AD-754 645

THE INTERACTION OF WAVES AND TURBULENCE IN WATER

John D. Skoda

California University

Prepared for:

Army Coastal Engineering Research Center

June 1972

DISTRIBUTED BY:

NTIS

National Technical Information Service
U. S. DEPARTMENT OF COMMERCE
5285 Port Royal Road, Springfield Va. 22151

AD754645

HEL 25-1

THE INTERACTION OF WAVES AND TURBULENCE IN WATER

by

JOHN D. SKODA

Reproduced by
NATIONAL TECHNICAL
INFORMATION SERVICE
U S Department of Commerce
Springfield VA 22151

DDC
RECEIVED
JAN 26 1973
C

HYDRAULIC ENGINEERING LABORATORY
COLLEGE OF ENGINEERING

UNIVERSITY OF CALIFORNIA
BERKELEY
JUNE, 1972

Approved for public release;
distribution unlimited.

R126

UNCLASSIFIED
Security Classification

DOCUMENT CONTROL DATA - R & D

(Security classification of title, body of abstract and indexing annotation must be entered when the overall report is classified)

1. ORIGINATING ACTIVITY (Corporate author)

Hydraulic Engineering Laboratory
College of Engineering
University of California

2a. REPORT SECURITY CLASSIFICATION

UNCLASSIFIED

2b. GROUP

3. REPORT TITLE

The Interaction of Waves and Turbulence in Water

4. DESCRIPTIVE NOTES (Type of report and inclusive dates)

HEL 25-1

5. AUTHOR(S) (First name, middle initial, last name)

John D. Skoda

6. REPORT DATE	7a. TOTAL NO. OF PAGES	7b. NO. OF REFS
June 1972	116	31

8a. CONTRACT OR GRANT NO.

DACW-72-68-C-0033

b. PROJECT NO

c.

d.

9a. ORIGINATOR'S REPORT NUMBER(S)

HEL 25-1

9b. OTHER REPORT NO(S) (Any other numbers that may be assigned this report)

10. DISTRIBUTION STATEMENT

Approved for public release; distribution unlimited.

11. SUPPLEMENTARY NOTES

12. SPONSORING MILITARY ACTIVITY

Department of the Army
Coastal Engineering Research Center
5201 Little Falls Road, N.W.
Washington, D. C. 20016

13. ABSTRACT

Report investigates a system in which water waves are generated and propagated in a turbulent flow field. Growth of wind wave spectra and decay of monochromatic waves are considered.

For monochromatic waves the turbulence in the water can greatly increase the rate of wave energy dissipation and that the data can be fitted by an equation with an eddy viscosity term proportional to the wave height, the phase speed of the waves, and the intensity of the larger scale turbulence.

Growth of wind waves on turbulent water is faster than in still water; however, maximum wave height in turbulent water is always lower than in still water. Wave energy spectra at the longer fetches in turbulent water show more wave energy at low frequency and less at high frequency than those for still water. Turbulence in water alters the rate of transfer of energy from the wind to the waves, the maximum height allowed and the distribution of wave energy among the various frequencies.

DD FORM 1473 NOV 65 — REPLACES DD FORM 1473, 1 JAN 64, WHICH IS OBSOLETE FOR ARMY USE.

UNCLASSIFIED

14. KEY WORDS	LINK A		LINK B		LINK C	
	ROLE	WT	ROLE	WT	ROLE	WT
Monochromatic Waves						
Wind Waves						
Water Turbulence						
Wave Energy						

University of California
Hydraulic Engineering Laboratory
Wave Research Projects

The work presented herein was submitted in partial fulfillment of the requirements for the Ph.D. in the Department of Civil Engineering, University of California, Berkeley, California. The work was partially supported by Contract DACW-72-68-C-0033 with the Coastal Engineering Research Center, Corps of Engineers, U.S. Army.

Technical Report
HEL 25-1

THE INTERACTION OF WAVES AND TURBULENCE IN WATER

by

John D. Skoda

Approved for public release; distribution unlimited.

Berkeley, California
June 1972

1C

ABSTRACT

This is a report of an investigation of a system in which water waves are generated and propagated in a turbulent flow field. The growth of wind wave spectra and the decay of monochromatic waves are considered.

For the monochromatic waves it is found that the presence of turbulence in the water can greatly increase the rate of wave energy dissipation and that the data can be fitted by an equation with an eddy viscosity term proportional to the wave height, the phase speed of the waves, and the intensity of the larger scale turbulence.

The growth of wind waves on turbulent water is found to be faster than in still water; however, the maximum wave height obtained in turbulent water is always significantly lower than the maximum height in still water. The wave energy spectra at the longer fetches in turbulent water show more wave energy at low frequency and less at high frequency than those for still water. Thus the presence of turbulence in the water alters the rate of transfer of energy from the wind to the waves, the maximum height allowed and the distribution of the wave energy among the various frequencies.

ACKNOWLEDGMENTS

Many of the staff and students in the Hydraulics Laboratory helped the author during the course of this research.

Professor H. A. Einstein suggested the topic and guided the study; his help, encouragement and consistent good humor are most appreciated. Professors F. S. Sherman and R. L. Wiegel are sincerely thanked for their suggestions and review of the study. During the entire course of the author's graduate studies Professor J. W. Johnson was always available to give advice and assistance. Professor J. V. Wehausen, Edward Noda, Charles Petrauskas and M.M. Das went out of their way to secure and transmit copies of publications pertinent to this study.

M. M. Das assisted in the initial experiments in the outdoor flume and Rahim Golchin helped in performing some of the experiments in the laboratory and in reducing data. The final design of the hot-film anemometer towing system was made by Karl Bermel. Bud Hewitt helped in developing the plans for the turbulence generators and these plans were executed by Walter Krogmoe. The author is also grateful to Jim Allison, Ray Campbell and Warren Matthew for friendly cooperation on occasions too numerous to mention in detail.

Finally, the drafting of William Kot and the typing of Patricia Tifft is gratefully acknowledged.

LIST OF SYMBOLS

A	constant in exponential regression equation (ft.)
B	constant in exponential regression equation (ft.)
C	constant in anemometer calibration equation (volts^2 sec./ft.)
c	phase speed of waves (ft./sec.)
C_G	group velocity of waves (ft./sec.)
D	rate of wave energy dissipation per unit area (lbs$_m$/sec^3)
D_B	rate of wave energy dissipation per unit area in Bowden's equation
D_D	rate of wave energy dissipation per unit area in Dobrokinoskii's equation
D_M	rate of wave energy dissipation per unit area measured by experiment
E	hot-film anemometer output (volts)
E_o	hot-film anemometer output in still water (volts)
e	natural log base (dimensionless)
F	length of fetch (ft.)
f	frequency of waves (sec^{-1} = Hertz)
g	gravitational acceleration (ft./sec.^{2})
h	wave height (ft.)
h_i	incident wave height (ft.)
$h_{i+\Delta x}$	attenuated wave height (ft.)
K_B	coefficient proportional to rate of energy dissipation in Bowden's equation (dimensionless)
K_D	coefficient proportional to rate of energy dissipation in Dobrokinoskii's equation (dimensionless)
k	wave number = $2\pi/L$ (ft.$^{-1}$)

L	wave length (ft.)
S	constant in anemometer calibration equation (dimensionless)
T	wave period (sec.)
Δt	incremental time between digitized data points (sec.)
U	horizontal velocity of flow (ft./sec.)
U_o	freestream wind velocity (ft./sec.)
X	horizontal distance (ft.)
ΔX	incremental horizontal distance (ft.)
δ	wave steepness = h/L (dimensionless)
κ	von Karman's constant = 0.4 (dimensionless)
ν	kinematic viscosity of water (ft.^{2}/sec.)
π	3.142 (dimensionless)
σ_{KB}	standard deviation of K_B (dimensionless)

TABLE OF CONTENTS

TABLE OF CONTENTS (cont'd.)

1. INTRODUCTION

In this chapter some qualitative observations which motivated this study are described. Because the interaction of waves and turbulence is a complex phenomenon with many aspects, it is necessary to place some limits on the study. These limits are defined in a positive way by stating what we wish to study, and in a negative way by listing some of the aspects which have been placed outside the scope of this study because they have already been treated by others or because they appear particularly intractable.

1.1 Wind Waves in Open Channels

When the resistance of a flow over mud deposits was studied in the outdoor 1000 ft. recirculating flume at the Richmond Field Station of the University of California in Berkeley, an interesting phenomenon was observed. The flume was fully exposed to the local winds which were usually blowing in the longitudinal direction of the flume. Over the length of 1000 ft. considerable wave action resulted both in the main channel and in the parallel return channel. As soon as the pump was started and the water in the two channels started to flow, the wave action practically disappeared in both channels.

The fact that the waves did not develop in either the main flume or the return channel proved that it was not the change of the wind speed with respect to the water that caused the change of the wind speed with respect to the water that caused the change, because in one channel this relative wind speed increased while it decreased in the other. Observation of the flow conditions showed that the wind actually created along the full length of both flumes the little ripples which always are the first indication of wave generation by wind. While in still water these ripples grow into waves did not grow, but remained always about the same. It was concluded from this observation that the flow or probably its turbulence interfered to prevent the growth of the waves beyond a certain size.

These open channel observations raised the following questions:

1) Is it actually the turbulence which interferes with the waves (taking energy from the waves faster than the wind puts energy into the waves)?

2) Does the turbulence interfere with the creation of waves by inhibiting the transfer of energy from the wind to the waves?

3) How important are the scale and the intensity of the turbulence in determining the size of waves which finally develops in the turbulent water?

1.2 Sea and Swell in the Turbulent Wake of a Ship

Observations were made of turbulent tug-boat wakes in San Francisco Bay from a sail boat moving through the wakes. It appeared that the long, low amplitude swell was unaffected by the wake, but shorter and steeper waves were almost completely eliminated. However, wind waves up to a few inches long soon appear in the wake. For several minutes the wake will persist with the very short wind waves and the long period swell, but with very little evidence of waves of intermediate length.

Refraction may play a role in the attenuation of waves in the locality of the wake if we consider the wake as a jet. Barber, 1969, points this out as well as the possibility that a ship with two screws whose blades are outward turning (as they reach their upper position such blades move outwards away from the center line of the ship) will cause water to rise along the center of the track and pass outwards near the sea surface. This pattern is like that created by pneumatic and hydraulic breakwaters. One might attribute all or most of the wave attenuation in a wake to refraction or the action of the surface current. There are however aspects which it does not seem to explain. One is the persistence of the wake. Barber, 1969, mentions this and an observation of a smooth ship wake in a large lake 10 minutes after the passing of a ship. Several of the above mentioned observations in San Francisco Bay were made when the direction of the wind and wave advance were at almost right angles to path of the ship and its wake. Here the jet driven backward from the propellers was essentially parallel to the oncoming wave crests. Under such conditions there would be no change in the height or length of the waves due to refraction by the jet current (see Johnson, 1947, or Wiegel, 1964, pp. 170-172 for refraction by currents for various angles of wave approach).

These observations of wakes in San Francisco Bay raised questions similar to those raised about wind waves in the open-channel.

1) Can turbulence be an important factor in causing the smoothing of the sea in a ship's wake?

2) Why do long waves pass through the wake relatively unaffected?

3) Why do very short wind waves and very long swell appear together in a wake while the waves of intermediate length seem to disappear?

1.3 The Scope of This Study

The main purpose of this study is to determine what effects turbulence has on water waves and on their generation by wind. The relative importance of intensity and scale of turbulent energy in wave attenuation is also investigated.

Because of the experimental difficulties and the expense of data reduction it was not possible to study the three-dimensional characteristics of the various turbulent flow fields.

The study is primarily concerned with time and space-averaged effects. For example, a statement saying that waves are attenuated a certain percent by a certain turbulent flow field means that after traveling a certain distance, in a certain time, the average wave height declined the stated percent. This should not be interpreted as ruling out the possibility of a wave being amplified as the instantaneous result of a wave - turbulence interaction.

Although turbulence in nature is generally associated with rivers, ocean currents and other flows of non-zero mean, this study concentrates on turbulent flow fields with a mean velocity of zero. This was done because of the difficulty of separating the effect on the waves of turbulence from the effects of a shear in the mean flow. This difficulty comes in turn from the fact that it is impossible to generate a turbulent flow, in a laboratory flume, with non-zero mean velocity which is uniform throughout the cross section.

As will be seen in the next section there have been several theoretical studies of the scattering of waves by turbulence. In these studies large scale turbulence is shown to be capable of redirecting wave energy by refracting and reflecting the waves. Because it has been well studied before, and because it could obscure other aspects of wave - turbulence interference an attempt was made to eliminate or at least minimize scattering in these experiments. In summary this study is concerned with a system which is non-conservative with respect to wave energy; whereas, the studies of scattering assume a closed system in which the total wave energy is conserved.

2. LITERATURE SURVEY

2.1 Theoretical Papers

The attenuation of waves moving across a deep turbulent liquid was considered by Phillips, 1959, assuming that the turbulence itself is not generating waves. He suggested two types of interaction which would cause attenuation of the incident waves; eddy viscosity interaction and scattering. Where characteristic scales of turbulent motion are of the same order as the wavelengths scattering will occur, and that, for turbulent conditions prevailing in the open ocean, attenuation is primarily due to scattering for waves of length greater than 3 meters. In either case the waves will decay exponentially and the problem is to predict the correct value of the exponent. Although only the scattering problem is solved in this paper, Phillips argues that a major difference between eddy viscosity interaction and scattering is that the wave steepness should be of much greater importance in eddy viscosity interaction than it is in scattering.

The scattering of waves by irregularities in the medium has been studied for electromagnetic, acoustic and elastic waves as well as for surface gravity waves. A general method to determine the average solution of a linear wave equation with random coefficients was presented by Keller, 1964.

Later Howe, 1971, solved the same problem by an alternative method and applied this method to a problem involving surface gravity waves. He found that the effect of inhomogeneities in a fluid with surface waves is to gradually randomize an initially coherent wave field. These inhomogeneities could be in the fluid depth (bottom topography) or in the velocity field (turbulence). He derives equations in which the attenuation of the coherent wave field appears to be due to a "psuedo-viscosity", and speaks of the energy of the coherent wave field being "absorbed" by the medium. Actually he assumes that total wave energy is conserved and the energy losses from the coherent (incident) wave field appear as gains in the random wave field.

Several authors have proposed methods of calculating an eddy viscosity to be used in determining the loss of wave energy due to turbulence generated by the motion of the wave itself. Dobrokinoskii, 1947, used Prandtl - von Karman turbulence theory and trochoidal wave theory to obtain an expression for the kinematic turbulent viscosity N_D , which is a function of the wave parameters and the depth. At the surface this expression is as follows:

$$N_D = \frac{\pi \varkappa^2}{18} \frac{h^2}{T} (1 - \pi^2 \delta^2)^3 \qquad (2.11)$$

where, h is the height; T the period, δ is the wave steepness = h/L; L is the wavelength; and $\varkappa$ is the von Karman constant equal to 0.4.

Bowden, 1950, on the basis of dimensional analysis, proposed that the kinematic viscosity in the wave dissipation equation be replaced by an eddy viscosity term, N_B, (due to turbulence generated by wave motion) as follows:

$$N_B = \frac{K\,Lh}{T} = K\ Ch \tag{2.12}$$

where; L is the length; h the height; T the period; and C the celerity of the wave. K is a nondimensional constant to be determined empirically; Bowden suggests that a K of the order of 5×10^{-5} would account for observed rate of decay of ocean swell. He also suggests that eddy viscosity may limit the steepness of wind waves which have grown so long that they travel at a speed approaching that of the wind.

Groen, 1954, proposed that an eddy viscosity proportional to the "4/3 power" of the wavelength he used to explain the decay of ocean swell in turbulence generated independently of the wave motion. The idea of using a "4/3 power" rule came from the work of Richardson, 1926, who found that the coefficient of diffusion applicable to dispersion of particles in the atmosphere was proportioned to the "4/3 power" of the distance separating the particles. Richardson and Stommel, 1948, also found that a "4/3 power" rule could apply to diffusion in the ocean. He also states that externally generated turbulence not only causes attenuation of waves, but is also responsible, through selective damping, for the increase in period of ocean swell that has been found to increase with distance traveled. Groen is concerned with the effects of external turbulence (existing independently of the wave motion and due to wind influences or currents in the sea) on waves; whereas, Dobrokinoskii and Bowden are primarily concerned with turbulence generated by the motion of the waves. This distinction seems somewhat academic because a wave may encounter turbulence generated internally by the previous passage of another wave.

A theory to explain the damping of waves by intense turbulence, such as that found in the wake of s ship, is given by Boyev, 1971. He assumes that the only turbulence which is important in damping of waves is that having the following properties:

1) The turbulence must be "long", i.e. having fluctuations whose scale is longer than the wavelength of the surface waves.
2) The turbulence must also be "fast" having fluctuations with a frequency greater than the frequency of the surface waves.
3) Only "long" and "fast" fluctuations in the vertical direction result in loss of total wave energy.

In deep water only the upper layer of water (of depth equal to the wavelength) participates in the wave motion. According to this theory the "long-fast-vertical" turbulence acts like an elevator. This elevator takes wave energy down below the wave layer where it cannot aid wave motion. On the upward trip the elevator brings turbulent energy which does not compensate for the wave energy taken down; therefore, this elevator action results in a downward flow of wave energy.

The horizontal motions of the turbulence are assumed to cause a redistribution (scattering) of wave energy but not any net gain or loss in total wave energy. This neglect of the effect of horizontal components of turbulence is one of the major weaknesses of this theory. The horizontal components of Boyev's "long" and "fast" turbulence could deform the surface waves enough to cause breaking or spilling. Also in water of depth less than or equal to the depth of the wave layer no "long" vertical turbulent components could exist, so, Boyev's theory would predict no significant attenuation by turbulence. Accurate measurements could perhaps be made to compare the wake of a ship in shallow water with the wake in deep water to test this theory (stereo photography would be one method of obtaining the necessary wave data). At this time no qualitative observations, such as those mentioned in the Introduction, have been found to give any indication of a decrease in damping by a ship's wake when the ship enters shallower water.

2.2 Experimental Studies

In a discussion of experiments with pneumatic breakwaters Kurihara, 1958, suggests that one factor causing attenuation might be turbulence. He found that as the scale of his experiments increased the efficiency of the larger scale pneumatic breakwaters was greater than that obtained by Froude Law extrapolation from the smaller scale tests. He gives two equations for pneumatic breakwater power requirements of attenuation - one for the case where eddy viscosity is negligible and another for the case where eddy viscosity is important. On the basis of these equations and his data he concluded that the greater efficiency of the larger scale pneumatic breakwaters is due to greater eddy viscosity in the larger scale experiments.

Dobrokinoskii and Kontoboitseva, 1966, studied the dissipation of wave energy in a wave flume in order to test the theory of Dobrokinoskii (1947) and to compare it with other theories such as that given by Bowden, 1950. The turbulence was generated by the motion of the waves and not from any external source. Interestingly both the theories agree well with the experimental results, although the theoretical equations (given above in Section 2.1) are different.

Paquin, 1962, performed an experiment in which he passed mechanically generated waves (of frequencies 1.2 to 12.3 Hertz) through a zone of turbulence in a wave flume. The turbulence was generated by oscillating a false-bottom grid up and down. He found that the waves were attenuated more in the turbulent water than in still water, but his data had considerable scatter. He does not mention the cause of this scatter but if we consider the method of wave generation, the frequencies generated and the width of his flume, it seems likely that cross waves were present in his flume. The problem of cross waves is discussed in Chapter 5 of this report and a comparison is made between Paquin's data and ours. Paquin also placed a hot-film anemometer into the turbulent zone and shows spectra of velocity fluctuations. Because the mean flow with respect to the anemometer was zero, it is impossible to determine the scales of the velocity fluctuations from his data.

An experimental wake was created by Savitsky, 1970, in order to study wave attenuation. He towed a grid through a wave tank and then propagated waves into the wake. It was found that the towed grid set up a current and that this current refracted the waves in such a manner that they were lower in the wake and higher away from the wake. No appreciable attenuation could be attributed to the turbulence. Several factors may have accentuated the effects of refraction over those of eddy viscosity:

1) The angle at which the waves approached the wake was that which would maximize refraction; i.e. the waves were traveling in the same direction as the towed grid.

2) The scale and intensity of the turbulence was probably very small relative to that of the waves. Although no turbulence measurements are reported the grid was made of wooden slates ranging in width from 0.80 to 1.60 inches as compared to waves ranging in length from 3 to 8 feet.

3) The waves studied were all very low (not steep) and

as has been noted in some of the theories (and will be further discussed in Chapter 5) the wave height is an important factor in attenuation by turbulence.

3. WAVES IN FLOWING WATER

In this chapter some measurements and photographs of waves in flowing water are given. As was stated in the Introduction the overall study concentrates on waves in turbulent flow fields with a mean velocity of zero; however, some wave measurements were taken in turbulent flowing water with a nonzero mean velocity. The purpose of these measurements was to quantitatively verify some of the qualitative observations which motivated the study and to gain further insight into the problem.

3.1 Wind Waves in Flowing Water

Wave gages (resistance type) were placed in the outdoor 1000 ft. recirculating flume at the Richmond Field Station of the University of California (see Fig. 3.11 for details of the flume and location of instruments). The flume was filled to a depth of 1.2 ft. and waves were generated in the flume by the local winds. Wave records were made with no flow in the flume, then the wave recorder was stopped briefly while the pump was turned on and the pump speed increased gradually up to that required to give a velocity of 1 ft/sec. in the channel containing the wave gages. When the pump was up to the required speed and the velocity in the flume appeared to be the same everywhere, the wave recorder was turned on again. During the entire procedure the wind speed was recorded by an anemometer on the roof of the pump house. The flow velocity was measured by timing the speed of a dye patch injected into the flume.

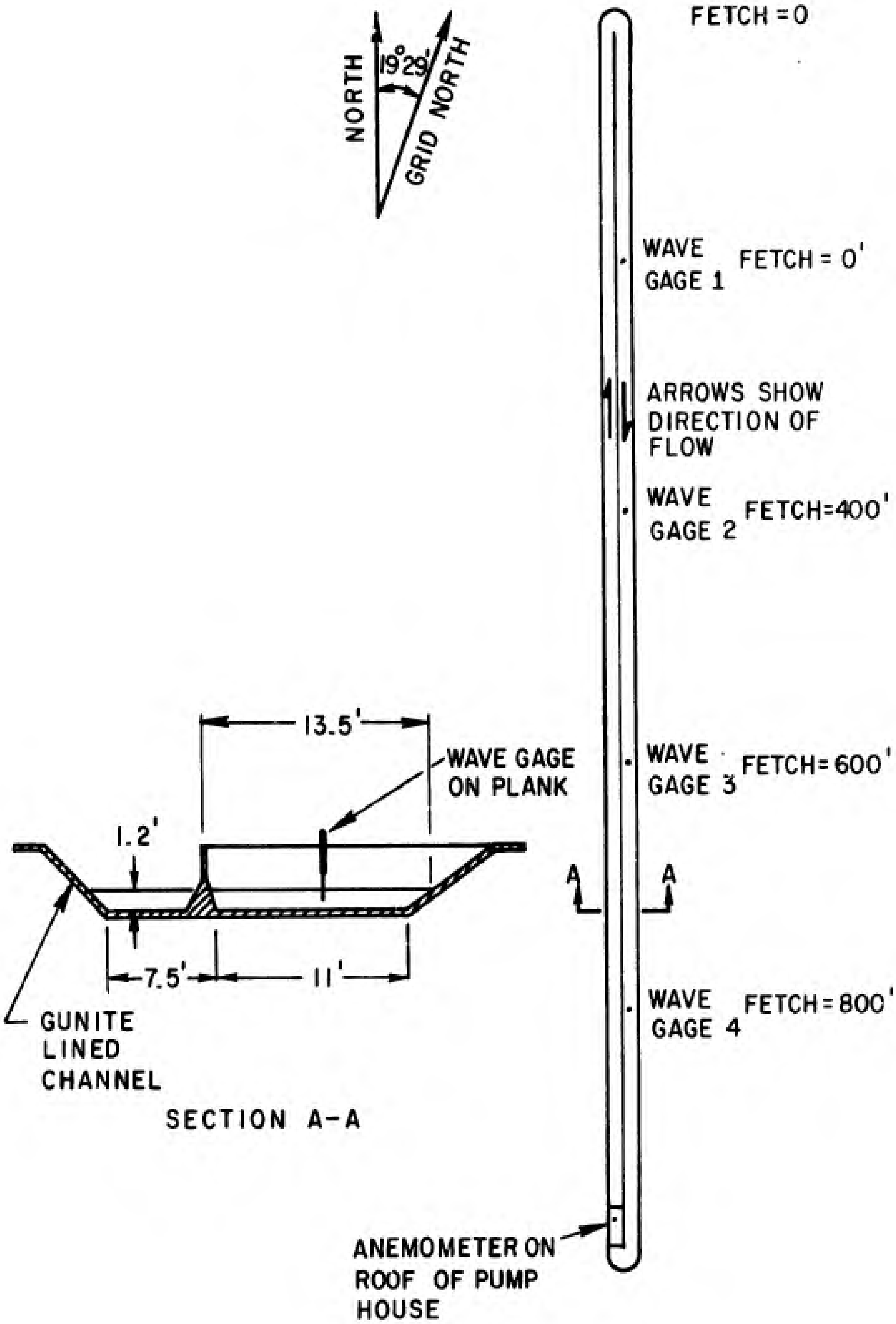

FIG. 3.11 OUTDOOR 1000 FT. FLUME

Records were obtained, in the above manner, during fairly steady wind for the following conditions:

1. Negligible wind coming from the SW at an angle of 45° to the long axis of the flume.
2. Wind of approximately 13 ft/sec. in the same direction as the flow.

The records under the first condition were taken to see if the turbulent flow alone was creating waves large enough to modify the wind waves. This disturbance of the water surface by the flow was found to be negligibly small.

Records for the second condition show that in the turbulent flow the growth of wind waves is considerably altered. Portions of the records are shown in Fig. 3.12. Figures 3.13 and 3.14 are photographs of the flume during test conditions. A 200 sec. portion of the wave records for 600 ft. fetch for both still and flowing water was digitized with a 0.1 sec. digitizing interval With available computer programs for spectral analysis (see Appendix A) the distribution of wave energy as a function of frequency was obtained. Figures 3.15 and 3.16 show spectra of wind-wave energy without flow and with turbulent flow for two different values of frequency band-width (0.05 Hertz and 0.25 Hertz). In the absence of turbulent flow the wind wave spectrum has a strong peak at 1.50 Hertz. This corresponds to a wave of period 0.67 seconds and a wavelength of 2.3 ft.

When the turbulent flow is present the spectrum of water surface fluctuations in the vicinity of 1.5 Hertz has a value of

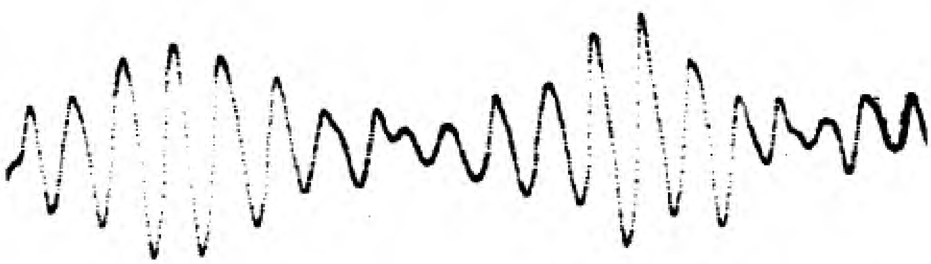

Waves in Still Water

Waves in Flowing Water

FIGURE 3.12 SAMPLE WAVE RECORDS
(Vertical Scale = 0.004 ft./mm;
Horizontal Scale = 0.1 sec/mm;
Wind Speed = 13 ft./sec;
Fetch = 600 ft.)

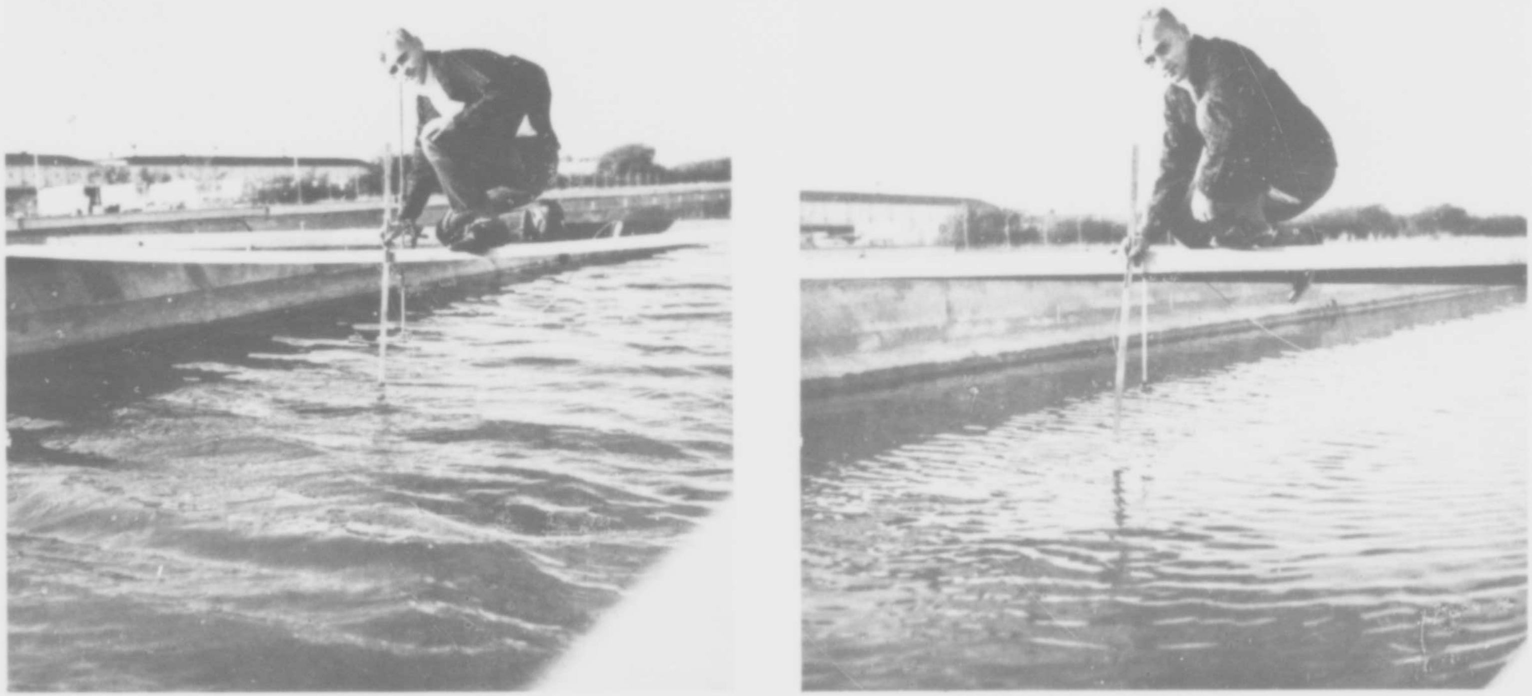

Channel Without Flow

Channel With 1 ft./sec. Flow (↗)

Waves with 13 ft./sec. Wind (↗) with 800 ft. Fetch
(Author holding yard stick)

Figure 3.13

Channels without Flow

Channel with 1 ft./sec. Flow (↑)

Waves with 13 ft./sec. Wind ( ) with 50 ft. Fetch in the Foreground

Figure 3.14

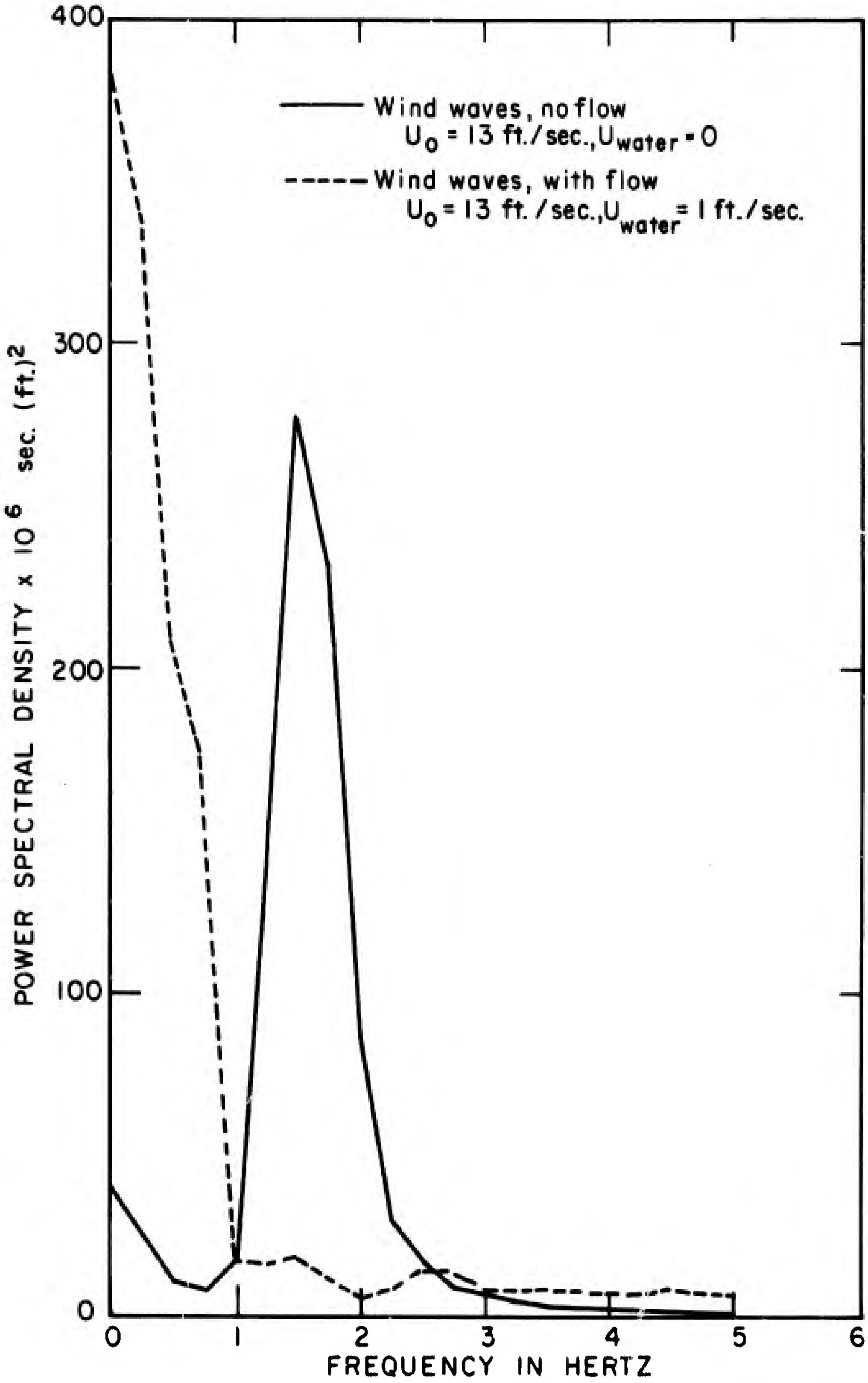

FIG. 3.15 SPECTRA OF WIND WAVES

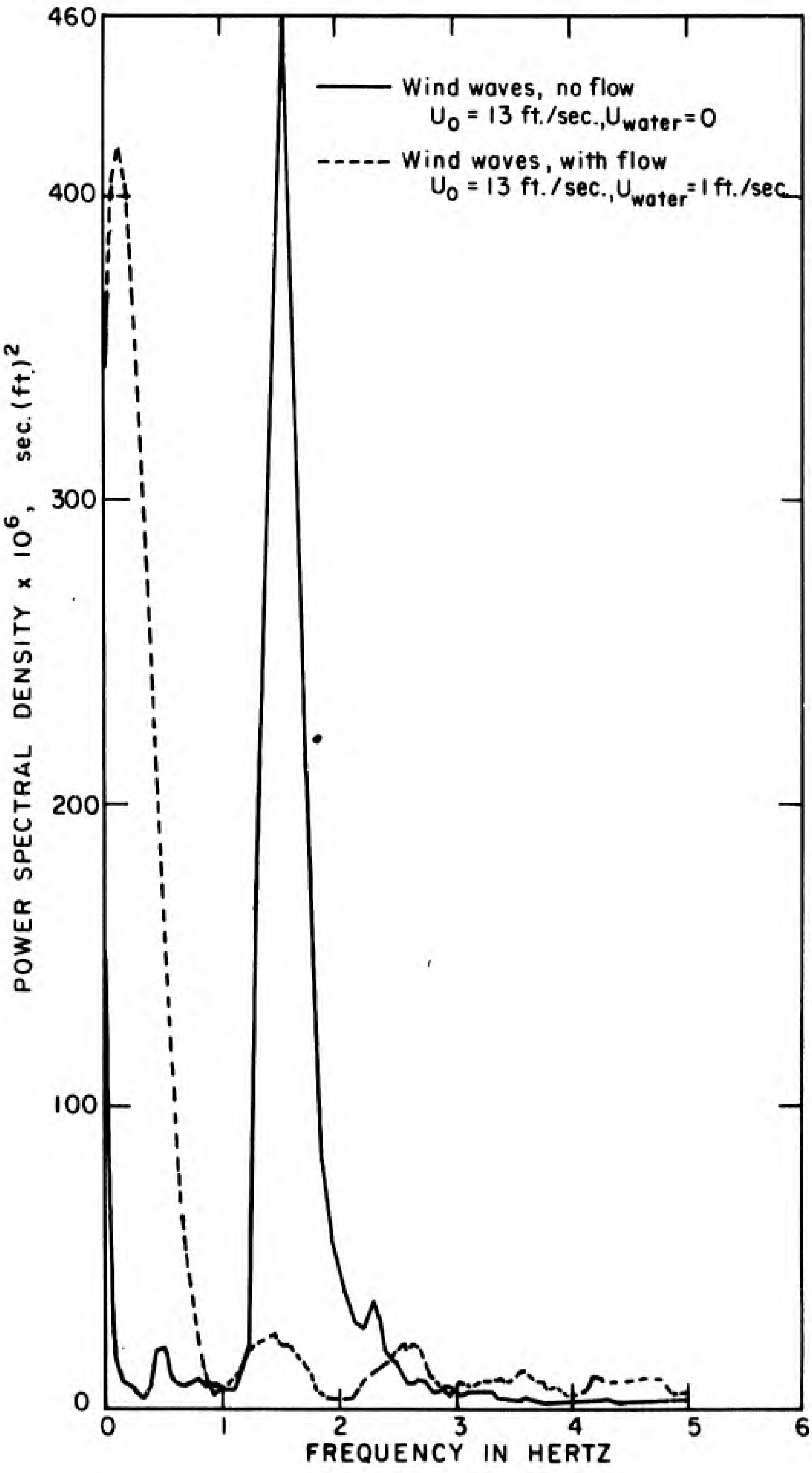

FIG. 3.16 SPECTRA OF WIND WAVES

only 5 to 10 percent of that for wind waves in the absence of turbulent flow. The frequency of a wave recorded in still water or in flowing water will remain the same provided that the gage is fixed (see Barber, 1969 for a discussion of this and Sawaragi, 1967 for experimental varification).

Several factors could be causing this significant reduction in wave energy. Because the wind and flowing water are going in the same direction, the wind speed relative to the water surface has been reduced as a result of the flow, but this reduction is only about 8%. Therefore it would not cause a 90 to 95 percent decrease in wave energy. Because the decline in relative wind speed cannot be expected to produce a reduction of 90 to 95 percent in the wave spectrum it seems that there must be another important factor effecting wind wave growth, and that could be the turbulence.

So far only that portion of the (Figs. 3.15 and 3.16) spectrum in the vicinity of 1.5 Hertz has been discussed. For frequencies near zero and up to 0.9 Hertz there is much more energy present in the flowing water. This is apparently due to very long period oscillations set up in the flume when the pump was turned on. For frequencies greater than 2.5 Hertz the spectrum shows 3 times as much wave energy in the turbulent flowing water as in the non-flowing water. This indicates that very short wind waves can exist and grow in turbulent water, but apparently as they grow longer they reach a length beyond which their growth is greatly inhibited.

Additional photographs of the outdoor flume under various wind and flow conditions are shown in Figs. 3.17, 3.18, and 3.19. Figure 3.17 shows the water surface near the beginning of the generating area. Figure 3.18 was taken from the window of the pump house with the camera facing into the wind. When flow is present three zones can be seen in the picture: 1) in the foreground the turbulent water leaving the pumps is creating strong surface fluctuations 2) in the middleground the water surface is greatly smoothed by the turbulence 3) in the background, where the turbulence is not so strong, short waves roughen the water surface. The second and third zones can also be seen in the same channel (the left channel) of Fig. 3.19, taken from the roof of the pump house.

3.2 Mechanically Generated Waves in a Recirculating Flume

Waves in flowing water were studied in the laboratory by placing a permeable paddle (dense screen), mechanical wave generator in a 2-ft-wide recirculating flume. The bottom of the flume was covered with corrugated plastic roofing sheets in order to obtain a fairly intense turbulence in slowly flowing water.

Waves from the generator were recorded at stations upstream from the wave generator both in still water and in turbulent water. Although it was noted that the shorter and steeper waves were attenuated more rapidly than the longer and less steep waves, the presence of standing cross waves in

Channels without Flow

Channels with 1 ft./sec. Flow (↕) (↕)

Waves with 15 ft./sec. Wind (↖) with 10 ft. Fetch in Foreground

Figure 3.17

Channel Without Flow

Channel with 1 ft./sec. Flow (↓)

Waves with 15 ft./sec. Wind (↓) with 900 ft. Fetch in the Foreground

Figure 3.18

Channels without Flow

Channels with 1 ft./sec. Flow
(↑) (↓)

Waves with 15 ft./sec. Wind (↓) with 900 ft. Fetch in Foreground

Figure 3.19

the flume made it impossible to obtain reliable data. These cross waves may have been generated by the wave generator or they may have resulted from the presence of shear in the mean flow. Naturally, the distribution of mean velocity cannot be uniform because the velocity must go to zero at the bottom and at the side walls. If most of the shear is near the bottom (i.e., if the velocity distribution is almost uniform in the upper part of the flow cross section), where the orbital velocities of the waves are fairly small, we can expect that the nonuniformity of the mean velocity will not have a large effect on the waves. Because the bottom of the flume is much rougher than the walls (corrugated roofing sheets on the bottom versus glass walls), the shear zone will be thicker at the bottom than at the walls, but both these shear zones can affect the attenuation of the waves in a way which is difficult to predict quantitatively. The reduced flow velocity near the side walls permits the waves to proceed faster at the wall (when the waves are traveling in a direction opposite to the flow) than in the center of the flume, bending the crests in such fashion that some of the wave energy is diverted from the wall towards the center of the flume. Cross components of the waves can be created in this process that result in standing waves across the channel. In this way, wave energy is diverted from the progressive wave under study by a process independent of the flow turbulence and makes the proper assessment of the latter effect impossible. Also, the measurement of the wave heights is almost impossible due to their strong three-dimensionality. To test if this three-dimensionality could be eliminated by using a different wave generator, a plunger-type wave generator was built and tested, but in flowing water the wave crests were bent and the waves became three-dimensional.

The presence of three-dimensional waves raises the question of how many wave gages are needed to define the wave surface. The electric field around our wave probes was large enough to prevent the close placing of probes without getting interaction. Thus, when two probes were within about 1 ft of each other, moving one probe up or down in the water would generate a signal on the other. This interaction could be alleviated by reducing the size of probes and thus reducing the size of the electric field; however, the overall number of probes and their requisite electronic equipment must be greatly increased if accurate measurements of three-dimensional waves are to be made. Obviously, the time and expense of data reduction is also greatly increased in the study of three-dimensional waves. It was decided, therefore, to change to a system in which turbulence is applied without systematic uni-directional flow. Such a system was built and the wave attenuation results are presented in the next chapter along with a more thorough discussion of cross waves.

4. A TURBULENT FLOW FIELD WITH A MEAN VELOCITY OF ZERO

4.1 Turbulence Generators

In order to study the effect on waves of turbulence alone (without any effects of a mean shear flow) two turbulence generators were built and tested.

The first turbulence generator consisted of a rough false bottom which was driven back and forth on skids by means of cables attached to a compressed air piston. Figure 4.11 shows photographs of the piston and the false bottom roughened with plastic corrugated sheeting. The turbulence thus generated was found to be effective in increasing the rate of attenuation of waves, but it had one serious drawback. It created a standing surface wave that was so high that the wave recorders would be driven off scale unless the sensitivity was greatly reduced. The wave made by the turbulence generator could be separated from the waves whose attenuation we wished to study be means of spectral analysis, because the waves were far apart on the frequency scale. However, if the sensitivity was reduced to keep the recorders on scale, the signal made by the waves under study became too small to detect accurately. Furthermore, the orbital velocities of the standing wave were also large relative to the velocities of the turbulent fluctuations making it difficult to define the turbulence spectrum accurately. In other words the spectra of velocity fluctuations for identical experiments were not sufficiently reproducible. Therefore, a

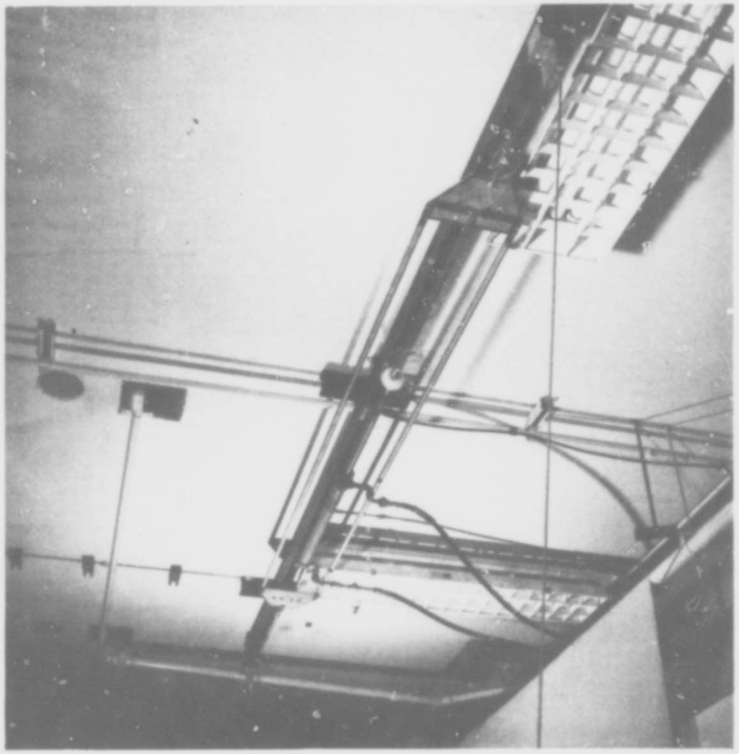

Pneumatic Piston
and Cable Drive

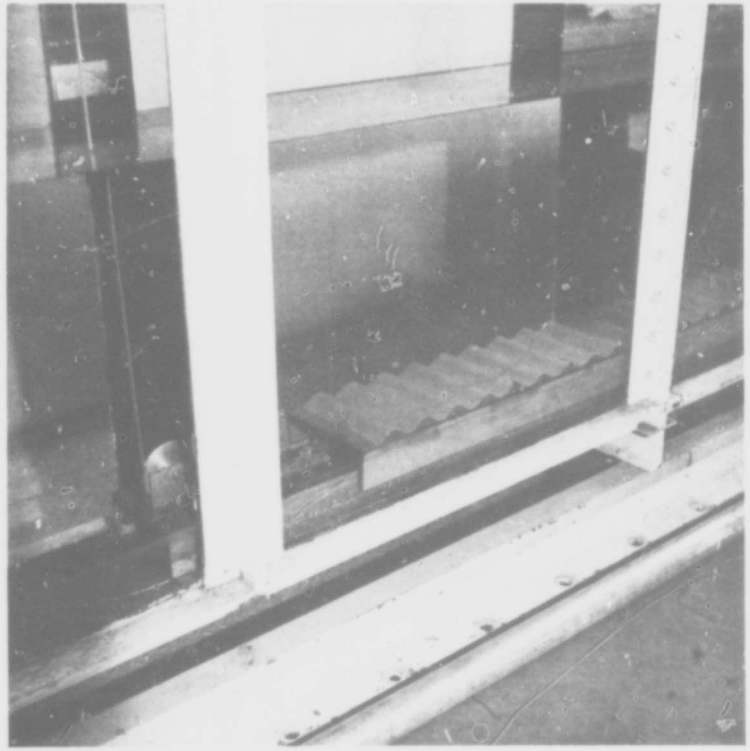

Cable Drive and Rough-False-Bottom
Turbulence Generator in 1 Foot Flume

Figure 4.11

new turbulence generator was designed with the aim of reducing the size of the unwanted surface wave and improving the reproducibility of the spectra of velocity fluctuations.

The second turbulence generator had a series of paddles attached to two 25-ft-long rode running lengthwise along the bottom of the 1-foot flume. The rode and attached paddles are rotated back and forth to produce turbulence. This design was successful in that it produced a much smaller surface wave and the spectra of velocity fluctuations were more nearly reproducible than was the case with the first turbulence generator. The design drawing is shown in Fig. 4.12 and photographs of the turbulence generator and its motor drive are shown in Fig. 4.13 and 4.14.

4.2 Calibration System for the Hot-Film Anemometer

The first calibrations of the hot-film anemometer were made in calibrators employing nozzles. Here a jet with measured discharge flows through the nozzle into a large body of water. The hot-film anemometer is placed at the center of the mouth of the nozzle. The velocity is calculated from the discharge, the cross sectional area of the nozzle, and the velocity distribution. The velocity distribution may be calculated or taken from data published by the nozzle manufacturer. The water is filtered and deaerated by passing it through a low pressure chamber or by heating it and then cooling it immediately prior to running the calibration. Several potential sources of error

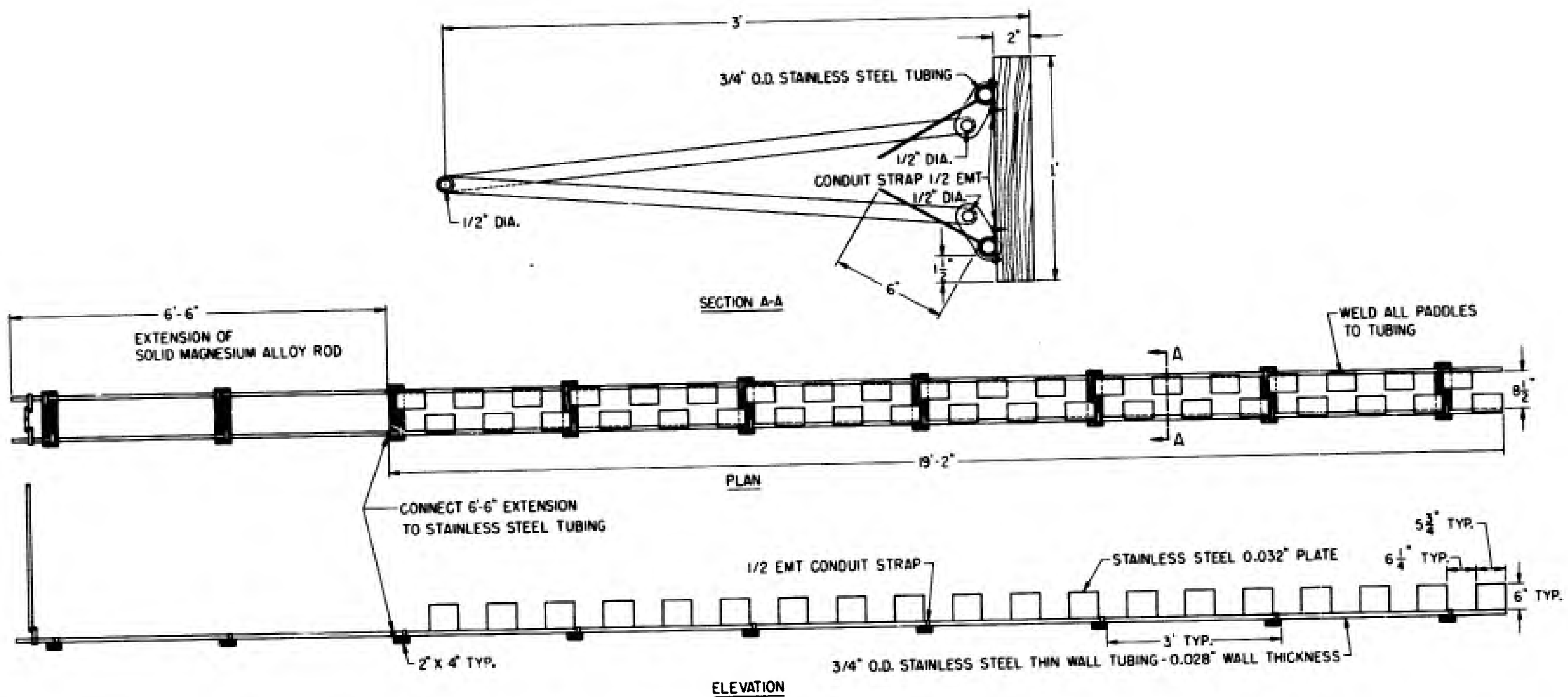

Figure 4.12 PADDLE TYPE TURBULENCE GENERATOR

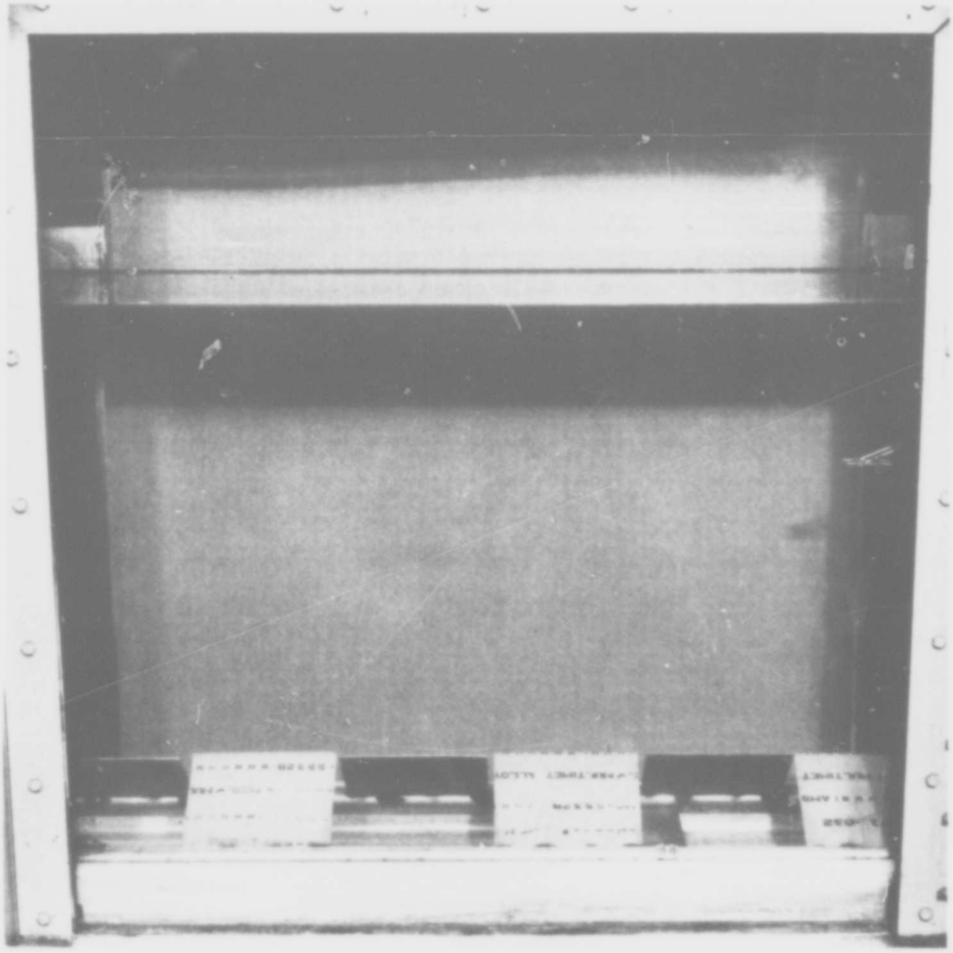

Figure 4.13 Turbulence Generator Paddles in the Flume

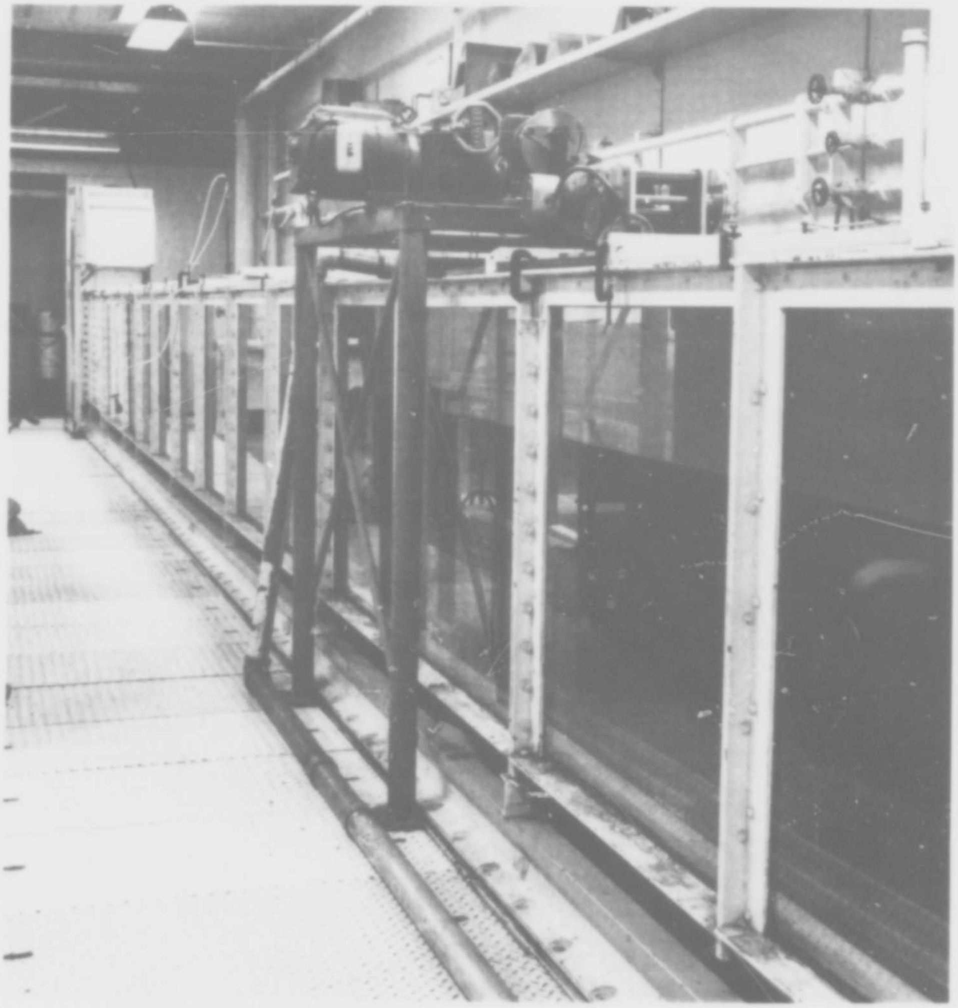

Figure 4.14 Motor Drive for the Paddle
Type Turbulence Generator

in the calibration system are as follows:

1. Errors can be made in measuring or calculating the discharge. In one test we found that the calibrator was leaking and only part of the measured discharge was passing through the nozzle.
2. An error can be made in attempting to place the hot-film anemometer at the exact center of the nozzle mouth.
3. Errors can be made regarding the velocity distribution at the mouth of the nozzle. Previously published data for the nozzle may be missinterpreted or in the case of calculation on theoretical grounds some of the assumptions may be incorrect or only approximately correct.
4. Sometimes the water in which the measurements are to be taken is of different temperature or purity from that in the nozzle calibrator. Corrections can be made for temperature differences, but contamination of the probe by impurities in the water may invalidate the calibration entirely.

Many of the problems and potential sources of error encountered in the use of a nozzle-type calibrator were eliminated in our final calibration system. In this system the probe is towed by a constant speed electric motor through still water. A gear box (see Fig. 4.21) made speed changes possible. The velocity can be obtained directly by measuring the distance and

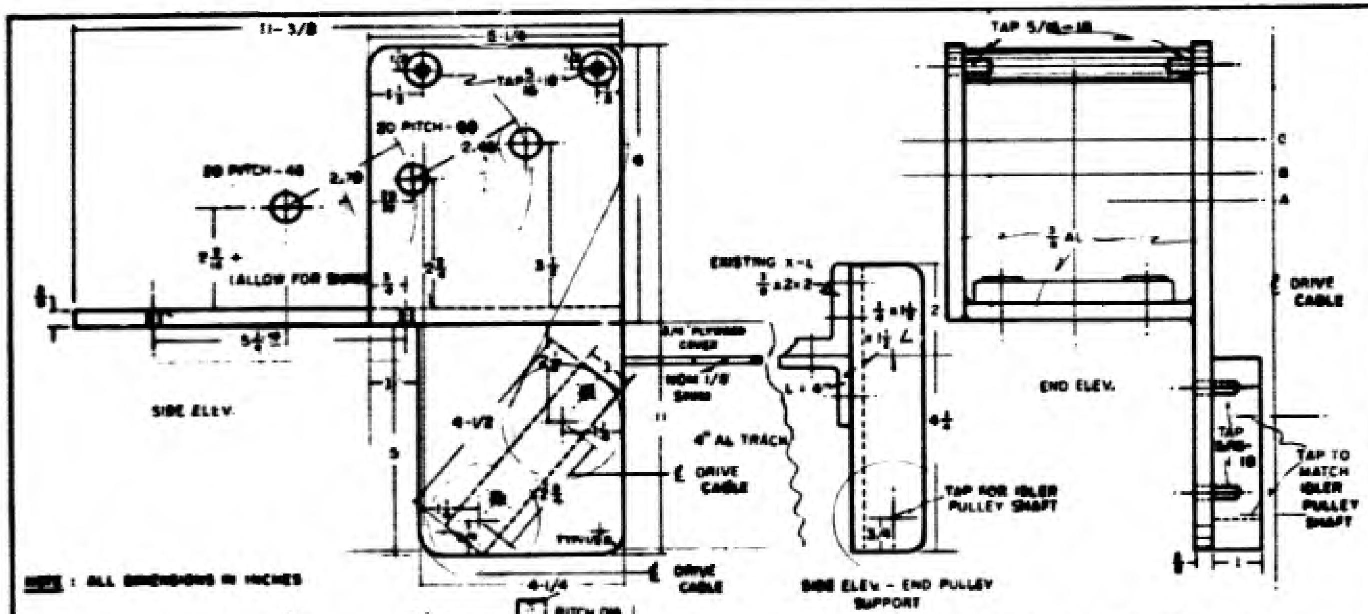

NOTE: ALL DIMENSIONS IN INCHES

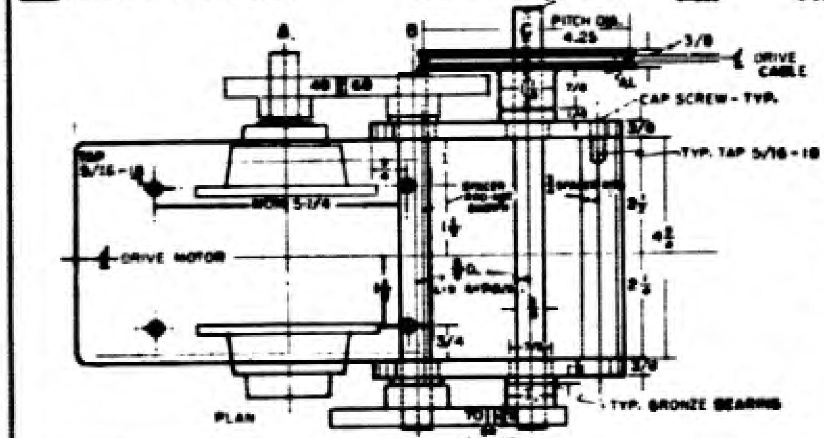

GEAR COMBINATIONS – OUTPUT SPEEDS

MOTOR-GEAR REDUCER INPUT-R.P.M. SHAFT A	GEAR ARRANGEMENT SHAFTS A-B	GEAR ARRANGEMENT SHAFTS B-C	DRIVE PULLEY P.D. 4.25" ● OUTPUT SPEED
34.5	48-60	28-70	0.20 FT/SEC.
"	"	40-58	0.35 "
"	"	*58-40	0.74 "
"	"	70-28	1.28 "
"	60-48	28-70	0.32 "
"	"	40-58	0.55 "
"	"	58-40	1.16 "
"	"	70-28	2.00 "

● ENTIRE RANGE CAN BE SHIFTED BY CHANGE P.D. DRIVE PULLEY
* PROVIDE SPACER COLLAR OR HUB (MIN 1" O.D.)

GEAR ASSEMBLY FOR INSTRUMENT CALIBRATION

Figure 4.21

travel time between two points. The following four towing speeds were used to determine the calibration equation: 0.210, 0.360, 0.757, 1.30-all in fee. per second.

The probe was clamped to a carriage (see Figs. 4.22 and 4.23) which rolls on an aluminum track suspended above the flume. This carriage was pulled by a taut steel cable running on pulleys driven by the constant speed electric motor.

The voltage output from the hot-film anemometer was connected to an analog to digital converter which recorded it, at intervals of 0.00853 seconds, as a binary number on a magnetic tape. This tape was then read by the computer which computed the average value for each run. To obtain the calibration equation, $(E^2 - E_o^2)$ was plotted versus U on log - log paper; where U is the towing speed in ft./sec., E_o is the average value of the anemometer output when the towing speed is zero, and E is the average value of the anemometer output when the towing speed is equal to U. The calibration curve will appear as a straight line in such a plot. Figure 4.24 shows such a calibration curve. The general form of the calibration equation is then:

$$U = \left(\frac{E^2 - E_o^2}{C}\right)^{1/S}$$

where S is the slope of the line when log $(E^2 - E_o^2)$ is the ordinate and log U is the abscissa, and where C is a constant which is determined by substituting the U and E coordinates of any point on the line into the equation and solving for C.

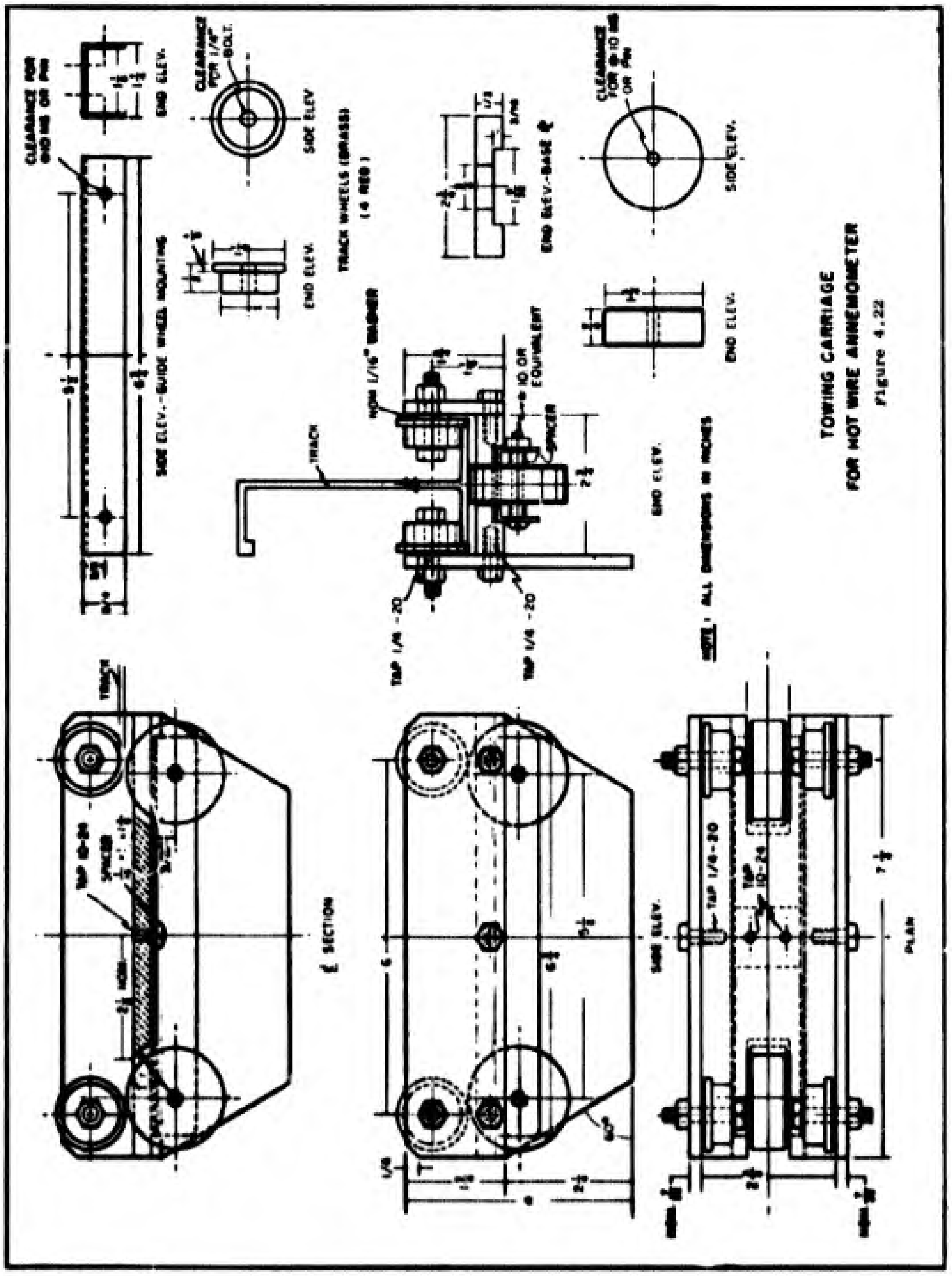

TOWING CARRIAGE
FOR HOT WIRE ANNEMOMETER
Figure 4.22

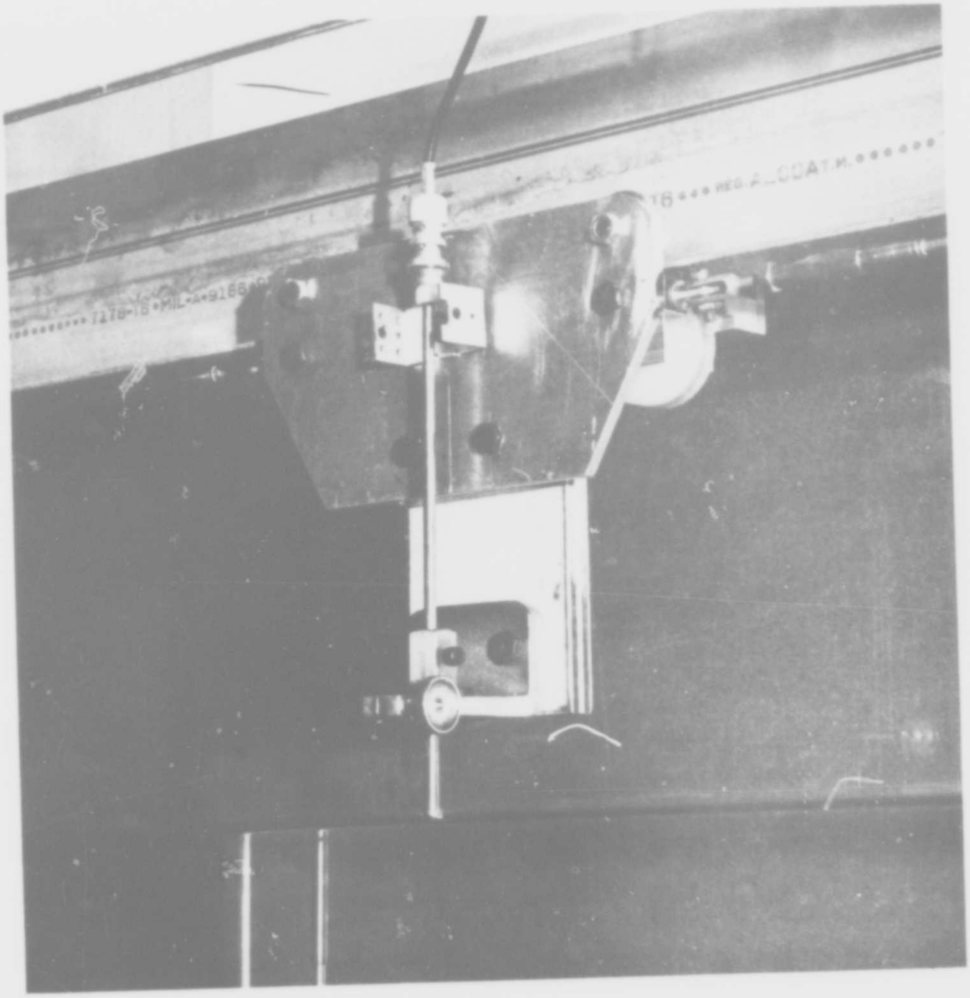

Figure 4.23 Towing Carriage for the
Hot-Film Anemometer

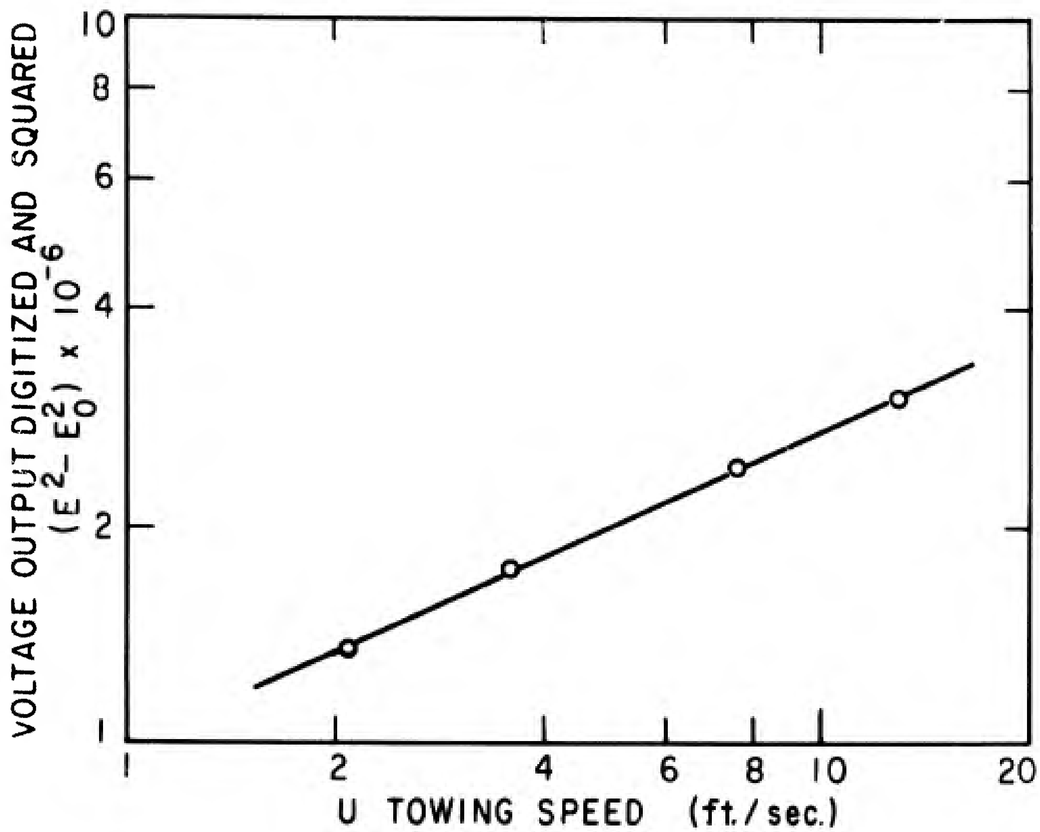

FIG. 4.24 HOT-FILM ANEMOMETER CALIBRATION CURVE

The equation for the calibration curve shown in Fig. 4.24 is thus found to be:

$$U = \left(\frac{E^2 - 520,000.}{2,679,000.}\right)^{2.30}$$

In order to minimize contamination of the hot-film anemometer by particulate matter in the water a 10 micron cartridge type filter with a flow capacity of 50 gal./min. was installed in the flume. Though the filter pump was not turned on when data was being taken the water in the flume was circulated through the filter continuously during the night prior to taking data.

All of the hot-film data was taken with a quartz coated cylindrical probe manufactured by Thermal Systems Incorporated. In order to minimize bubble formation on the probe, without employing a deaeration system, we used the low overheat ratio of 3%.

4.3 Analysis and Interpretation of Hot-Film Anemometer Data

After calibration, the hot-film probe was towed at 1.30 ft./sec. at a depth of 4.5 inches below the surface through the water made turbulent by the paddle type generator. The paddles were driven at three different rates (0.57, 0.92 and 1.52 cycles/sec.) to produce what will hereafter be called "Turbulence A", "Turbulence B" and "Turbulence C".

Just as in the calibration records the analog to digital converter recorded the velocity digitally at intervals of 0.00426 seconds on the magnetic tape. The records were each

12 seconds long in which time the probe traveled 15.6 feet. By performing spectral analysis on the data we can get the distribution of turbulent energy as a function of frequency up to the Nyquist frequency, 1/2 Δt .

In our data Δt is 0.00426 second; therefore the Nyquist frequency is 117 Hertz. We can also make a geometric interpretation of the velocity spectra because we know that the probe is passing through the water at 1.30 ft./sec. This speed is much higher than the velocity of the turbulent fluctuations; therefore there are no reversals of flow direction only changes in the magnitude of the velocity. Turbulent energy in the spectrum at any given frequency means that the probe is detecting a pattern whose scale in feet in the direction the probe is traveling is equal to 1.30/f where f is the frequency in Hertz. Although no measurements of turbulence were attempted in the plane perpendicular to the longitudinal axis of the channel, we know that away from the paddles the turbulence will be relatively isotropic. Because the flume is 1.0 ft. wide no isotropic turbulence could exist at scales greater than 1.0 ft. i.e. no isotropic turbulent energy at frequencies less than 0.8 Hertz.

Figure 4.31 shows spectra obtained from towing the probe through still water and through Turbulence A. Ideally there should be negligible energy in the spectrum for a tow through calm water, yet several areas of considerable energy appear;

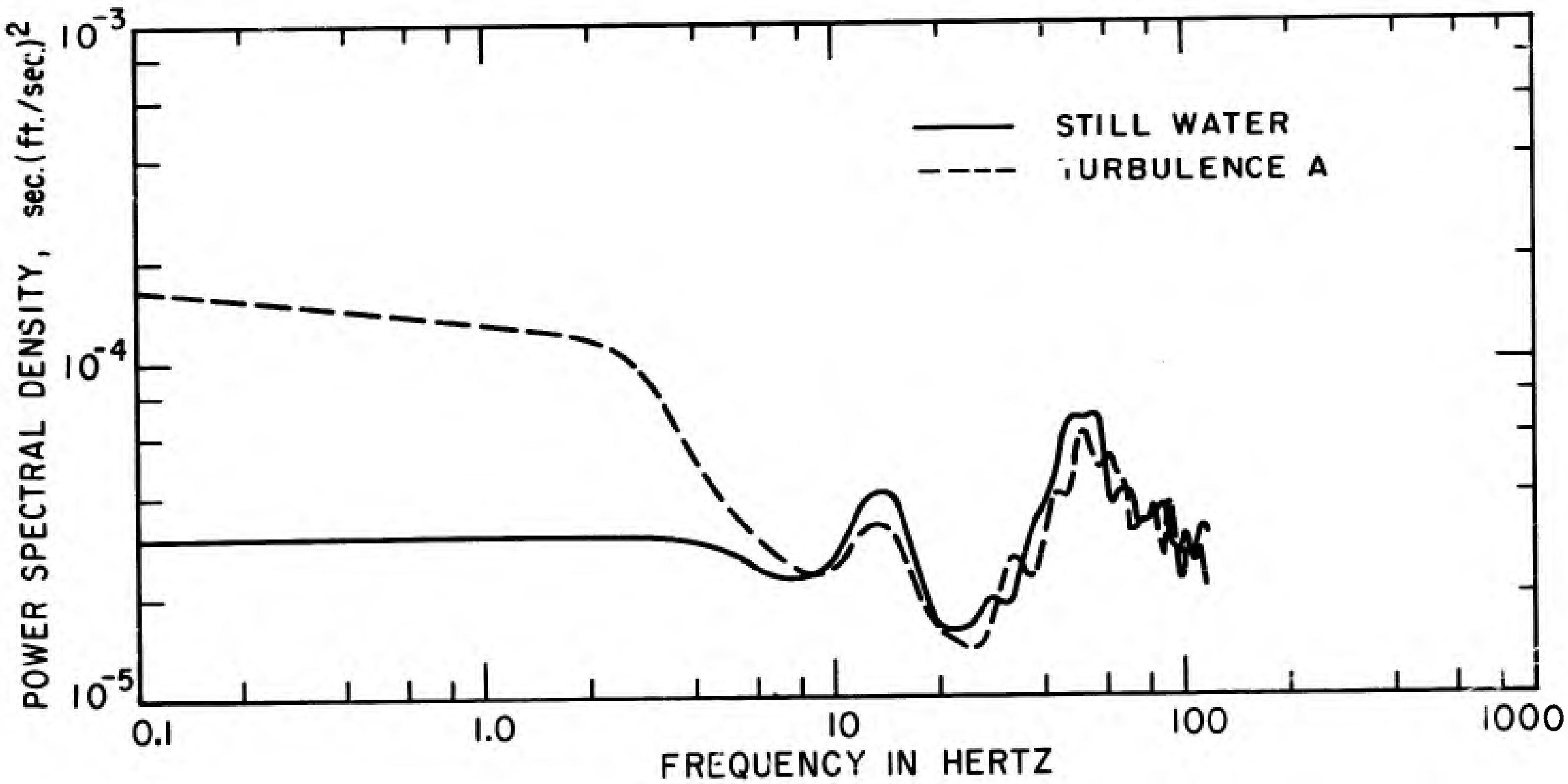

FIG. 4.31 VELOCITY SPECTRA FROM HOT-FILM DATA

one at about 14 Hertz, and another larger one at 50 to 60 Hertz. These peaks are practically identical in all the spectra of data taken at 1.30 ft./sec. towing speed. Spectra of the calibration tows at 0.360 and 0.757 ft./sec. through still water seem to show less energy in these peaks (see Fig. 4.32). These peaks could be due to a vibration of the carriage or probe support which is more violent at high speeds or possibly to electronic noise. For some reason the spectra obtained in turbulent water seem to have slightly less energy in these peaks. Fortunately this background pattern is consistent and most of the turbulent energy effective in the damping of the waves is found at frequencies lower than these peaks i.e. at frequencies less than 14 Hertz and length scales greater than about 1 inch.

Figure 4.33 is another spectrum of Turbulence A. Figure 4.34 shows two spectra of Turbulence B and Fig. 4.35 shows two spectra of Turbulence C. For Turbulence A, B and C the two available spectra are averaged and these average spectra are shown in Fig. 4.36 along with the background spectrum for still water. In this Figure the abscissa is shown both as a frequency and as a length.

Because the type of turbulence present makes a big difference on the rate of wave damping (as will be shown in Chapter V) we will compare the spectra for Turbulences A, B and C as percentages of each other. Figure 4.37 shows the spectra

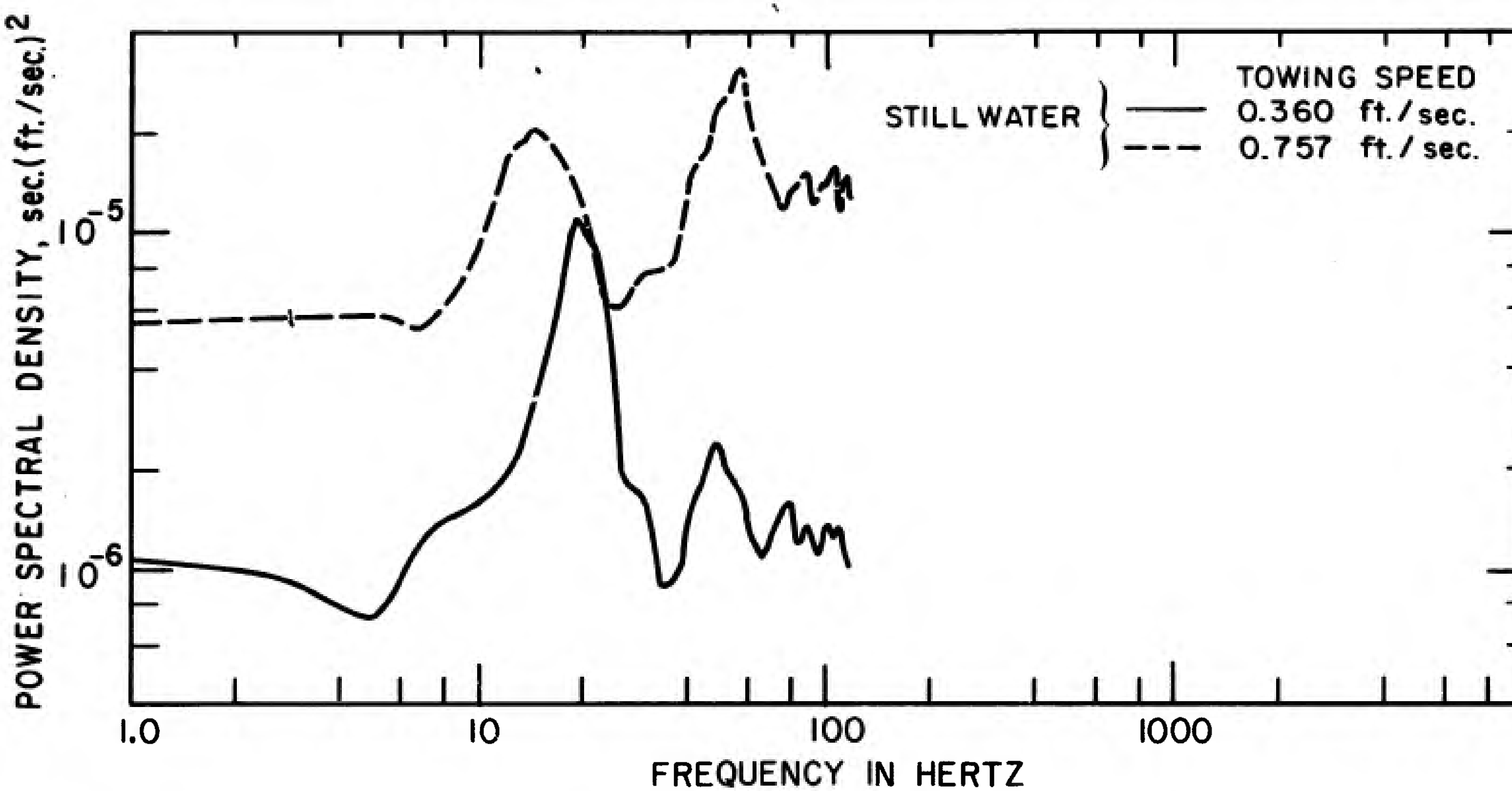

FIG. 4.32 VELOCITY SPECTRA FROM HOT–FILM DATA

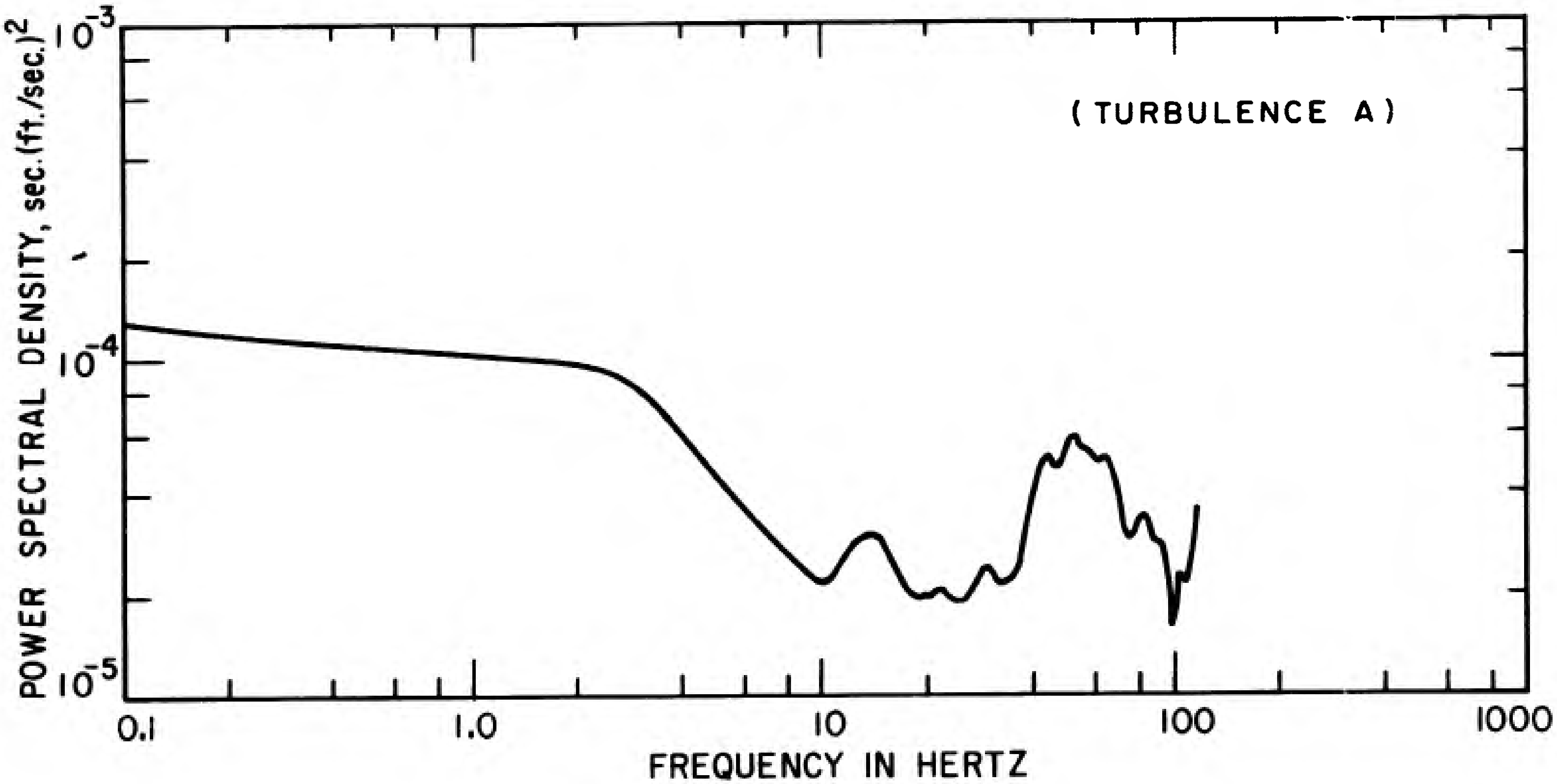

FIG. 4.33 VELOCITY SPECTRUM FROM HOT-FILM DATA

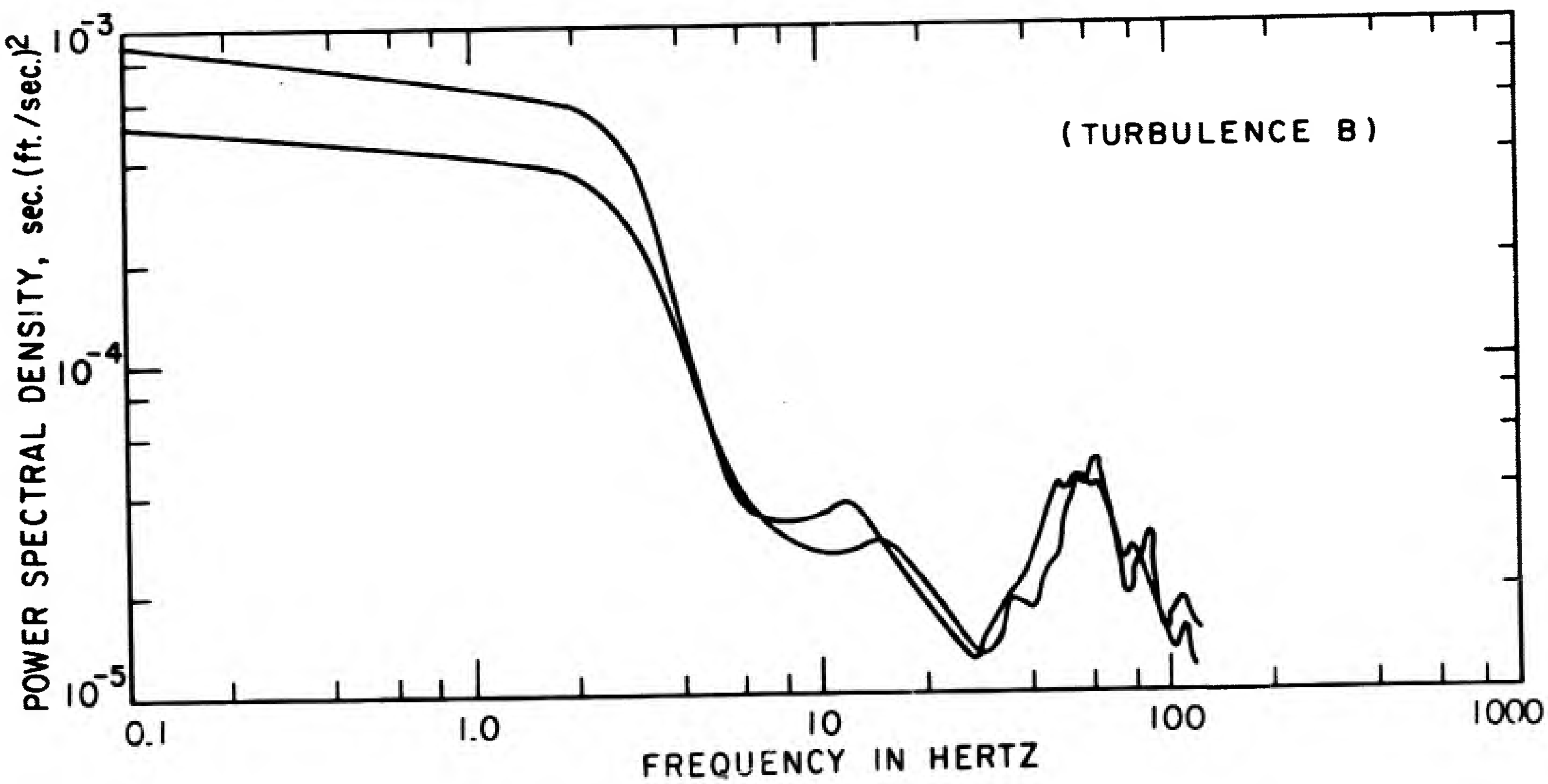

FIG. 4.34 VELOCITY SPECTRA FROM HOT-FILM DATA

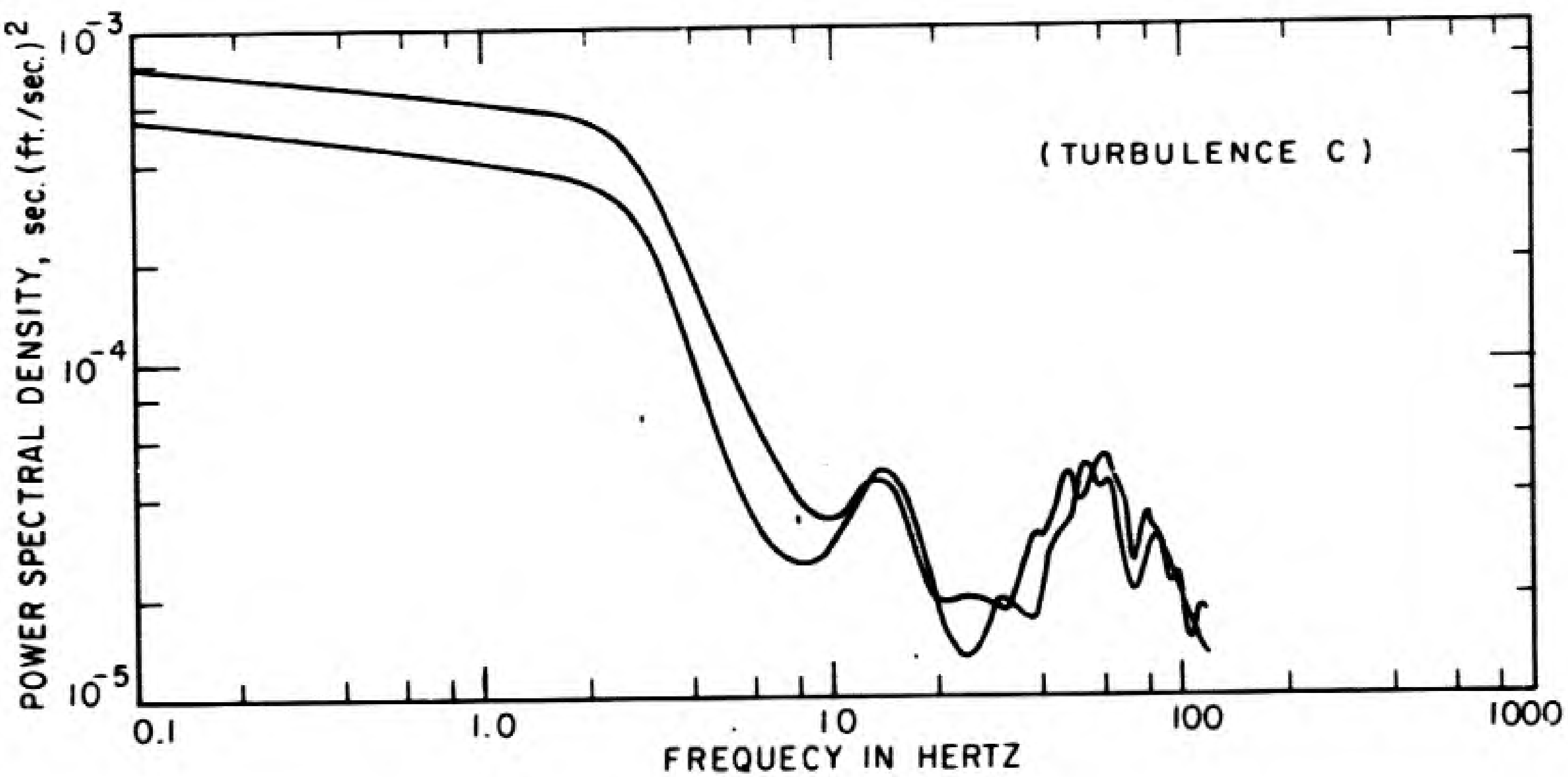

FIG. 4.35 VELOCITY SPECTRA FROM HOT-FILM DATA

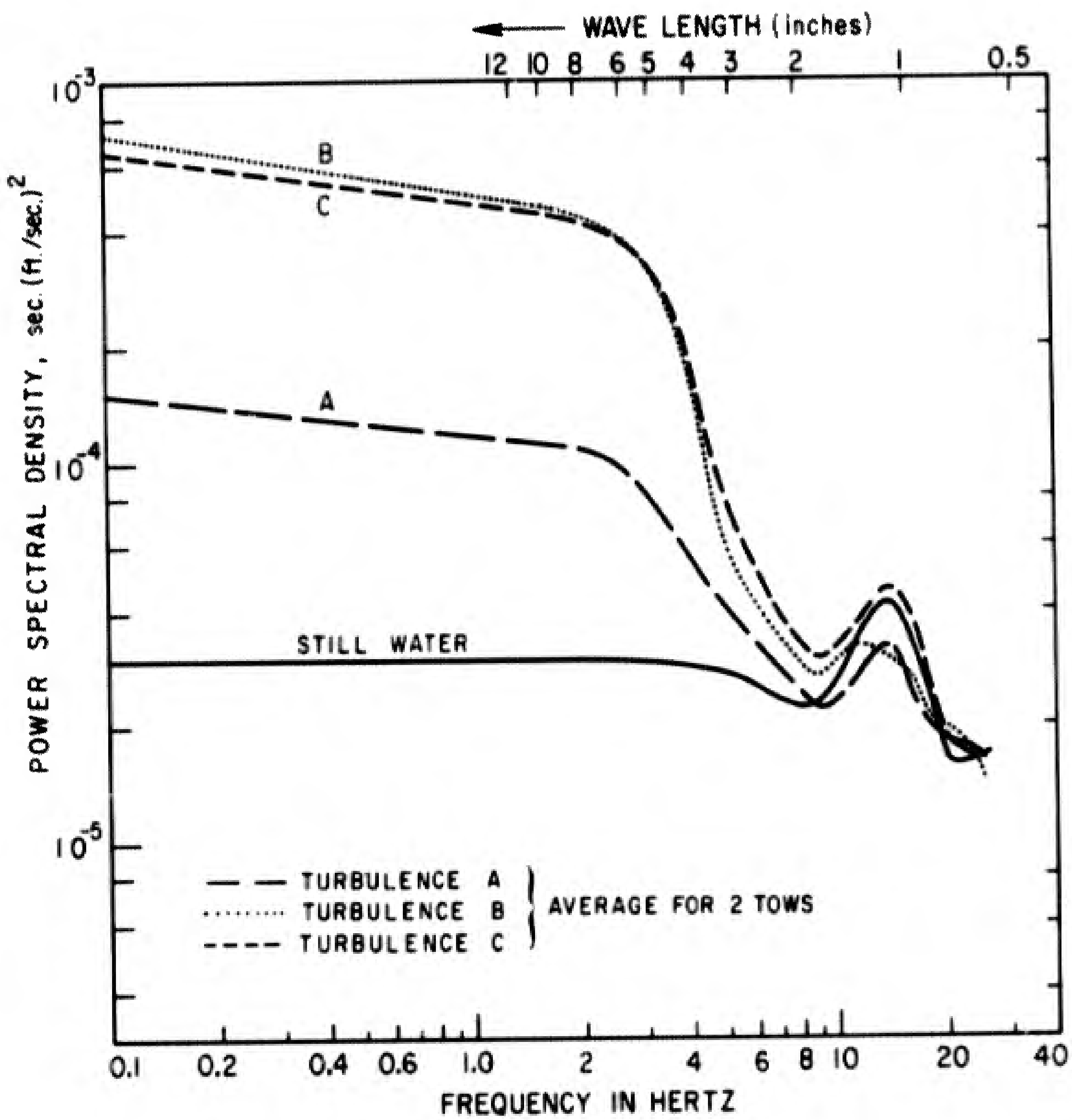

FIG. 4.36 VELOCITY SPECTRA FOR ALL CONDITIONS

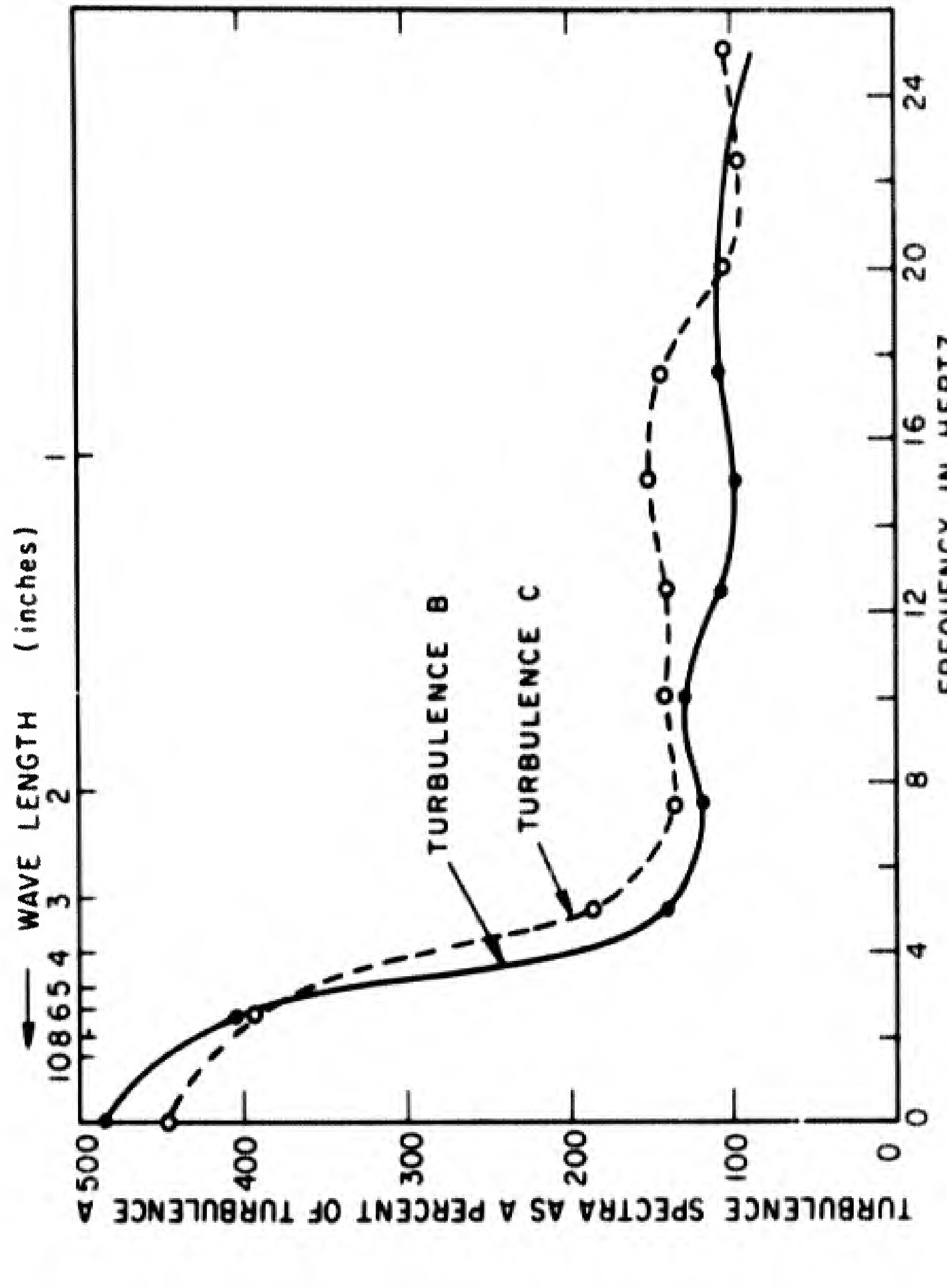

FIG. 4.37 COMPARISON OF TURBULENCE SPECTRA B & C TO A

as percents of the spectrum for Turbulence A. For turbulence of length greater than 3 or 4 inches (less than 4 or 5 cycles/sec.) B and C are much greater than A. In Turbulence A waves attenuate about 3 times faster than in still water, but in Turbulence B & C waves attenuate almost 6 times as fast as in still water.

One question to be answered is why Turbulences B and C are about equally effective in damping waves. In Fig. 4.37 it can be seen that for frequencies greater than 5.0 cycles/sec. spectrum C is generally greater than spectrum B. This is even more dramatically demonstrated in Fig. 4.38 where the spectra are shown as percentages of spectrum B. Yet another way of comparing the spectra is to integrate the area under them - this area is directly proportional to the turbulent energy. Between 5 and 20 Hertz B has 6.% more energy than A, and in this range C has 37.% more energy than A. Clearly this portion of the spectrum (length scales of from 3 inches to less than 1 inch) is not nearly as important in determining the effect of the turbulence on the waves as is the portion of the spectra representing scales larger than 3 inches.

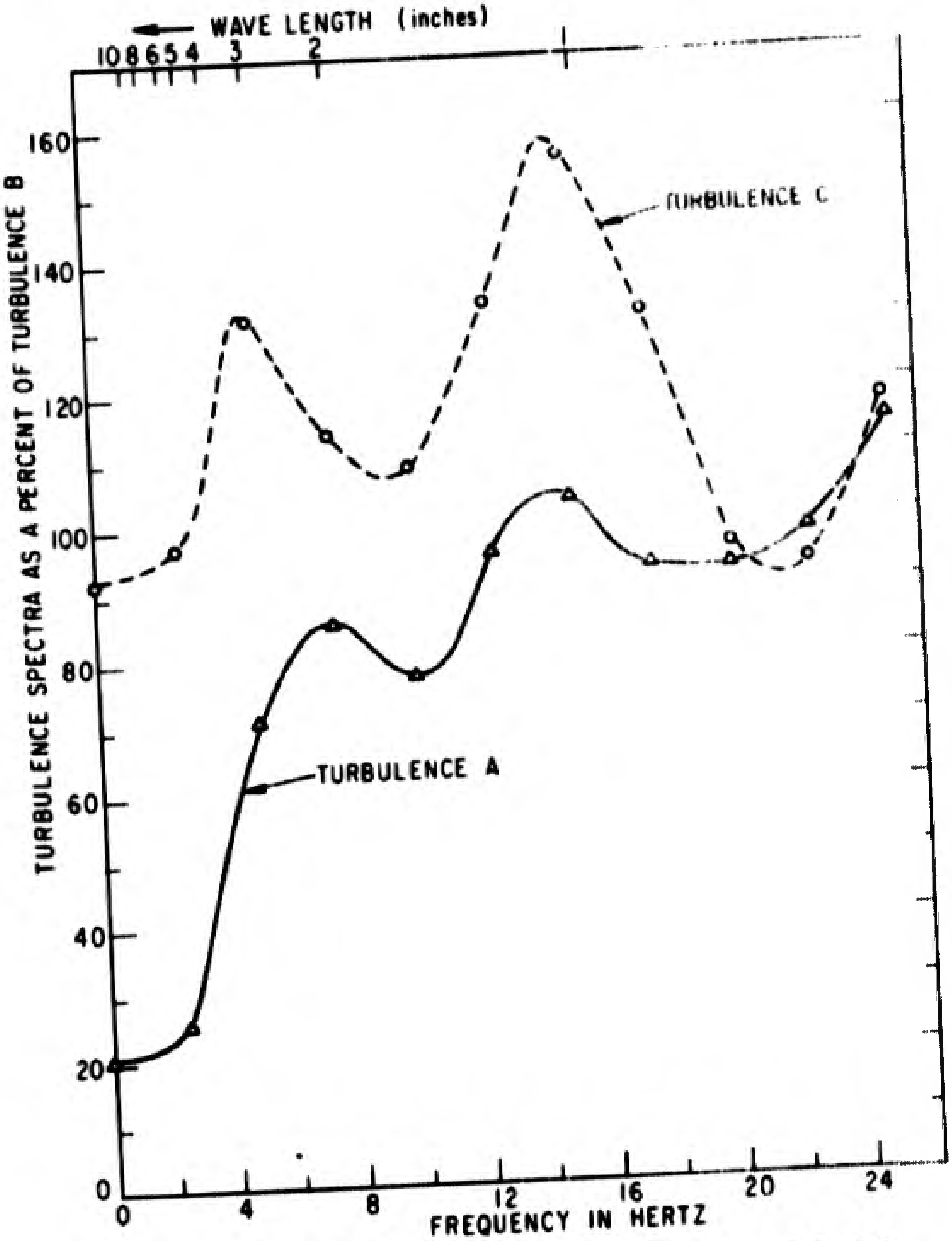

FIG. 4.38 COMPARISON OF TURBULENCE SPECTRA A & C TO B

5. MONOCHROMATIC WAVES IN A TURBULENT FLOW FIELD

In Chapter 4 the generation and measurement of a turbulent flow field with a mean velocity of zero was described. In this chapter the effects of such a turbulent flow field on mechanically generated wave trains are described. In the first attempts to study such wave trains several serious difficulties arose. These problems and their solution are discussed first and then the experimental results are presented. All of the experiments reported in this chapter were performed in a flume 1 foot wide, 100 feet long with a water depth of approximately 2 feet.

The first experiments were performed in the 1-ft flume containing the rough false bottom driven back and forth to generate turbulence. A rough corrugated sheet lying close to and parallel with the bottom of the flume was agitated back and forth along the bottom by means of a cable drive driven by a pneumatic piston above the flume. The turbulence generated by this means then diffuses up through water and along the flume. Figure 4.11 shows this turbulence generator and the piston cable drive, and the data shown in Fig. 5.21 were obtained using this type of turbulence generator. For the reasons given in Chapter 4 this turbulence generator was later replaced with the paddle-type turbulence generator shown in Figs. 4.12 and 4.13. Except for the data shown in Fig. 5.21, all of the data presented in this chapter were taken in the flume equipped with the paddle-type turbulence generator.

The waves were generated by a plunger-type wave generator which had been built previously for the 1-ft flume. The plunger is shaped like a triangular wedge and the entire wave generator can be moved along the top of the flume to any desired location. Figure 5.11 shows the plunger in position in the flume and removed for better view.

5.1 The Attenuation of Waves by a Surface Film

In the initial experiments it was found that if the wave length was very long compared to the scale of the turbulence, then little or no attenuation could be detected by our wave gages. The largest scale of turbulence was limited by the size of the paddles and the width of the flume; therefore, in order to determine the effects of turbulence on waves shorter than the scale of the turbulence, it became necessary to generate very short waves. Such very short gravity waves can be rapidly damped by a surface film and it was found that very soon after filling the wave flume with clean water a surface film developed which did greatly attenuate the waves we wished to study. Eventually it was discovered that this surface film was caused by the leaching of chemicals from the paint (Inertol brand) covering the steel parts of the flume (the only non-steel section of the 100 foot long flume is the glass walled center section 20 feet long).

The surface tension was measured with a tensiometer for various waters with and without surface films. The surface

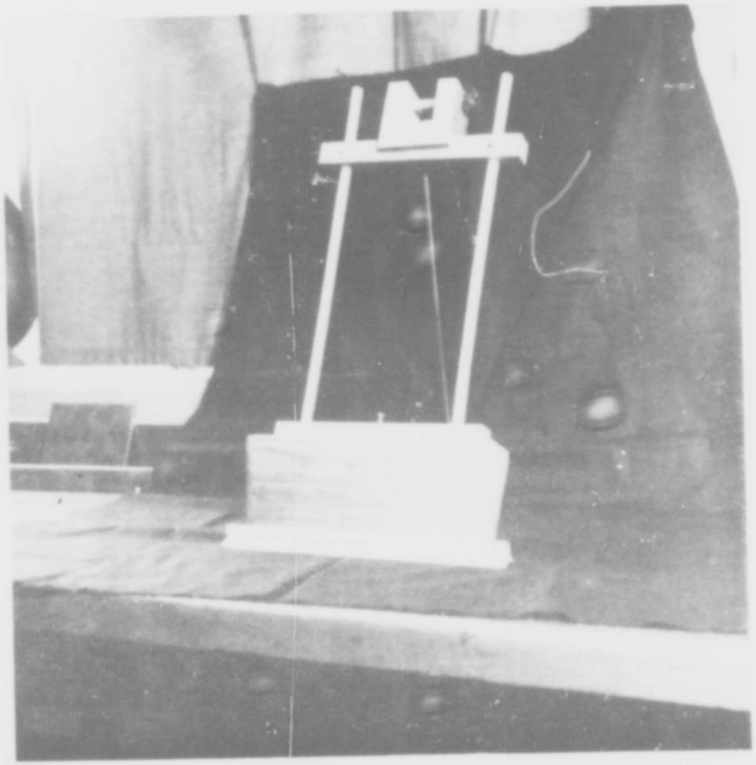

Wedge - Shaped Plunger

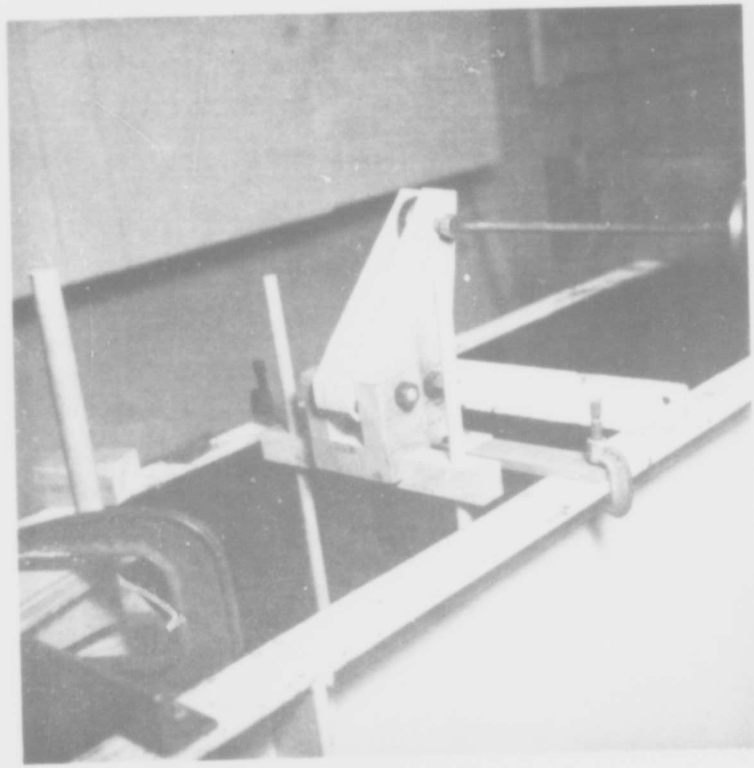

Plunger in Position
in the 1 Foot Flume

Figure 5.11

tension was about 15 dynes/cm less when the Inertol film was fully developed than it was in clean water. It should be noted that a fully developed surface film often causes less damping than a partially developed one. In other words a small change in surface tension may cause more damping than a larger change. This was already noted by Davies, 1962, and by Garrett, 1967. For this reason the ordinary platinum wire tensiometer is not sufficiently sensitive to be of use in determining whether or not the surface is clean enough for short waves. In fact the rate of damping of a short wave is a more sensitive measurement of surface tension than the standard tensiometer. Davies, 1962, states that the main cause of damping of short waves is due to the "reversals in the surface stress as the wave pass, caused by the marked compressional elastic behavior of surface films"; only at frequencies much higher than gravity waves is the surface viscosity important in causing damping.

Various attempts were made to clean the surface. Skimming the surface with a double layer of clean cheese cloth tied to a wooden float effectively removed the film, but a new film developed so rapidly that there was not enough time to perform experiments before the film developed sufficiently to affect the results. Complete removal of this paint was found to be prohibitively costly; therefore, some covering which would prevent the leaching of the surface film agent was sought. Small scale tests showed that a covering of clear acrylic was very effective in containing the surface film agent, but later it was found that the acrylic covering did not wear well. Finally the flume was lined with polyethylene sheeting and the surface was skimmed at regular intervals of about 20 minutes. This kept the surface clean enough that no significant wave damping was caused by the surface film and yet allowed adequate time between skimmings to perform the experiments.

5.2 The Problem of Cross Waves

In the generating of waves with lengths close to or shorter than the width of the flume it was found that in addition to the wave progressing down the long axis of the flume there were also present cross components causing a variation of wave height (measured at various points) across the width of the flume. This pattern appeared as soon as the wave generator was turned on; therefore, it could not be caused by any reflections from the ends of the flume. Figure 5.21 shows some of the data taken (with a single wave probe at each station) when cross waves were present. The presence of cross waves makes it very difficult to get reproducible data because the cross components may increase the wave height near the center of the flume at one point and further along these components may decrease the wave height near the center and increase it near the walls. This pattern may be stationary or it may move along the flume.

Lin and Howard, 1960, showed both theoretically and experimentally that cross waves could be generated by interactions

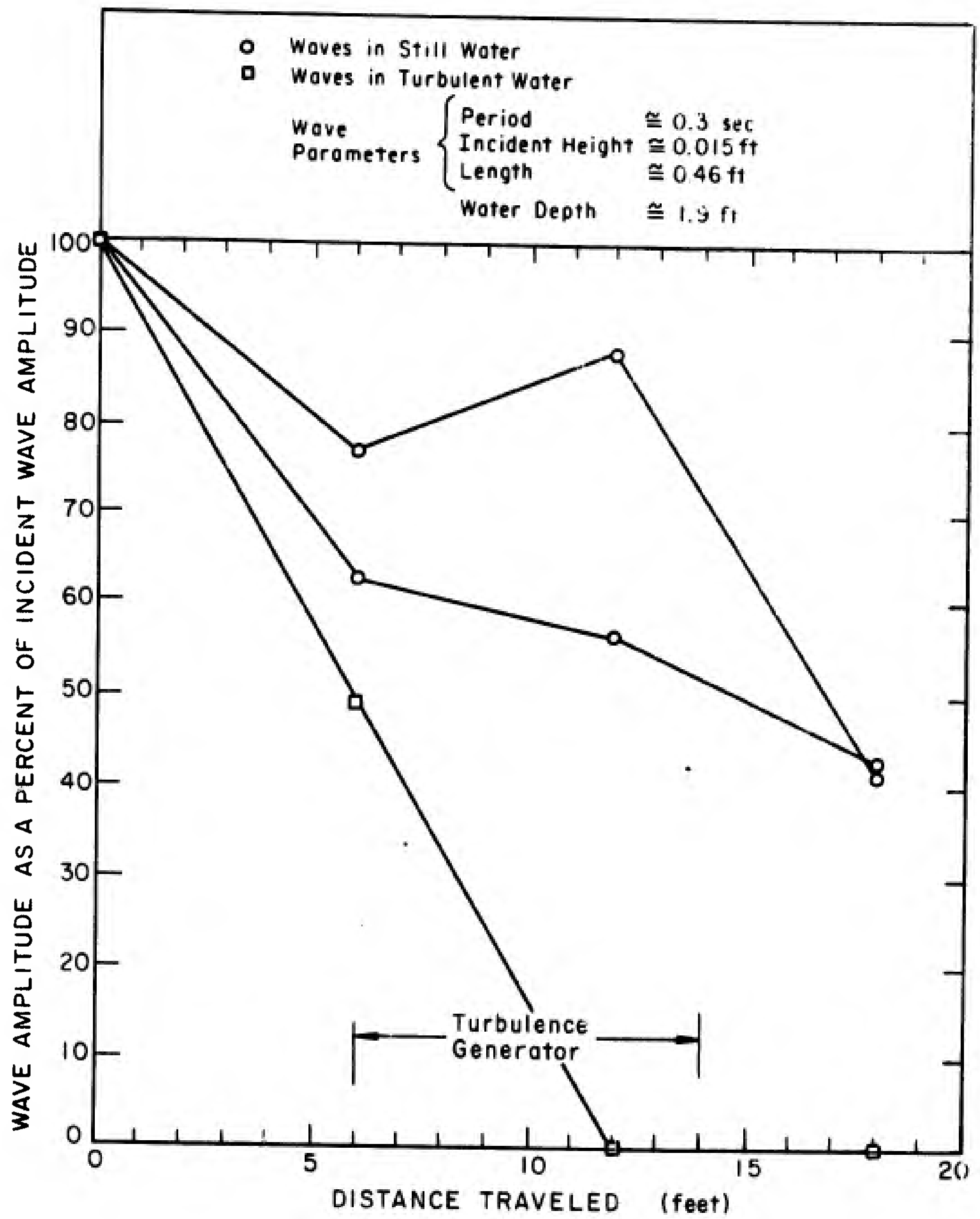

FIG. 5.21 ATTENUATION OF WAVES BY TURBULENCE

between a wave generator and reflected waves in a very short flume. As previously stated the cross waves in our flume appeared immediately when the wave generator was turned on; furthermore, the end of the flume was 50 feet away and equipped with a rubberized hair wave energy absorber, so reflections would be negligible even if enough time had elapsed for the wave to travel to the end and back.

Recently, Mahony, 1971, applied the theory of resonant interactions to cross waves in a channel of infinite length. He found that when the primary waves are shorter than the width of the channel, cross waves of a frequency of half that of the wave generator may appear. Although viscous dissipation is neglected in Mahony's analysis, he notes that the growth rate of the cross waves must exceed the decay rate; therefore, there is a minimum amplitude of wave-generator motion below which cross waves will not be generated Furthermore, he argues that this minimum amplitude will be significantly greater for an infinitely long channel than for a short, closed-end channel, but this seems to contradict his other statement that cross waves originate in the field close to the wave maker - how the end of the channel being moved from 20 feet to 200 feet, or to infinity can affect the field close to the wave maker to require a larger amplitude of excitation as the end is moved away from the wave generator is not clear. One should keep in mind that the cross waves we observed appeared immediately - not after reflections could alter the flow.

Mahony could find no resonant interaction which would transfer energy from the primary waves to the cross waves in the absence of a wave maker; also he notes that "cross waves do not appear to have been observed in naturally generated wave systems." All of this supports Mahony's theory that cross waves originate in the field close to the wave generator; but cross waves can be seen in wind waves generated in a wind-wave tunnel in the laboratory. Perhaps this would not be considered "naturally generated". In any case many questions regarding the generation, propagation, and dissipation of cross waves remain to be answered. Mahony has shown how a pure cross wave mode may be generated in the forced field close to the wave generator. How such a pure cross wave mode can propagate energy down the channel is not clear. It may even be that viscous effects at the side walls enable cross waves to obtain energy from the primary progressive waves.

We found that if the amplitude of the wave generator was continually increased, eventually waves with crests normal to the face of the plunger would form. The same thing happened if the amplitude was fixed and the frequency was increased continuously - eventually these waves would appear. Once these waves formed the wave generator no longer produced the progressive waves. Tatsumo, Inoue and Okabe, 1969, reported such waves appearing with crests radial to a vertically oscillating cylinder. As in the case of the cross waves studied by Mahony, 1971, the frequency of these waves is one half that of the motion of the wave generator. Thus we find: 1) At low enough amplitude or frequency pure progressive waves are generated. 2) At intermediate amplitude or frequencies progressive waves and cross waves propagate together. 3) At high amplitudes or frequencies the cross waves dominate and they do not seem to propogate away from the wave generator.

There is no easy way to avoid cross waves in our system. Mahony, 1971, states that there is no simple way to avoid generating cross waves unless one could invent a wave generator with no bulk mobement of the fluid and no surface displacement. Therefore we built six-pronged resistance probes to average the wave height across the width of the flume. A drawing of this probe is shown in Fig. 5.22. This averaging of the wave height served the purpose of reducing scatter sufficiently to enable the pattern of the wave damping to be clearly seen. This idea that the cross components can be averaged away assumes that the interaction of the progressive waves and the cross waves is not a major factor in determining the rate of attenuation of the progressive waves either in calm or in turbulent water.

Mahony, 1971, does not discuss the effect of changing the width of the flume. Many model studies are performed in wide basins with waves very much shorter than the width and apparently the cross waves do not modify the progressive waves enough to create a problem. Either they are not generated or they are

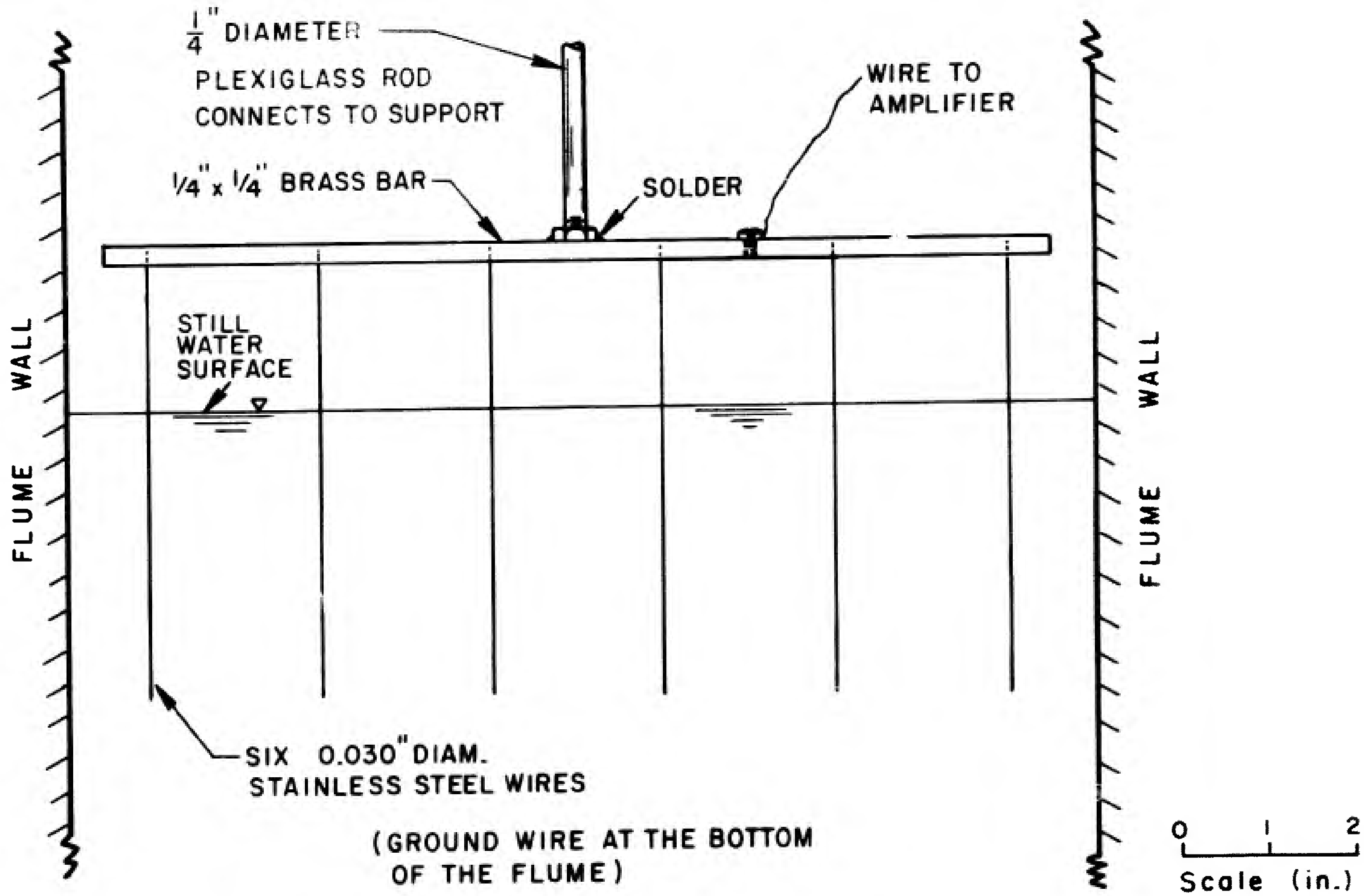

FIG. 5.22 SIX-PRONGED RESISTANCE PROBE

damped out before they can travel across the width of the basin.

5.3 Analysis and Interpretation of the Wave Date

Various wave records were taken in the 1-ft flume, both with and without turbulence. The waves generated by the plunger travel past four wave gages spaced 6 feet apart and were recorded as analog signals on a chart recorder. At the same time, these analog signals were sampled for a period of 18 sec. at a rate of 58.6 samples/sec/wave gage by the digitizer, converted to binary numbers and recorded on magnetic tape. Figure 5.31 shows the mechanical drive for the wave generator, the chart recorder, the amplifiers and the analog-to-digital converter. Spectral analysis (using a Fast-Fourier Program see Appendix B) of this digital data then separated the low-frequency surface disturbances caused by the turbulence generator from the short, higher frequency waves generated by the wave generator. The wave height is then directly proportional to the square root of area under the spectral spike found at the frequency of the wave generator. This wave height data for the various frequencies is given in Appendix C.

Even with the use of the multi-pronged averaging probes there was considerable scatter in the data, and for wave lengths between one and two times the width of the flume the wave height either decreased only slightly with distance or even showed an apparent increase. Therefore, only the data for waves shorter than the width of the flume is included in the analysis below.

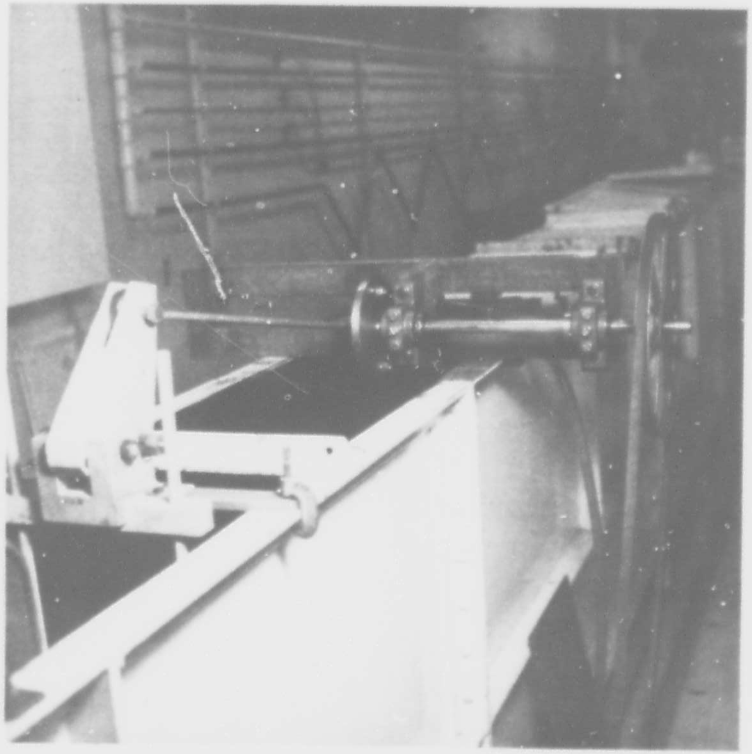

Mechanical Drive for Wave Generator in 1 Foot Flume

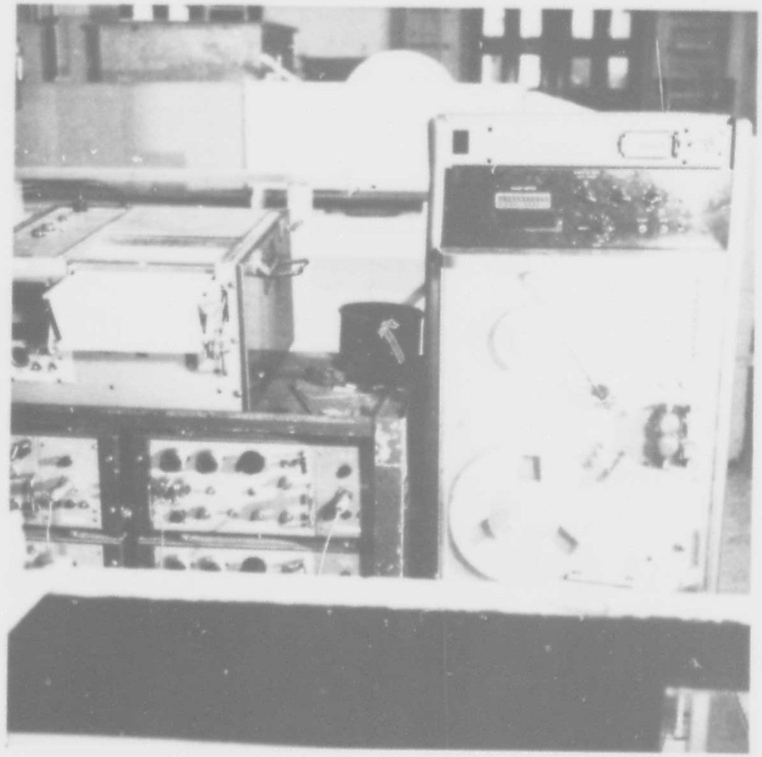

Chart Recorder, Amplifiers and Analog-to-Digital Converter

Figure 5.31

The four wave gages were located above and exactly spanning the turbulence generator at x = 8, 14, 20, and 26 feet where x is the distance away from the wave generator. In the first analysis h(11), the value of the wave height at x = 11 ft; was estimated to be the average of the values at x = 8 ft. and x = 14 ft. and h(23) was estimated to be the value at x = 23 ft. by averaging h(20) and h(26). Then h(11) is the incident wave height and h(23) is the attenuated wave height after traveling a distance of 12 feet.

These values of wave height were analyzed in various ways to see the dependence on parameters such as wave length, wave celerity, wave height, etc. Because both the wave height and the speed appeared to be important parameters, the proposal of Bowden, 1950, that the kinematic viscosity in the wave dissipation equation be replaced by an eddy viscosity term, proportional to the product of the wave height and the celerity was followed. The rate of dissipation by molecular viscosity as given by Lamb, 1932 (p. 623) is:

$$D = 2\rho \nu k^3 c^2 h^2 \tag{5.31}$$

where; D is the rate of wave energy dissipation per unit area, ρ is the density of water, k is the wave number equal to $2\pi/L$, L is the wave length, and ν is kinematic viscosity. When ν is replaced by c h :

$$D_B = K_B \, 2\rho \, k^3 \, c^3 \, h^3 \tag{5.32}$$

where : K_B is some constant to be determined.

Using the values obtained from the flume data of the incident and the attenuated wave heights:

$$D_M = \frac{\rho g (h_i^2 - h_{i+\Delta x}^2) C_G}{2 \Delta x} \tag{5.33}$$

where: D_M is the measured rate of wave energy dissipation per unit area, g is the acceleration due to gravity, h_i is the incident wave height, $h_{i+\Delta x}$ is the attenuated wave height after the wave has traveled a distance Δx , and C_G is the group velocity of the wave equal to half the phase speed for deep-water gravity waves.

The values of D_B (assuming $K_B = 1$) and D_M for the experiments in still and turbulent water are plotted in Fig. 5.32. Although considerable scatter is present, it is clear that the turbulence greatly increases the rate of wave energy dissipation. One reason that the data is not spread very evenly over the whole range of dissipation rates in Fig. 5.32 is that in turbulent water the steeper waves were greatly attenuated before they could travel to the first gage; therefore, there is more data for low amplitude waves in turbulent water than there is in still water.

The value of K_B in Eq. 5.32 is equal to:

$$K_B = \frac{D_M}{2 \rho k^3 c^3 h^3} \tag{5.34}$$

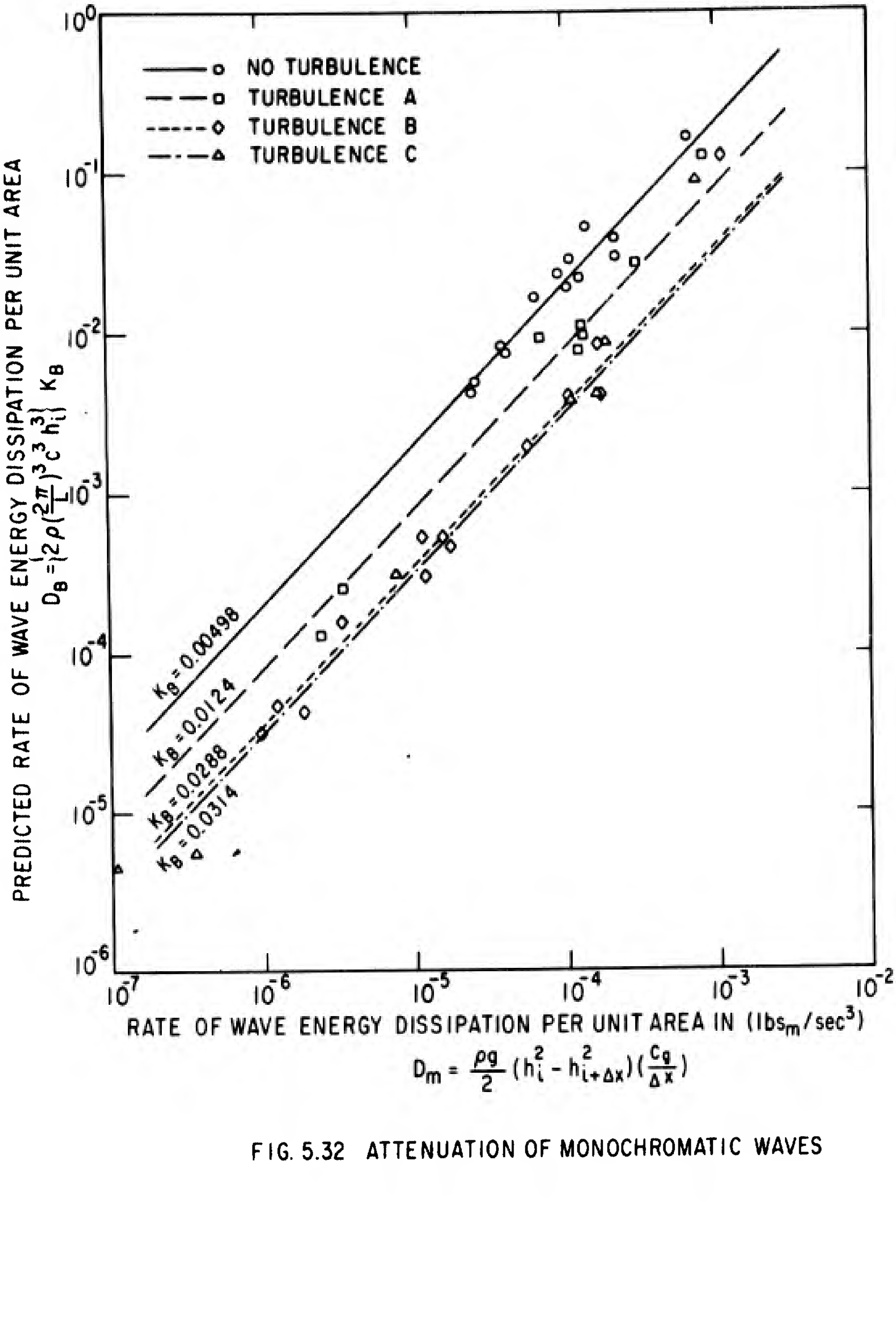

FIG. 5.32 ATTENUATION OF MONOCHROMATIC WAVES

The average value, $\overline{K}_B$, and the standard deviation, σ_{KB} , for the points plotted in Fig. 5.32 are shown in Table 5.31.

TABLE 5.31

Condition of Water	$\overline{K}_B$	σ_{KB}	$\sigma_{KB}/\overline{K}_B$ in per-cent	Number of points in sample	$\overline{K}_B / \overline{K}_B$ for still
Still Water	4.98×10^{-3}	1.19×10^{-3}	24%	13	1.
Turbulence A	12.4×10^{-3}	4.08×10^{-3}	33%	8	2.5
Turbulence B	28.8×10^{-3}	9.91×10^{-3}	34%	13	5.8
Turbulence C	31.4×10^{-3}	16.7×10^{-3}	55%	8	6.1

The wave height data was also analyzed in another way using exponential regression. If the waves decay exponentially then:

$$h(x) = A\ e^{BX} \tag{5.35}$$

where: A and B are constants calculated by the least squares method and e is the natural log base. The value of A, B and the wave heights calculated from the above equation are given in Appendix C. As before the incident wave was taken to be h(11) and the attenuated wave to be h(23); these values were then used in Eqs. 5.32 and 5.33 to calculate the rate of wave energy dissipation. The results are plotted in Fig. 5.33. This

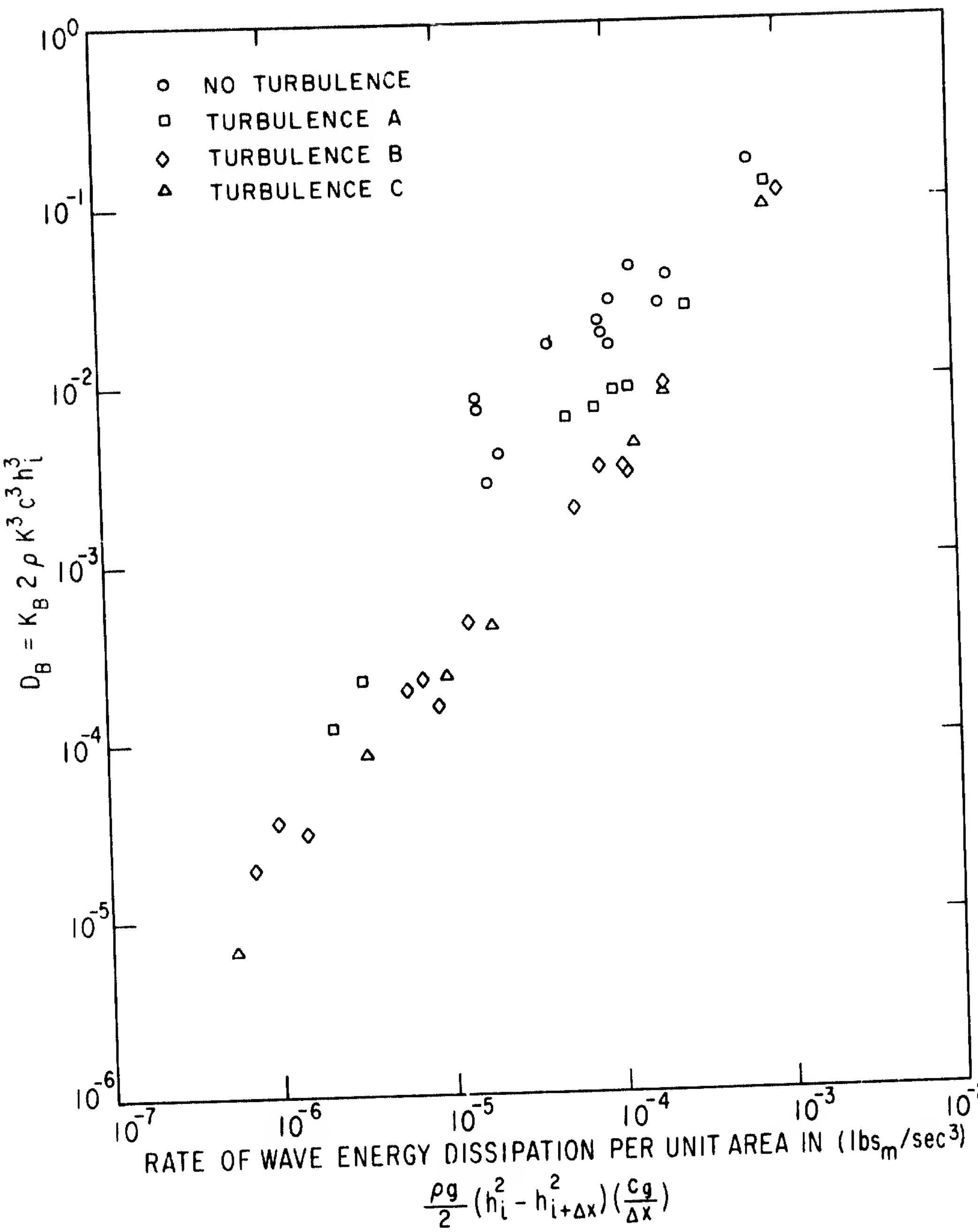

FIG. 5.33 ATTENUATION OF MONOCHROMATIC WAVES
(CALCULATING USING EXPONENTIAL REGRESSION)

figure is very similar to Fig. 5.32. The same pattern of increased rate of energy dissipation for the various turbulent conditions is seen; however, there is no marked improvement in the scatter.

Previously in the survey of literature (Chapter 2) the experiments of Paquin, 1962, were mentioned. His data was used to calculate D_B and D_M by Eqs. 5.32 and 5.33. The results are plotted in Fig. 5.34, although the rate of attenuation is generally greater in the turbulent water the scatter is very great. Paquin measured the wave heights at only two points and many of the waves were shorter than the width of the flume; therefore, it seems likely that he had cross waves in the flume. His wave gages were far enough apart that the wave height was always less at the second gage, so he probably did not suspect cross waves. Furthermore, cross waves of low amplitude are not easily noticed by eye when they are superimposed on a progressive wave train.

Another proposal mentioned in Chapter 2 is that of Dobrokinoskii, 1947. He proposed replacing the kinematic viscosity in Eq. 5.31 by the following expression:

$$N_D = \frac{\pi \kappa^2 h^2}{18\,T} (1 - \pi^2 \delta^2)^3 \qquad (5.36)$$

where: T is the wave period, δ is the wave steepness equal to h/L, and κ is the Von Karman constant equal to 0.4. Doing

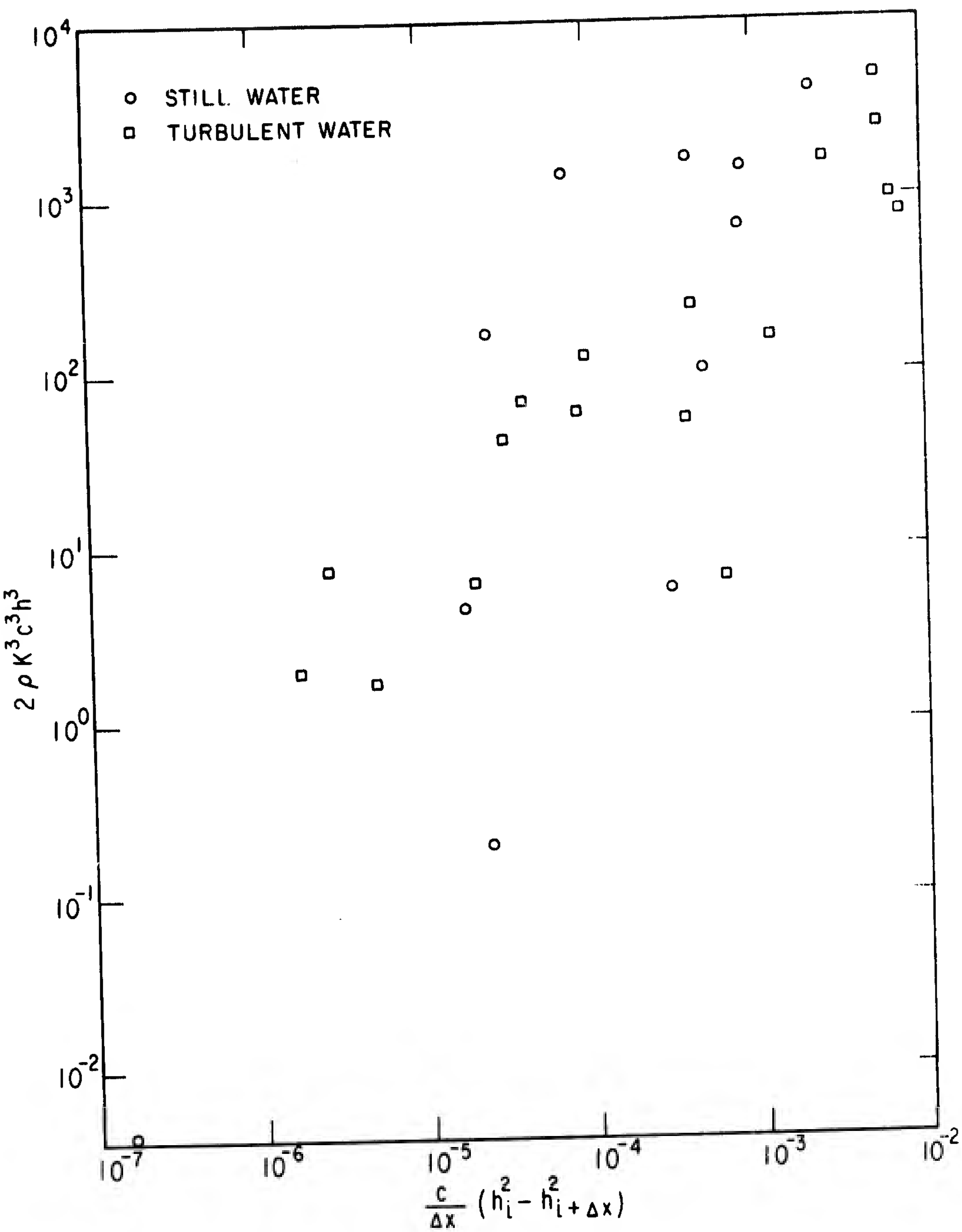

FIG. 5.34 ATTENUATION OF WAVES
(Data of J.E. Paguin)

this gives:

$$D_D = K_D\{2\rho k^3 c^2 h^2 (1 - \pi^2 \delta^2)^3 \kappa^2 \frac{h^2}{T} \frac{\pi}{18}\} \tag{5.37}$$

A plot of D_D versus D_M is shown in Fig. 5.35. This can be compared to Fig. 5.32. In view of the difference between Eqs. 5.32 and 5.37, there is remarkable similarity between the two graphs; however, there is greater scatter and separation of the different turbulence conditions in Fig. 5.35.

If one compares the eddy viscosity terms (N_B and N_D) proposed by Bowden and Dobrokinoskii, (Eqs. 2.12 and 2.11 or 5.36) they have in common that the eddy viscosity is inversely proportional to the period T; however, N_B is directly proportional to L and h, whereas N_D is proportional to $h^2(1 - \pi^2\delta^2)^3$. If the wave steepness, δ, is small N_D is approximately proportional to h^2/T; in other words, N_D is approximately proportional to $N_B\delta$. Therefore, for data not having a great range of values for δ, either Bowden's or Dobrokinoskii's eddy viscosity may appear to fit the data equally well.

In summary we find that monochromatic waves of high frequency and height are dissipated the fastest and long, low waves are dissipated the slowest. Furthermore, a short period gravity wave losing energy at the same rate as a long period wave will disappear much sooner because the short wave is transmitting energy at a much slower rate (the wave energy

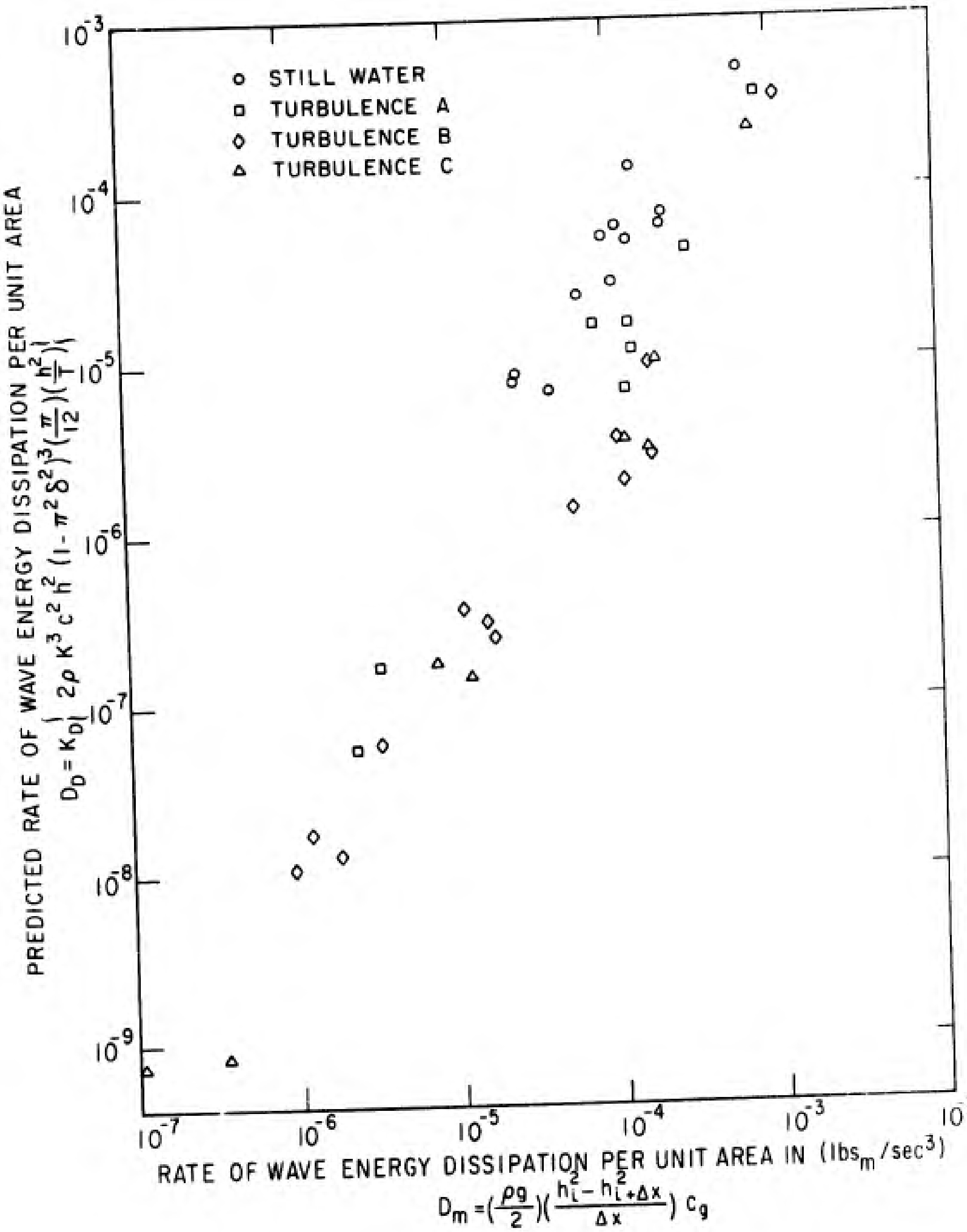

FIG. 5.35 ATTENUATION OF MONOCHROMATIC WAVES

being transmitted at rate equal to the group velocity). This confirms some of the observations of ship wakes mentioned in Chapter 1 and answers some of the questions raised there. Turbulence is an important factor in attenuating waves, especially waves of high frequency and height. The rate of attenuation of waves in Turbulence B and C was very nearly equal; although, the intensity of turbulence in Turbulence C was found (Chapter 4) to be greater overall and particularly for turbulent fluctuations of a scale less than 4 inches. This implies that the scale of turbulence is an important factor, but if the scale of the turbulence is much smaller than the wave length an increase in turbulent intensity does not cause a significant increase in the rate of wave attenuation. The intensity of turbulent fluctuations is an important factor if the scale is large enough to be comparable to the length of the waves. This is shown by the significant increase in rate of wave energy dissipation when the data for Turbulence B and C are compared to those of Turbulence A---keeping in mind that the intensities of turbulent fluctuations for scales of motion longer than 4 inches were found (Chapter 4) to be much greater in Turbulence B and C than in A.

One question which merits further study is: What becomes of the energy lost by a wave moving in turbulent water? In some instances very small increases in wave energy developed in the side band frequencies adjacent to the spectral peak of the monochromatic wave after passing through the turbulent zone;

however, these increases could only account for a very small fraction of the loss to the incident monochromatic wave. Although we have no direct evidence as yet, some of the wave energy no doubt adds to the turbulent energy. If this is so, it could be the explanation to the remarkable persistance of wakes.

Our results conflict with the theory of Boyev, 1971. His theory shows turbulence will cause attenuation only when the velocities of the turbulence are greater than the oribital velocities of the particles in the wave. Clearly higher (i.e. steeper) waves have higher orbital velocities and therefore should be less affected by the turbulence (or perhaps we should say that a smaller percentage of the particles in the turbulence will be traveling faster than the particles in the orbital wave motion.) Our study indicates that the steeper wave will lose energy faster than a less steep wave of the same length.

Some of the questions which motivated this study but which have not yet been answered concern wind waves. This is the subject of the next chapter.

6. WIND WAVES IN A TURBULENT FLOW FIELD

In this chapter the results of experiments in which air was blown over turbulent water to produce wind waves are described. Three turbulent conditions (A, B, and C) were generated by the paddle type generator described in Chapter 4.

All of the experiments were performed in the 1-ft. flume with a still water depth of 2-ft. The four single wire (resistance type) wave gages were located above and exactly spanning the turbulence generator at F = 5, 11, 17 and 23 feet, where F is the fetch length. Although the first five feet of fetch was not directly above the turbulence generator, we assume that the turbulence diffuses along the flume sufficiently that for the entire fetch the wind was blowing over turbulent water. At F = 0 the air entered at the flume from the top and was turned to the horizontal by metal vanes. At the far end of the flume (F = 65 ft.) the waves broke on a beach of metal shavings covered by rubberized hair. The mean free-stream wind speed was recorded by means of a pitot tube at F = 52 ft. The wave gages were recorded on a chart recorder and simultaneously digitized at the rate of 29.3 samples/sec/wave gage. In each of the digitized recording was begun 5 seconds after the start of the wind and all the records continued for a period of 100 seconds. Spectral analysis (see Appendix A for computer program) of the digital data was done for a frequency resolution of 0.299 Hz.

6.1 Wind Wave Theory and Definition of Terms

At the present time no wave prediction model exists which is sufficiently accurate under all wind and wave conditions; however, much progress has been made in this direction and at least the overall pattern of wave growth can be described qualitatively. Figure 6.11 shows a typical growth curve as proposed by Barnett and Sutherland, 1968. When the wind first blows over the water the wave height grows linearly for some distance; this is followed by a range of exponential growth. Further along the growth rate drops off and a maximum height is reached which is greater than the eventual equilibrium -- this is termed "overshoot". Some of the data presented by Barnett and Sutherland, 1968, show a decline in wave height to below the equilibrium value following the overshoot -- this is termed "undershoot" -- and because it occurs at a longer fetch than overshoot, not as much data is available to establish it as a general rule. As more data becomes available for long fetches it may even be found that the wave height oscillates somewhat about the equilibrium -- repeatedly overshooting and undershooting. An accurate definition of a growth curve such as Fig. 6.11 requires at each increment of fetch a wave record long enough to calculate the spectrum with a narrow confidence band. With this in mind, it is easy to see that a maximum or a minimum such as occurs in overshoot or undershoot could be missed if the wave gages are too few or improperly spaced.

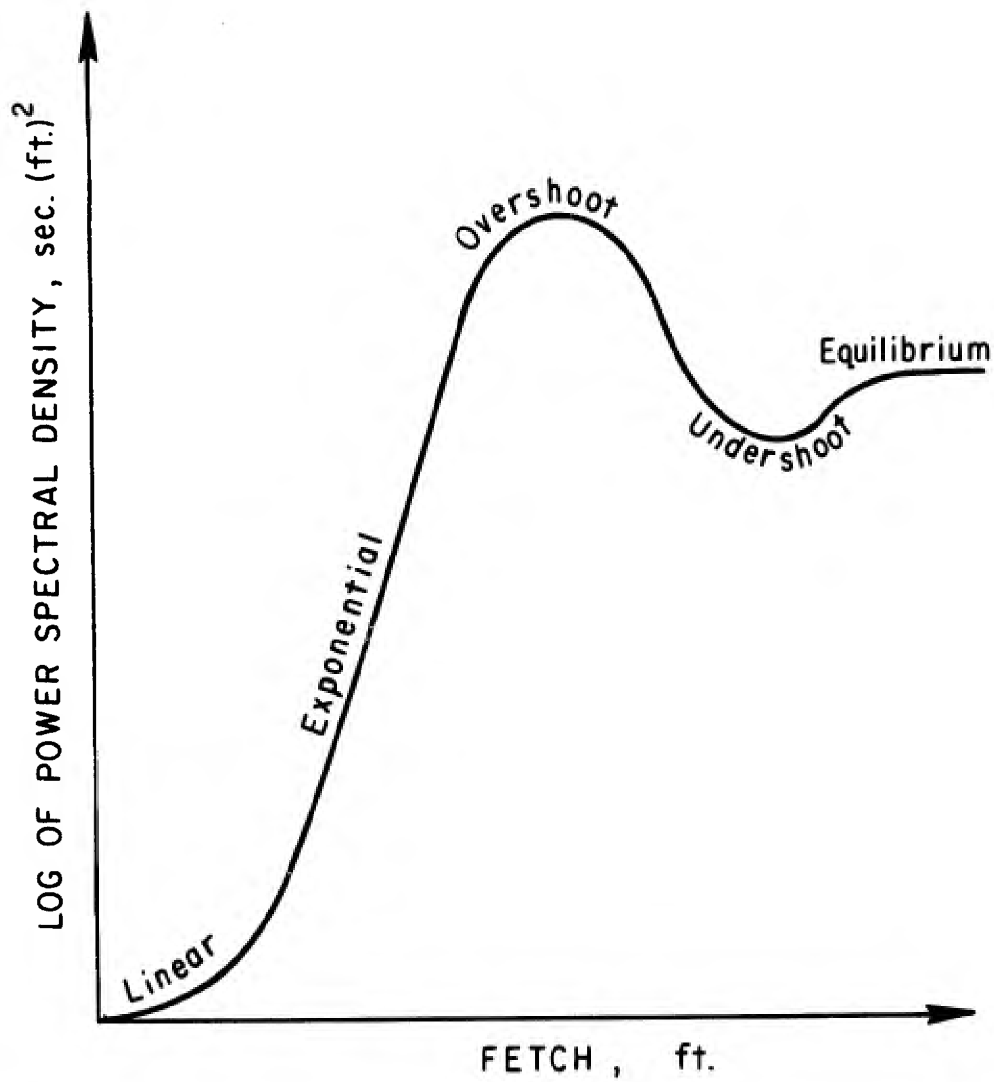

FIG. 6.11 WAVE HEIGHT GROWTH CURVE
(FOR A PARTICULAR FREQUENCY AND WIND SPEED)

Various theories have been developed to predict the wave-growth curve. Phillips, 1957, developed a theory which predicts a linear growth under certain conditions. Miles, 1957, and Phillips, 1966, published theories for the exponential portion of the growth curve assuming that the waves perturb the wind. These theories do not accurately predict measured data (see Sutherland, 1968, for a comparison of measured and predicted growth) and they require a great deal of knowledge of the wind conditions. For example the resonance theory of Phillips requires one to know the three dimensional spectrum of an atmospheric pressure fluctuations plus a turbulent scaling factor.

Hasselmann, 1962, has developed a nonlinear wave-wave interaction theory. When such energy transfer between waves is coupled with Phillips' and Miles' theories prediction is greatly improved. One of the problems with the nonlinear interaction theory is that it assumes that the wave-wave interactions are conservative. In an experimental study, Mitsuyasu, 1968, found that:

> "The dissipation mechanism remained unsolved, because the conservation of wave energy which should be a consequence of wave-wave interaction was not satisfied in the measured rate of energy transfer."

6.2 Effects of Turbulence on the Growth of Wind Waves

Before describing the differences between wave growth in still and in turbulent water it is necessary to be sure that the cause of the noted differences is in fact the presence of externally generated turbulence. As was mentioned in Chapter 4, an undesirable feature of our system of generating turbulence is the long low wave it produces. Phillips, 1966, states that there is no energy transfer between coexisting waves of different lengths as long as the wave lengths are not close to being equal. Certainly a monochromatic wave can encounter another monochromatic wave of significantly different length without transfer of energy; however, wind waves have some energy spread over a wide range of wavelengths and in addition to the possible wave-wave interaction the presence of the long wave might affect the air flow above. Mitsuyasu, 1966, studied a system of wind waves co-existent with longer oscillatory waves. He found that there will be no change in the wind wave spectrum as long as the steepness of the long regular waves is small. Table 6.11 shows the frequencies and steepnesses of the long waves made by the turbulence generator in the wind wave experiments.

TABLE 6.11

Turbulence Condition	Frequency of Turbulence Generator and Wave	Average Steepness h/L
A	0.57 cycles/sec.	.00019
B	0.92 cycles/sec.	.00082
C	1.52 cycles/sec.	.00076

In view of the very low steepness of the long turbulence generator waves, as shown in Table 6.11, and in view of

Mitsuyasu's results, we assume that these long, low waves do not significantly affect the growth of the wind waves.

Wave records were obtained for conditions of: 1) Still Water; 2) Turbulence A; 3) Turbulence B; 4) Turbulence C; for freestream wind velocities of 18 and 23 ft./sec. Spectra of wave heights for these are shown in Figs. 6.21 through 6.28. One of the clearest differences between the spectra in still and turbulent water is that the peak of the spectrum is at a lower frequency for the turbulent water. Also Turbulence C's spectral peak is at a lower frequency than B's and B's is at a lower frequency than A's.

In order to develop a wave growth curve like Fig. 6.11, one plots the spectral values for a single frequency versus the fetch. This has been done in Figs. 6.29 through 6.33 for frequencies 4.5, 6.0, 7.5, 9.0, and 10.5 Hz.

The only growth curve plotted which shows linear growth is that of frequency 4.5 Hz for the lower wind speed in Fig. 6.29. Sutherland, 1968, also found that he obtained linear growth only in the lower frequencies. All the other curves show exponential growth and at least some indication of overshoot. In most of the cases the exponential growth is higher when turbulence is present.

When overshoot takes place as in the 7.5 and 9.0 Hz curves (Figs. 6.31 and 6.32), it takes place at a lower fetch than in still water. Furthermore, Turbulence C has overshoot

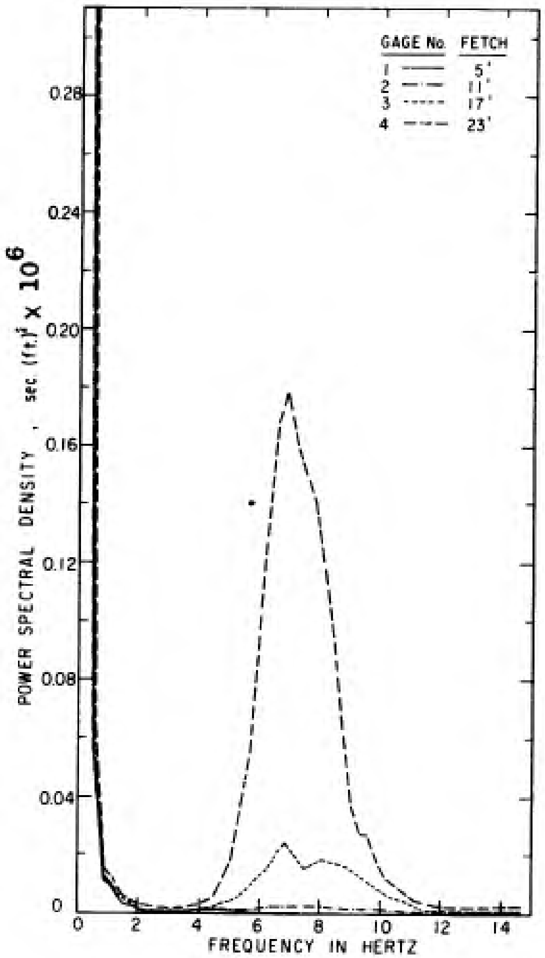

FIG. 6.21 WIND WAVE SPECTRA FOR INITIALLY STILL WATER
U_0 = 18 ft./sec.

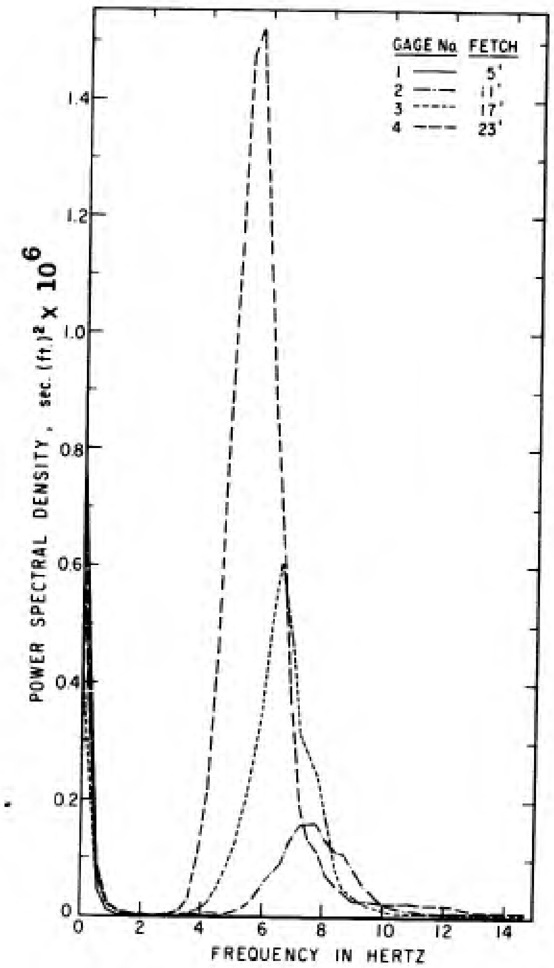

FIG. 6.22 WIND WAVE SPECTRA FOR INITIALLY STILL WATER
U_0 = 23 ft./sec

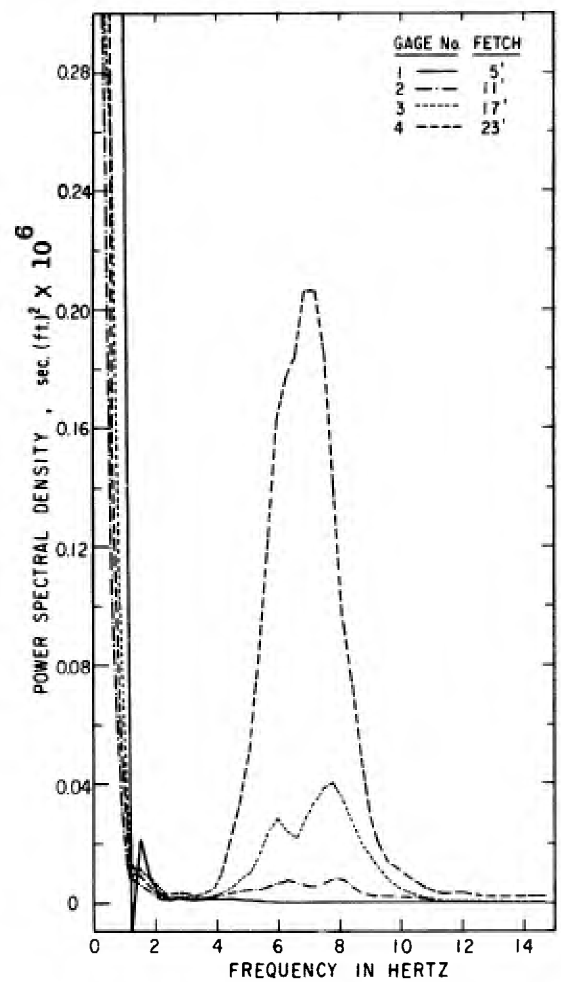

FIG. 6.23 WIND WAVE SPECTRA FOR TURBULENT CONDITION A
U_0 = 18 ft./sec.

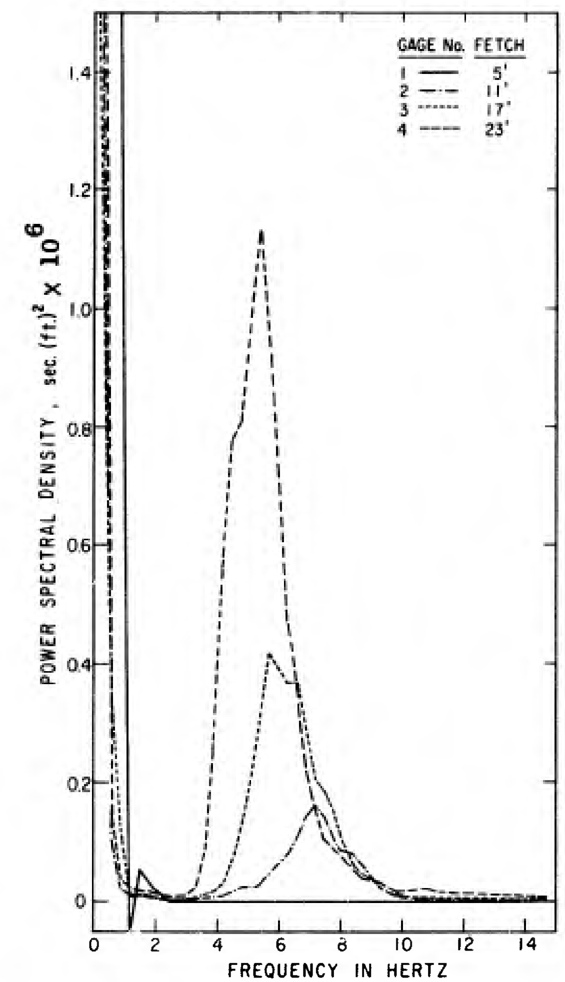

FIG. 6.24 WIND WAVE SPECTRA FOR TURBULENT CONDITION A
U_0 = 23 ft./sec.

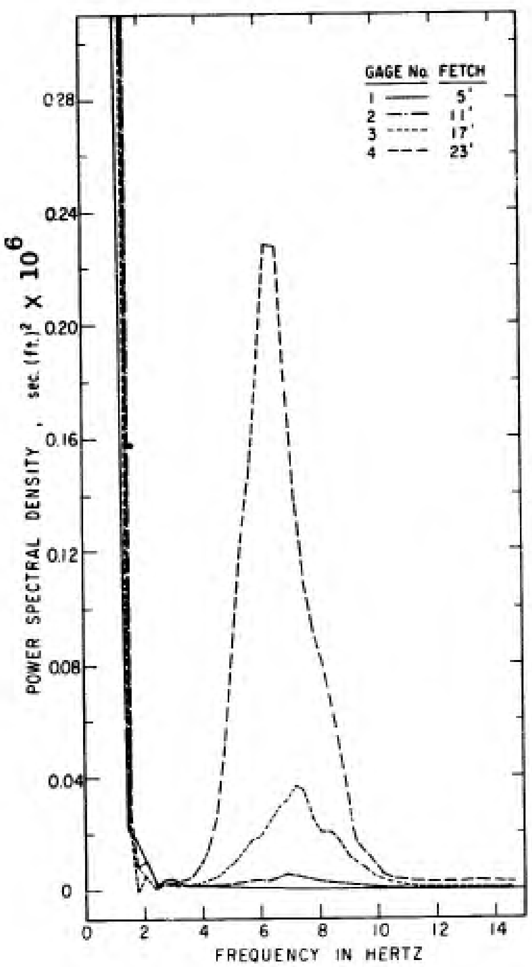

FIG. 6.25 WIND WAVE SPECTRA FOR TURBULENT CONDITION B
U_0 = 18 ft./sec.

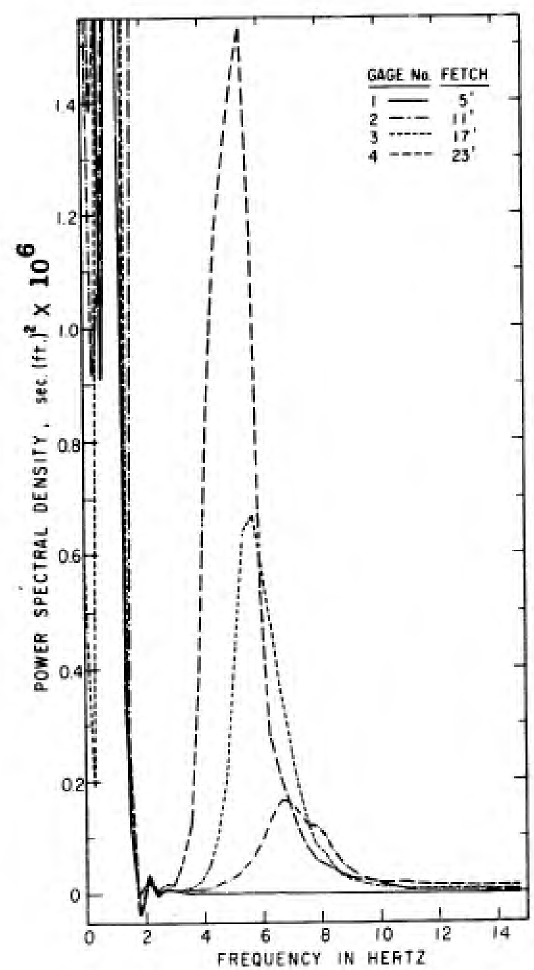

FIG 6.26 WIND WAVE SPECTRA FOR TURBULENT CONDITION B
U_0 = 23 ft./sec.

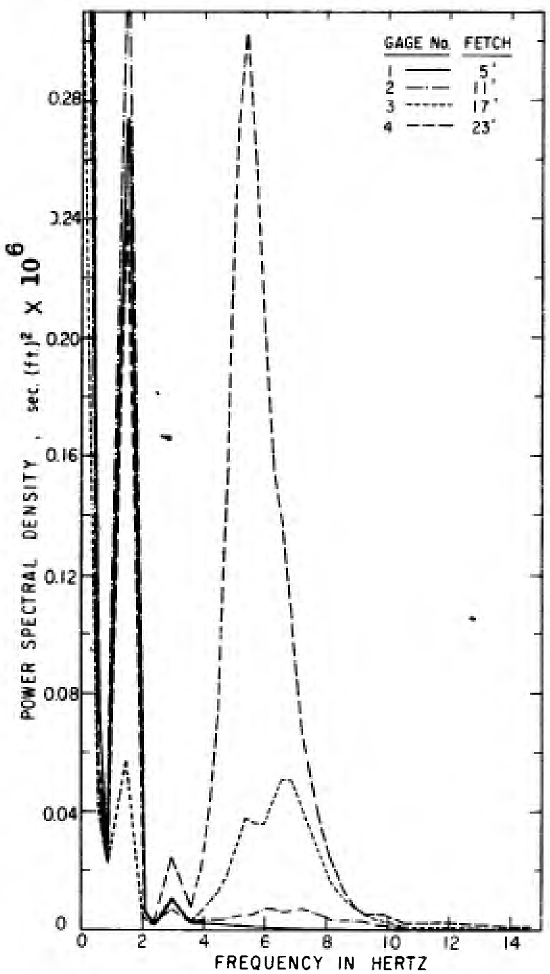

FIG. 6.27 WIND WAVE SPECTRA FOR TURBULENT CONDITION C
U_0 = 18 ft./sec.

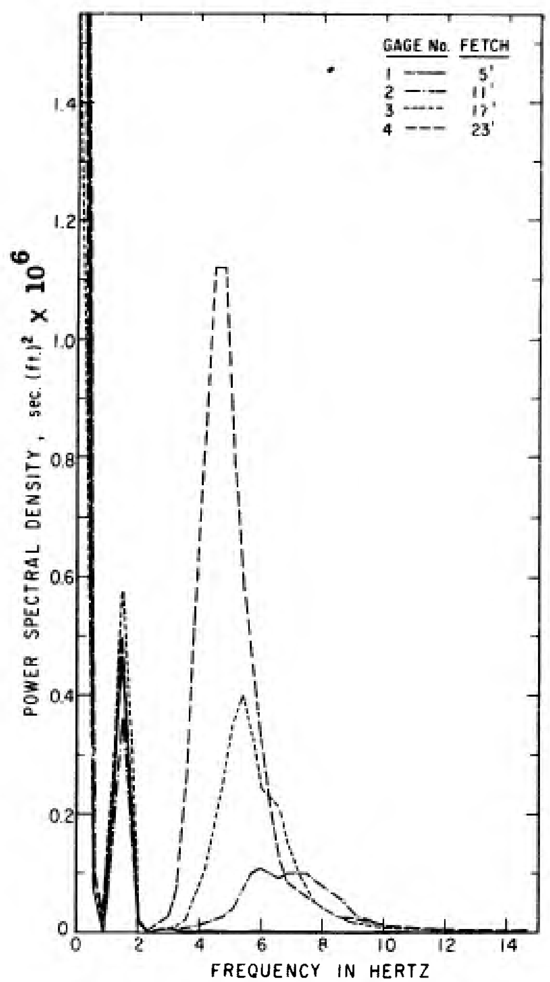

FIG. 6.28 WIND WAVE SPECTRA FOR TURBULENT CONDITION C
U_0 = 23 ft./sec.

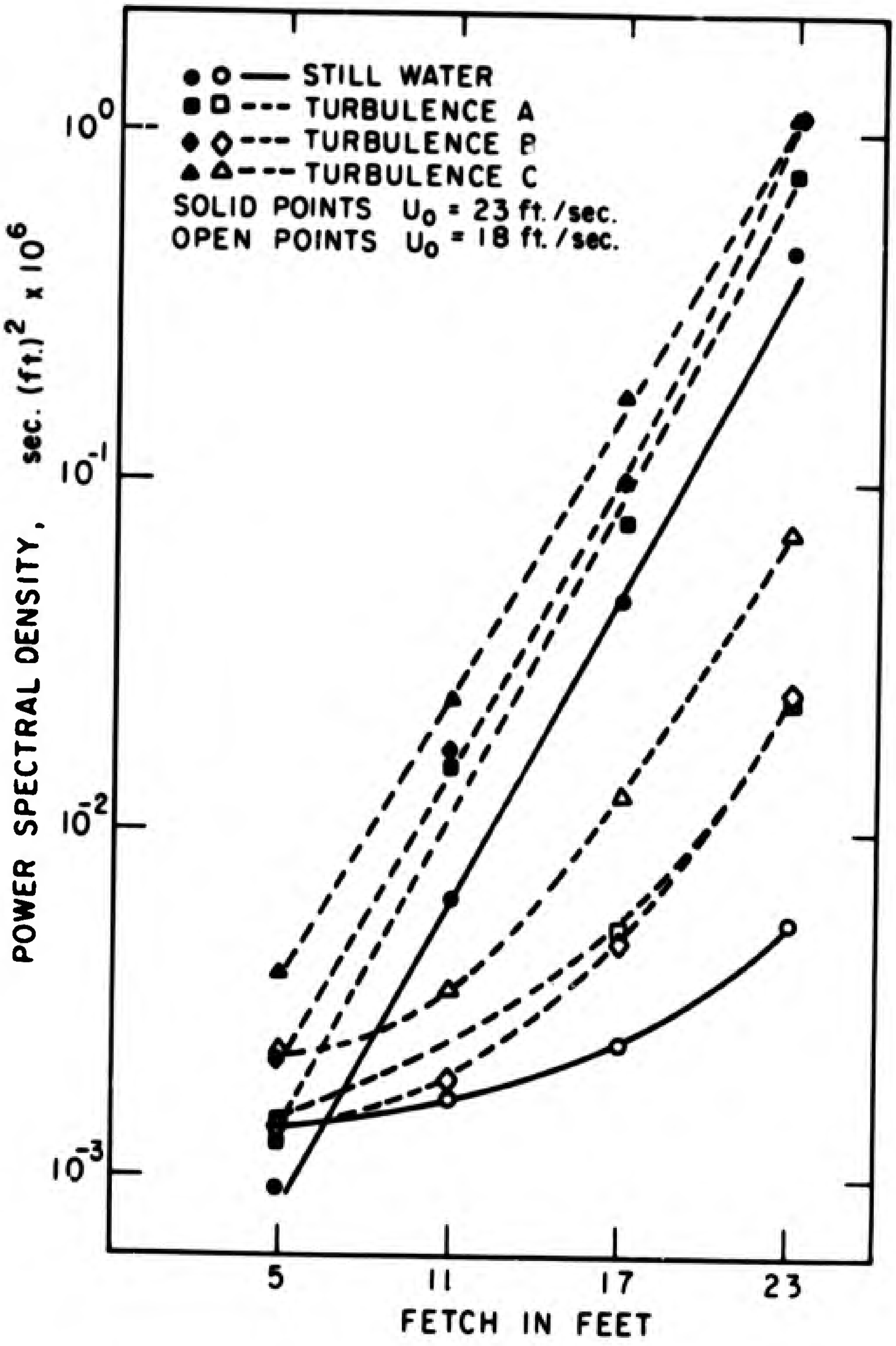

FIG. 6.29 WIND WAVES GROWTH CURVES (4.5 Hertz)

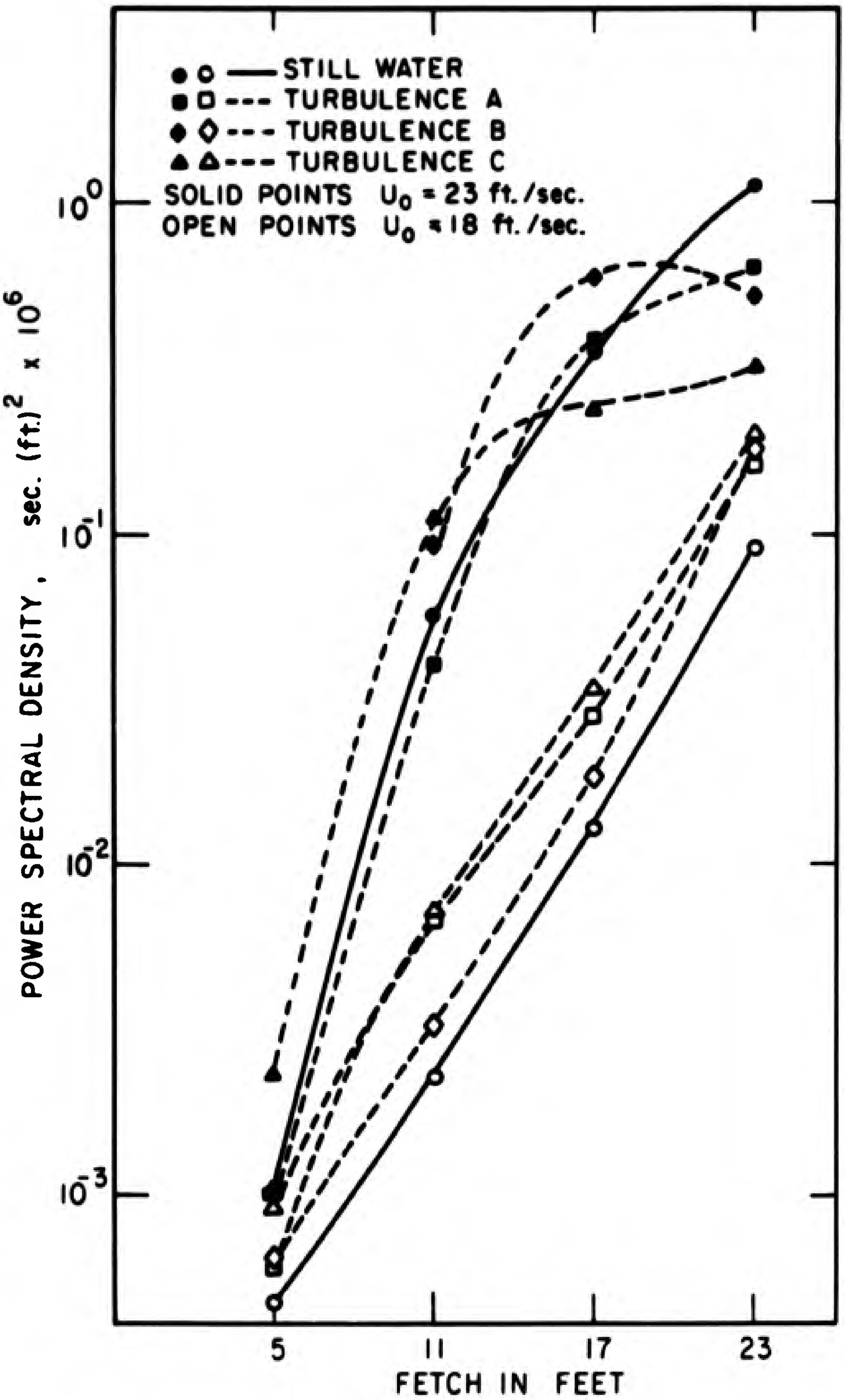

FIG. 6.30 WIND WAVES GROWTH CURVES (6.0 Hertz)

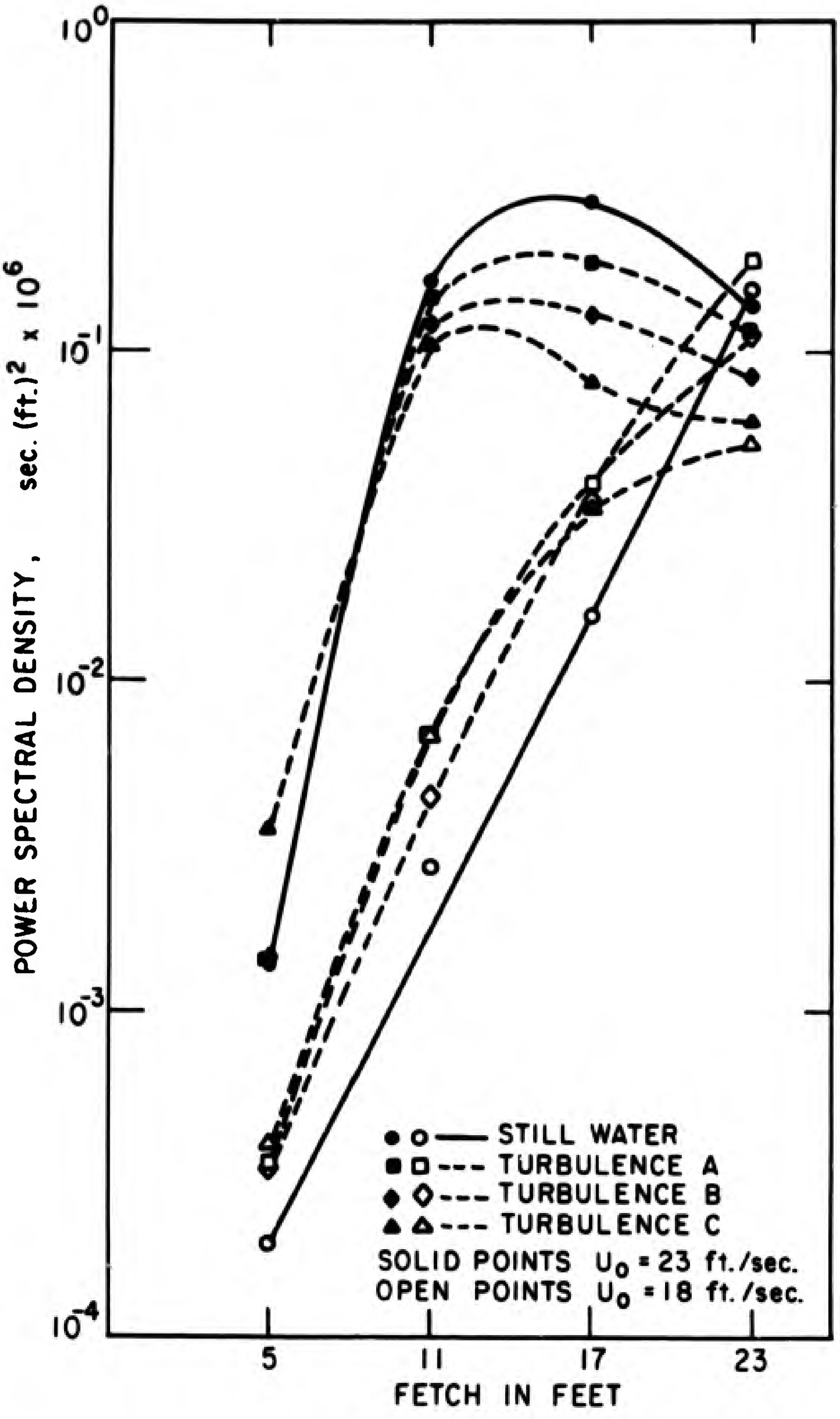

FIG. 6.31 WIND WAVES GROWTH CURVES (7.5 Hertz)

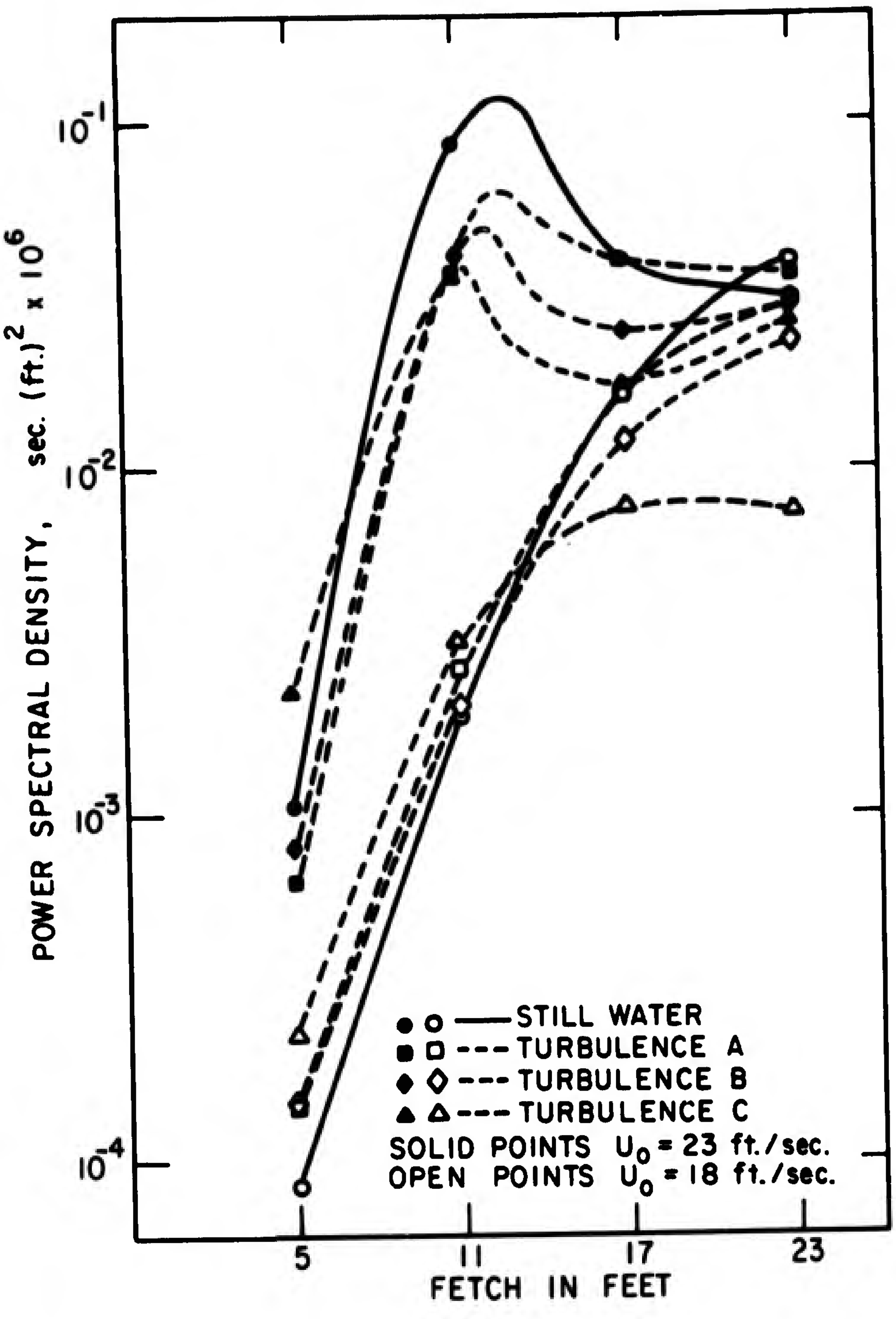

FIG. 6.32 WIND WAVES GROWTH CURVES (9.0 Hertz)

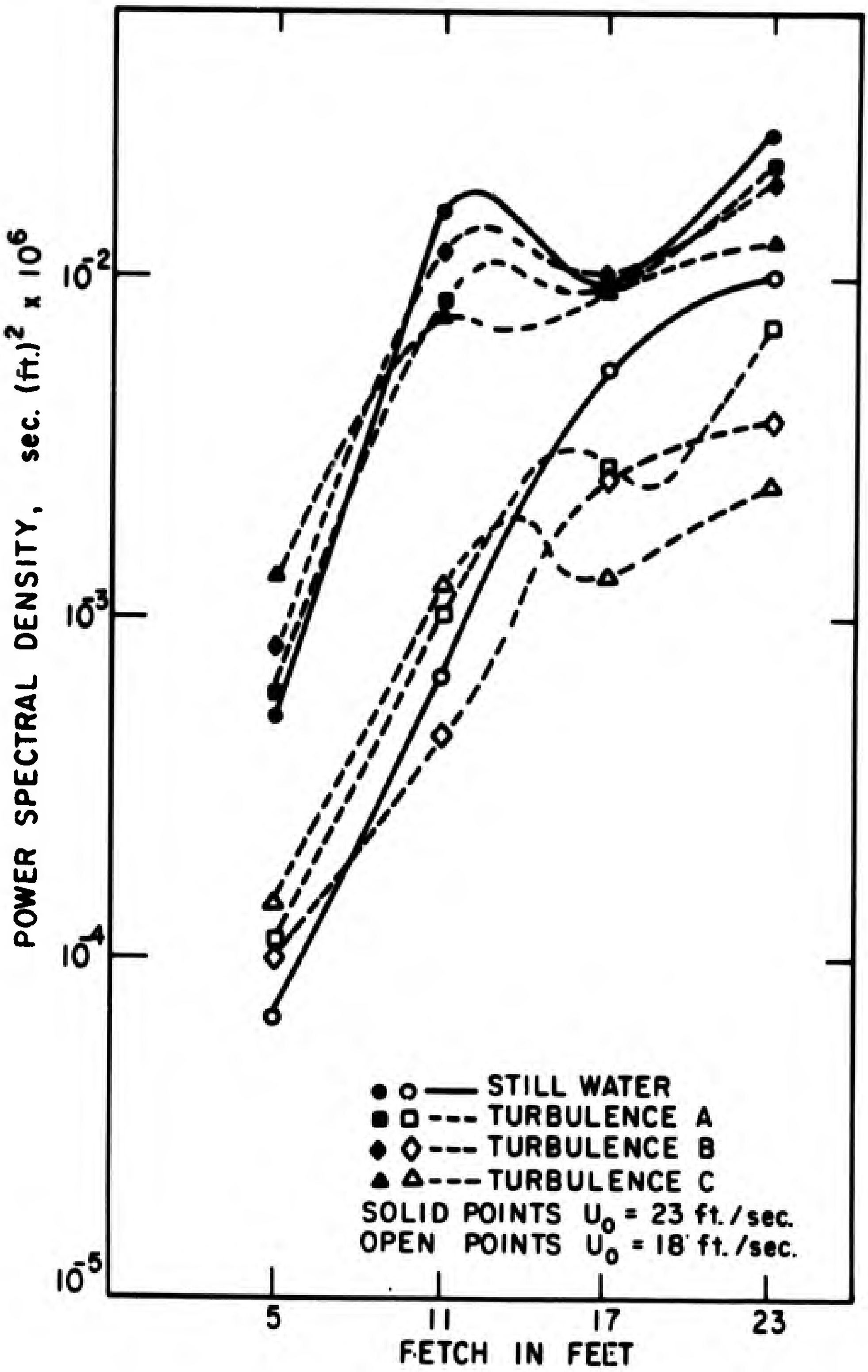

FIG. 6.33 WIND WAVES GROWTH CURVES (10.5 Hertz)

at a lower fetch than Turbulence B, and B has it at a lower fetch than A. The maximum value of these growth curves also follows a pattern -- arranged from highest to lowest in still water, Turbulence A, B, and C.

Whether or not the equilibrium values are also less than the still water is not clear, because fetch (roughly equal to the length of the turbulence generator) is not long enough to allow equilibrium to be reached. The growth curves for 10.5 Hz (Fig. 6.33) are much more erratic -- Sutherland, 1968, also found this to be the case for his higher frequency growth curves.

What is the explanation of these results? In the initial stages the turbulence may roughen the water surface and thus increase the wind drag; however, this does not seem sufficient to explain the shift of spectral peaks to lower frequencies and the decreased overshoot. The theory of wave-wave interactions predicts that an infinitesimal lower frequency wave receives energy from a finite wave of slightly higher frequency. Apparently turbulence aids in this transfer.

One possible way in which this could be is that for the waves studied here the turbulence had components whose scale was close to that of the wave lengths; this turbulence could generate very small yet finitely high waves of the right length to receive energy of nonlinear wave-wave interaction with well developed waves of higher frequency.

The spectra of surface disturbances caused by the turbulence in the absence of wind are shown in Figs. 6.34 through 6.36. Note that the scale has been magnified by a factor of 200 times the scale of Figs. 6.21 - 6.28. These spectra shows that the surface disturbances increase from Turbulence A to B to C. These surface fluctuations are in part due to the turbulence, but higher harmonies of the previously mentiored long wave and mechanical vibrations from the turbulence generator may also be present.

In order to show more clearly and concisely the pattern of wave growth a normalized curve can be drawn. To normalize, the fetch is divided by the wavelength and the power spectral density is divided by the maximum power spectral density achieved in overshoot in non-turbulent water. Of course, such a curve can only be drawn for those frequencies which clearly exhibit overshoot at fetches where data is available (this rules out low frequency waves) and for which an accurate estimation of the maximum power spectral density can be made (this rules out high frequency waves where the specing of the wave gages is large in terms of the wavelength). These conditions are adequately fulfilled only at the higher wind speed of 23 ft./sec. in the frequency range 6.6 to 8.1 Hz. The normalized growth curve for these conditions is shown in Fig. 6.37 and from this curve the following conclusions can be drawn: 1) By the

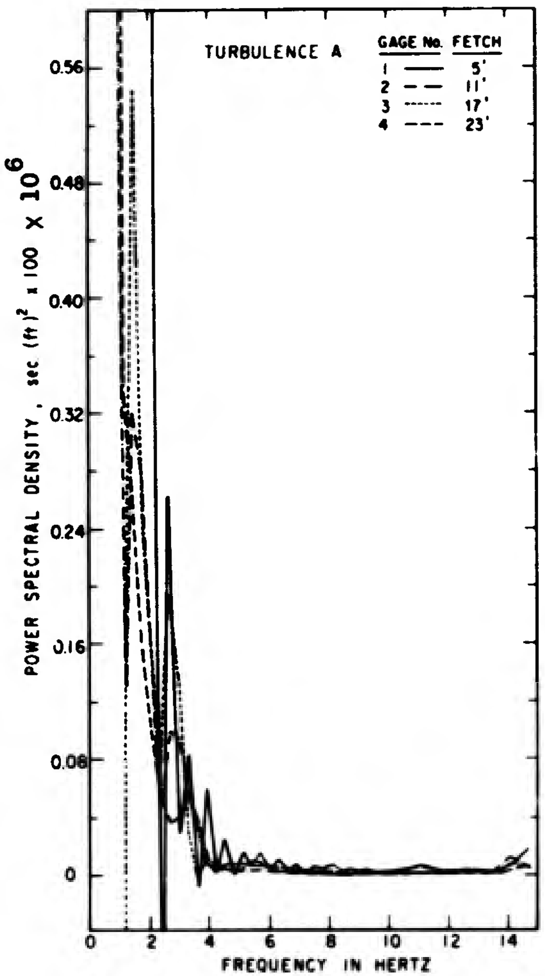

FIG 6.34 SPECTRA OF WATER SURFACE FLUCTUATION CAUSED BY THE TURBULENCE GENERATOR

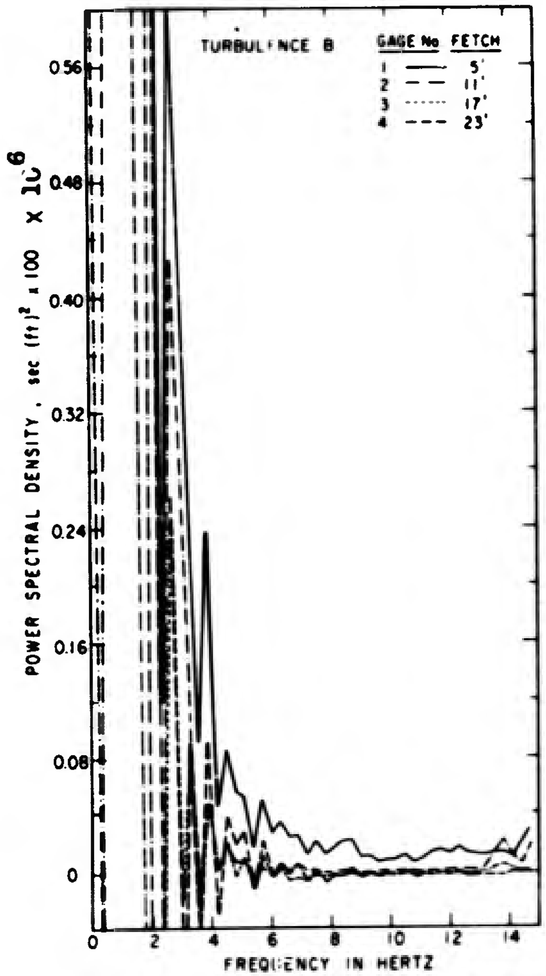

FIG 6.35 SPECTRA OF WATER SURFACE FLUCTUATION CAUSED BY THE TURBULENCE GENERATOR

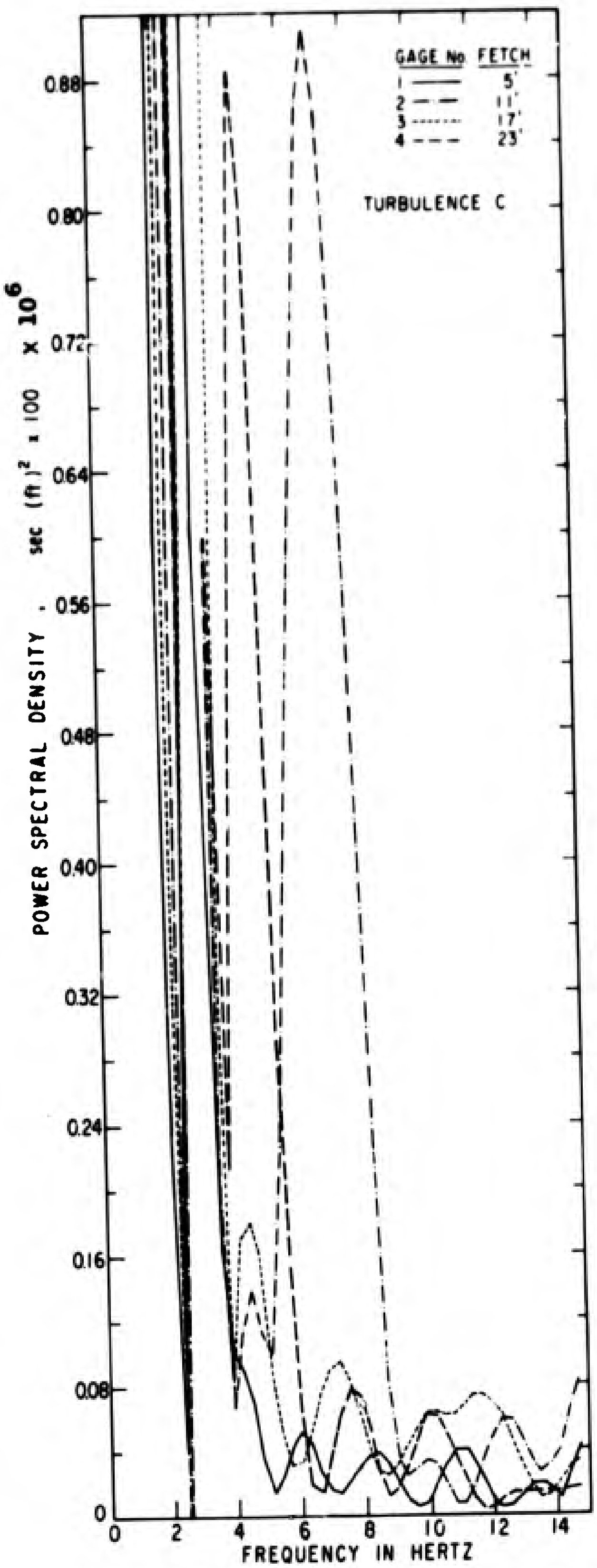

FIG. 6.36 SPECTRA OF WATER SURFACE FLUCTUATION CAUSED BY THE TURBULENCE GENERATOR

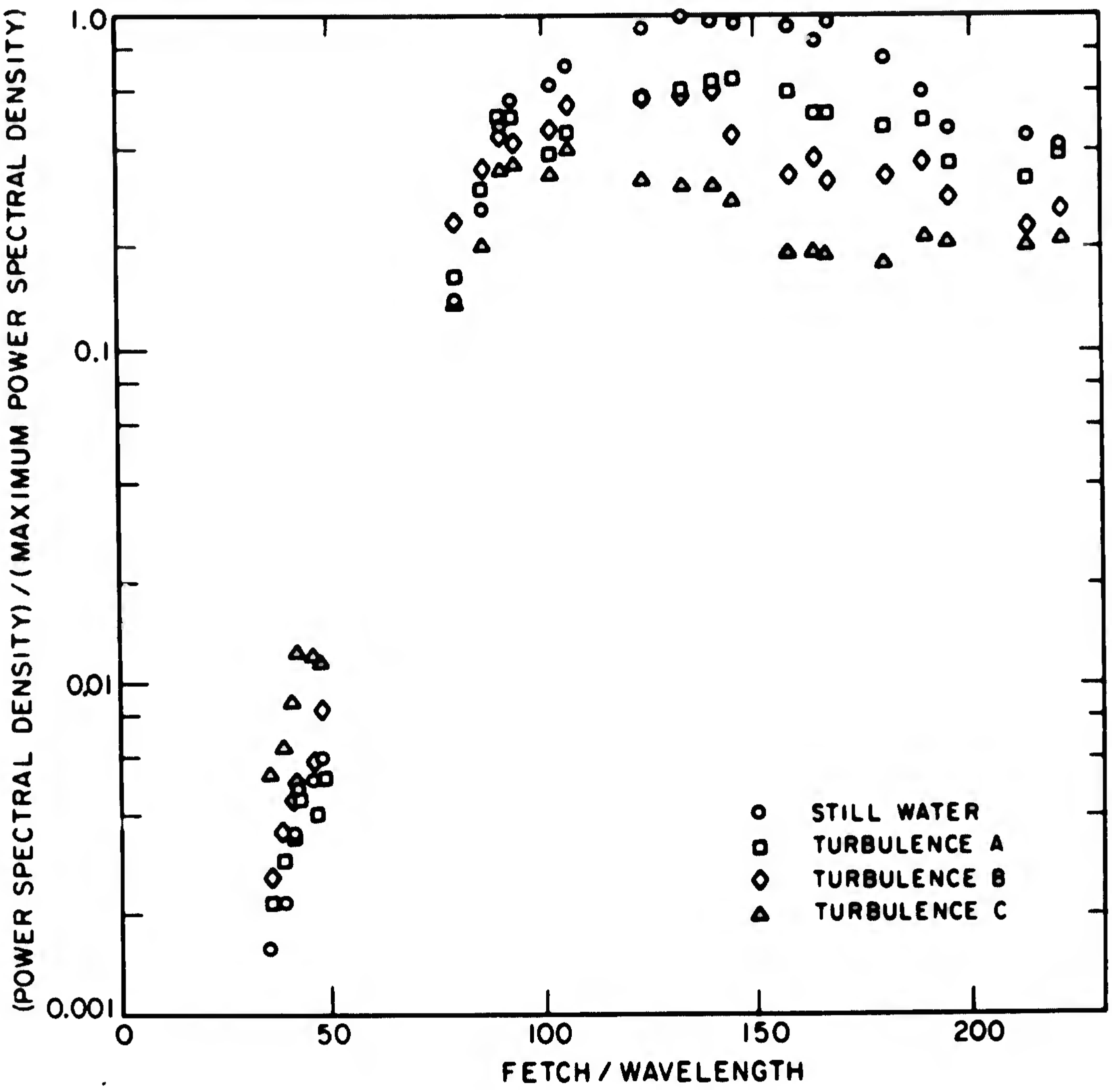

FIG. 6.37 NORMALIZED WIND WAVE GROWTH CURVES (U_0 = 23 ft./sec.)

time exponential growth is achieved the waves in turbulent water are higher than those found in initially calm water and in general those waves in turbulence C are higher than those in B which in turn are higher than those in A; 2) The waves in turbulent water tend to overshoot sooner than those in still water; 3) The maximum wave height achieved in overshoot is much less in turbulent water than in still water; 4) For the ranges of fetches observed here the wave height after overshoot remained lower in the turbulent water than in the still water and the waves in Turbulence C remained lower than those in B which in turn remained lower than those in A.

One outstanding difference between the results for monochromatic wave attenuation and those for growth of wind waves is that the rate of wave energy dissipation in Turbulence B and C was found (Fig. 5.32) to be roughly equal; whereas, the wind wave growth curves (such as those shown in Fig. 6.34) show that the effects of Turbulence C differ from those of B by at least as much as the effects of Turbulence B differ from those of A. One reason for this may be the difference in wave lengths. The wave lengths represented in Fig. 6.37 are all very short -- between 1 and 2 inches long, but the monochromatic waves shown in Fig. 5.32 range in length from 2 to 8 inches. Turbulence C was found to have higher intensity than B for length scales lower than 3 inches (Figs. 4.37 and 4.38). It may well be that monochromatic wave data for shorter waves would show a greater difference in the rate of wave attenuation between Turbulence B and C; and data for longer wind waves might show less difference in growth curves between Turbulence B and C.

Another possible reason for the greater differentiation of results between Turbulence B and C may be that the water surface fluctuations caused by the turbulence and the mechanical vibrations from the turbulence generators were significantly greater for Turbulence C than for A or B (as shown in Figs. 6.34 - 6.36). It may be that the water surface fluctuations are more important in the transfer of energy from wind to water and from one wave length to another, and that monochromatic waves are not affected as much by the surface fluctuations.

Comparison of the growth curves in turbulent and still water shows the differences that are noted above. The exact mechanism bringing about these differences cannot be proved at this point; however, some suggestions can be made. The increase in the initial growth rate of the high frequency waves in turbulence may be a result of the turbulence roughening the water surface; in this case the growth curve in turbulent water might be described as being like that of still water growth curve for a longer fetch. In the case of the lower frequency components of the waves, which receive energy from the higher frequency components, the increased rate of growth in turbulence strongly suggests that the presence of turbulence enhances the transfer of energy to the longer waves by wave-wave interaction.

In this regard, the findings of the Joint North Sea Wave Project (conducted in 1968 and 1969) reported by Barnett, 1972, should be noted. It was concluded that on the average 60-70% of the wave growth was due nonlinear wave-wave interactions. Barnett further states that:

> "The steep forward face of the spectrum is in essence maintained by the wave-wave mechanism. In the mid-frequency range of the spectrum, the wave-wave transfer (and perhaps other dissipative mechanisms) overcomes all atmospheric input. The net result is a loss of energy in this frequency range. This behavior explains the overshoot effort previously discussed by Barnett and Sutherland (1968). At relatively high frequencies the wave-wave mechanism joins forces with the atmospheric growth mechanism. These positive inputs are balanced by some unknown dissipative mechanism (wave breaking)."

If the steep forward face of the wind wave spectra obtained in turbulent water is in fact maintained by wave-wave interactions, then the hypothesis of enhanced transfer of wave energy by wave-wave interaction ih the turbulent water can help explain both the increased growth of lower frequency components and the lowering of the maximum height obtained in overshoot in turbulent water. If one attributes all of the lowering of the maximum height obtained in overshoot in turbulent water to increased dissipation, then there would be less energy at high frequency to pass on to lower frequency.

One of the qualitative observations which motivated this study was that short wind waves appear in the turbulent wake of a ship soon after the ship passes, and that for several minutes the wake persists with the very short wind waves and the very long period swell, but with little evidence of waves of intermediate length. From the work on monochromatic waves, it is clear that the shortest and highest waves coming into the turbulent wake will be attenuated the fastest. This explains why of all the incoming waves only the long low amplitude waves pass through the wake without significant loss of energy. In this chapter it has been shown that the presence of turbulence in the water results in faster growth initially when compared to growth in still water and that the maximum height is attained sooner but its value is less than it would be in still water. The apparent scarcity of waves of intermediate length in the wake may be explained in the following manner. The turbulence will cause the intermediate-length waves to gain energy faster from the short waves, but the intermediate-length waves will also interact and pass energy onto the longer waves which were not as drastically attenuated on encountering the turbulence. In this respect our experiment in the laboratory is quite different from the situation in the wake of the ship. In the ship wake a whole spectrum of wind waves encounters turbulence and the higher frequency side is initially attenuated, then the spectrum is redeveloped starting at the high frequency side.

This redevelopment cannot take place instantaneously and so for some time the spectrum will have two overlapping peaks - the remains of the incident spectrum at low frequency forming one peak and the new spectral peak at high frequency growing upward and toward the lower frequency peak. In the laboratory experiment there was a steep spectral spike representing the long low wave made by the turbulence generator isolated by a band of near-zero wave energy from the spectral peak representing the growing wind waves. Because the sloping side bands of the spectral peaks did not overlap there was no wave interaction resulting in energy exchange between them.

The fetch in this study was too short to allow waves longer than the scales of turbulent motions present to develop; therefore, one can only speculate what would happen in such a case. In discussing the effects of surface films on wind waves, Davies, 1962, notes that the damping of the short waves by surface films will lower the wind drag on the longer waves. However, if the long waves are close to breaking the damping of the short waves reduces the disturbances acting on the longer waves and thus reduces the chances of breaking. Perhaps small scale turbulence could have similar effects on long wind waves.

None of the wave theories predicts the overshoot phenomenon; however, the theory of wave-wave interactions does provide the idea that the energy lost by one frequency in overshoot is partially transmitted to lower frequencies. However, it seems clear that wave-wave interactions are not conservative and less conservative for interactions as the steepness of the interacting waves increases. Even in the absence of externally generated turbulence, wind waves could become sufficiently steep to interact in a manner that produces turbulence. Thus it seems that it may be necessary to study the effects of turbulence created in the generation area in order to understand the growth of wind waves. Both the transfer of energy from wind to waves and the transfer of energy from one wave length to another may be affected by this turbulence.

7. CONCLUSIONS AND SUGGESTIONS FOR FURTHER STUDY

7.1 Turbulence and Monochromatic Waves

The rate of dissipation of wave energy by turbulence can be represented by the equation:

$$D_B = K_B \, 2\rho \, k^3 \, c^3 \, h^3$$

where K_B depends on the scale of turbulence, the intensity of turbulence, and on the length of the waves, K_B was found to be from 3 to 6 times greater in the turbulent flow fields studied; however, for very long waves K_B was the same in still and in turbulent water. For scales of turbulent motion comparable to or greater than the length of the waves a significant increase in the intensity of turbulence will cause a significant increase in the rate of wave energy dissipation. For scales of turbulent motion smaller than the length of the waves a significant increase in the intensity of turbulence did not result in a comparable increase in the role of wave energy dissipation.

An area for further study is to define K_B for the transition range between very long waves unaffected by small scale turbulence and the short waves significantly attenuated by turbulence. The more difficult problem of tracing the energy lost by the monochromatic wave should also be studied.

7.2 Wind Waves and Turbulence

The presence of turbulence in the water has several very definite effects on the growth of wind waves. The following effects in particular were noted:

1. In the linear and exponential portions of the growth curve the waves were higher in the turbulent water.
2. Overshoot generally occurs at a shorter fetch in the turbulent water.
3. The maximum wave height achieved in overshoot in turbulence is as little as one half that achieved in still water.
4. After overshoot the waves remained lower in the turbulent water than in the still water.
5. In general the above effects appeared to be roughly proportional to the intensity of the turbulence of a scale comparable to the length of the waves.
6. The wave energy spectra at the longer fetches in turbulent water show more wave energy at low frequency and less at high frequency than those for still water.

The effects of turbulence on wind wave growth appears to be a very promising area for further research. The fetch in this study was too short to allow waves to attain the equilibrium height or to develop longer than the scales of turbulent motion present. This can be done by lengthening the turbulence generator and/or decreasing the scale of turbulence generated.

In order to accurately locate and measure the maximum in overshoot, one needs many wave gages closely spaced.

Another problem which could be studied in light of the findings presented above is that of non-conservative wave-wave interactions. Do the wind waves create turbulence (by non-conservative wave-wave interactions, whitecapping, breaking, etc.) which in turn effects the rate of viscous dissipation and the rate of energy transfer from wind to waves and the rate of transfer of energy from the shorter to the longer waves? What conditions and what wave parameters determine whether or not wave interactions are conservative with respect to wave energy or not?

Some progress has been made in this study on the effects of turbulence on monochromatic waves. Because of the possibility of greater wave-wave interactions when waves of many frequencies are present, the effects of turbulence on a decaying polychromatic spectrum should also be studied.

REFERENCES

Barber, N. F., 1969, Water Waves, Wykeham Publications Ltd., London.

Barnett, T. P., 1972,"Observations of Wind Wave Generation and Dissipation in the North Sea: Implications for the Offshore Industry," Offshore Technology Conference, Preprints, Vol. 1, pp. 43-50.

Barnett, T. P., and Sutherland, A. J., 1968, "A Note on an Overshoot Effect in Wind-Generated Waves," Jour. Geophys. Res., Vol. 73(22), pp. 6879-6885.

Bowden, K. F., 1950, "The Effect of Eddy Viscosity on Ocean Waves, Philos. Mag. (7), Vol. 41, pp. 907-917.

Boyev, A. G., 1971, "The Damping of Surface Waves by Intense Turbulence, Izv., Atmospheric and Oceanic Physics, Vol. 7(1) pp. 50-59.

Davies, J. T., 1962, "Some Effects of Surface-Active Agents on Waves and Ripples," Chemistry and Industry (May), pp. 906-910.

Dobrokinoskii, S. V., 1947, "Turbulent Viscosity in the Surface Layer of the Sea and Wave Motion," Prac. (Dokl.) Acad. Sci. USSR, Vol. 58(7).

Dobrokinoskii, S. V., and Kontoboitseva, N. V., 1966, "An Experimental Investigation of Turbulent Viscosity in Monochromatic Waves," Izv., Atmospheric and Ocean Physics, Vol. 2(1), pp. 64-74.

Garret, W. D., 1967, "Damping of Capillary Waves at the Air-Sea Interface by Oceanic Surface-Active Material," Jour. Mar. Res., Vol. 25(3), pp. 279-291.

Groen, P., 1954, "On the Behavior of Gravity Waves in a Turbulent Medium, with Application to the Decay and Apparent Period Increase of Swell," Kingdom of the Netherlands Meteorological Institute, Mededelingen en Verhandelingen 63, pp. 1-23.

Hasselmann, K., 1962, "On the Nonlinear Energy Transfer in a Gravity Wave Spectrum, Part 1," Jour. Fluid Mech., Vol. 12, pp. 481-500 (see also Vol. 15, pp. 273-298).

Howe, M. S., 1971, "Wave Propagation in Random Media," Jour. Fluid Mech., Vol. 45(4), pp. 769-804.

Johnson, J. W., 1947, "The Refraction of Surface Waves by Currents," Trans. Amer. Geophys. Un., Vol. 28(6), pp. 867-874.

Keller, J. B., 1964, "The Velocity and Attenuation of Waves in a Random Medium,: Proc. Symp. Appl. Math., Providence, R.I.: Amer. Math. Soc., Vol. 16, p. 145.

Kurihara, M., 1958, "Pneumatic Breakwaters I, II, and III," IER Tech. Rep. No. 104.

Lamb, H., 1932, Hydrodynamics (effects of viscosity on water water waves), Dover Pub. Inc., New York, pp. 623-628.

Lin, J. D., and Howard, L. N., 1960, "Nonlinear Standing Waves in a Rectangular Tank Due to Forced Oscillation," Mass. Inst. Tech Hydro. Lab. Rep. No. 44, 108 pp.

Mahony, J. J., 1971, "Cross Waves," Univ. Essex Fluid Mech. Res. Inst., Rep. No. 6, 25 pp.

Miles, J. W., 1957, "On the Generation of Surface Waves by Shear Flows," Jour. Fluid Mech., Vol. 3, pp. 185-204.

Mitsuyasu, H., 1966, "Interactions Between Water Waves and Winds (I) - Co-existent System of Wind Waves and Regular Oscillatory Waves," Rep. Res. Inst. Appl. Mech. (Japan), Vol. 14 (48), pp. 67-89.

Mitsuyasu, H., 1968, "A Note on the Nonlinear Energy Transfer in the Spectrum of Wind-Generated Waves," Rep. Res. Inst. Appl. Mech. (Japan), Vol. 16(54), pp. 251-264.

Paquin, J. E., 1968, "A Laboratory Experiment on Surface Wave Attenuation Due to Underwater Turbulence," Naval Postgraduate School, M.S. Thesis (unpublished), Monterey, 60 pp.

Phillips, O. M., 1957, "On the Generation of Waves by Turbulent Wind," Jour. Fluid Mech., Vol. 2, pp. 417-445.

Phillips, O. M., 1959, "The Scattering of Gravity Waves by Turbulence," Jour. Fluid Mech., Vol. 5 (2), pp. 177-192.

Phillips, O. M., 1966, The Dynamics of the Upper Ocean, Cambridge University Press, 261 pp.

Richardson, L. F., and Stommel, H., 1948, "Notes on Eddy Diffusion in the Sea," Jour. Meteor., Vol. 5, pp. 238-240.

Savitsky, D., 1970, "Interaction Between Gravity Waves and Finite Turbulent Flow Fields," Stevens Inst. Tech. Rep. 1469, (Presented at 8th Symp. Naval Hydrodyn. Cal. Inst. Tech.), 60 pp.

Sawargi, T., 1967, "Fundamental Studies on Generation and Development of Longshore Bar Near Rivermouth," Coastal Eng. in Japan, Vol. 10, pp. 59-66.

Sutherland, A. J., 1968, "Growth of Spectral Components in a Wind-Generated Wave Train," Jour. Fluid Mech., Vol. 33 (3), pp. 545-560.

Tatsumo, M., Inoue, S, and Okabe, J., 1969, "Transfiguration of Surface Waves," Rep. Res. Inst. Appl. Mech. (Japan), Vol. 17 (59), pp. 195-215.

Wiegel, R. L., 1964, Oceanographical Engineering, Prentice-Hall Inc., Englewood Cliffs, N. J., pp. 170-172

APPENDIX A

```
C AS GIVEN HERE THE INPUT IS ON TAPE AND THE OUTPUT IS FOR VELOCITY SPECTRA
C A FACTOR OF 2 MUST BE APPLIED TO THE  AREA UNDER THE SPECTRUM
C IN ORDER TO OBTAIN THE VARIANCE
RUN,,,,,,PRF.
REQUEST,TAPE1,HI,4000
LGO,PRF.
RUN.
LGO.
,
      PROGRAM PRF(TAPE1,TAPE9,INPUT,OUTPUT)
      DIMENSION A(3200)
      NSKIP=0
      NRAN=0
      REWIND 1
99    READ (1)  (A(I),  I=1,6)
      NRAN=NRAN+1
      NSKIP=NSKIP+1
      IF (NSKIP .LT. 14) GO TO 99
100   READ (1)  (A(I), I=1,3128)
      NRAN=NRAN+1
      IF(NRAN .EQ. 27) GO TO 101
      IF(NRAN .EQ. 31) GO TO 101
      IF(NRAN .EQ. 32) GO TO 102
      GO TO 100
101   CONTINUE
      WRITE (9) (A(I), I=1,3128)
      GO TO 100
102   CONTINUE
      END
,
      PROGRAM INSPEC (INPUT,OUTPUT,PUNCH,TAPE9)
C    SPECTRAL DENSITIES WITH MAGNETIC TAPE INPUTS
      DIMENSION PPS(150,10),SUMPS(150,1)
      DIMENSIONA(3200,1),AC(150,10),II(150),PS(150,10),FREQ(150),F1(150)
      PI = 3.1415926536
      READ 1300,NRUN
      NRAN=0
1     READ 1300, NGAGE, NTIME, NFREQ
      PRINT  1390
      PRINT 1330
      REWIND 9
1301  FORMAT ( 5X, 10I10 )
1302  FORMAT ( 5X,  10F10.6)
4     READ 1910, WATERD, WINSPD, IDATMO, IDATDY, IDATYR
      READ 1310, FN, FACTOR
    2 READ 1300, INDIC, IFACTOR, NPRINT , IPRINT
C*******************PRINT OUT THE INPUTS**********************************
      ML = NFREQ + 1
      LAGS = NFREQ
      FBAND = FN / FLOAT( NFREQ )
      IF ( IFACTOR .EQ. 1 ) FACTOR =  1. / (2. * FBAND )
```

```
      PRINT 1301,INDIC, IFACTOR, NPRINT , IPRINT, NFREQ
      PRINT 1302, FN, FACTOR
      PRINT 1352, NGAGE
      PRINT 1351, NTIME
      PRINT 1350, FBAND
      PRINT 1340, LAGS
      PRINT 1920,IDATMO, IDATDY, IDATYR
      PRINT 1940, WATERD
      DO  8  LL= 1, ML
      LLM1 = LL - 1
      F1(LL) = FLOAT (LLM1) * FBAND
      I1(LL) = F1 (LL) * 10.
    8 CONTINUF
      DELTA - F1(2) - F1(1)
9     READ (9) (A(J,1), J=1,NTIME)
      AAA=0
      DO 11 J=1,NTIME
      A(J,1)=A(J,1)+AAA
11    CONTINUF
      DO 7777 J=1,NTIME,4
      A(J,1)=((A(J,1)**2.-510941.)/2512617.)**2.304
      A(J+1,1)=((A(J+1,1)**2.-508360.)/2522042.)**2.304
      A(J+2,1)=((A(J+2,1)**2.-528522.)/2558850.)**2.304
      A(J+3,1)=((A(J+3,1)**2.-531441.)/2556262.)**2.304
7777  CONTINUF
      NRAN=NRAN+1
      NN=NGAGE-1
      NSER = 0
      DO 99 K= 1, NN
      LURCH = K + 1
      PRINT 1411
      DO 14 I = 5, 10     , 5
      I1 = I - 4
      ID = I / 5
      PRINT 1400, ( A(M,1), M= I1, I), K , ID
   14 CONTINUF
      CALL DETRND(A(1,1), NTIME, A(1,1), 2)
      DO 90 L= LURCH, NGAGE
      NSER = NSER + 1
      NG = NG + 1
   45 CALL AUTCOV( A(1,1), NTIME, AC(1, K), LAGS , IPRINT )
      CALL FOURTR( AC(1, K), LAGS, PPS(1, K), INDIC , IPRINT )
   90 CONTINUF
      DO 81 I = 1, ML
       PS(I, K) =PPS(I, K) * FACTOR
   81 CONTINUF
      SUMPS(1,K)=PS(1,K)
      DO 82 I=2,ML
      SUMPS(I,K)=PS(I,K)+SUMPS(I-1,K)
   82 CONTINUF
      PRINT 1421
      DO 86  I = 1, ML
      IM1 = I - 1
       IF( MOD( IM1 , 50) .NE. 0 ) GO TO 86
       IF ( I .NE. 1 ) PRINT 1390
      PRINT 85
   86 PRINT 84, F1(I), PS(I,K),SUMPS(I,K)
```

```
      M=0
      DO 83 J=1,ML,5
      J1=J+4
      M=M+1
      PUNCH 89, (PS(I,K), I=J,J1),M
 83   CONTINUE
 89   FORMAT (5E15.7,I5)
   99 CONTINUE
C*********************************************************************
94    FORMAT ( 4X,F9.5,5X, 6E15.7 ,6X,6E15.7)
95    FORMAT( 10X, 4HFREQ, 13X, 3HPSD,      10X, 6HSUMPSD)
1300  FORMAT(12I6)
1310  FORMAT( 8F10.4)
1330  FORMAT ( 30X, 41H-----------THE GIVEN INFORMATION----------/)
1340  FORMAT(30X,18HNUMBER OF LAGS =   , I6/)
1350  FORMAT(30X,22HFREQUENCY BAND WIDTH = ,F6.3/)
1351  FORMAT ( 30X, 36HNUMBER OF DATA GIVEN FOR EACH GAGE =,I10/)
1352  FORMAT(30X,16HNUMBER OF GAGE =, I6/)
1370  FORMAT ( 1H1 )
1400  FORMAT ( 5X= 5E14.7, 5X, 3HCH, I3, I5
     1    , I3/ )
1411  FORMAT (1H0, 24X,  43H VELOCITIES IN FT. PER SEC.              )
1421  FORMAT(1H1,1X,22HPOWER SPECTRAL DENSITY)
1910  FORMAT(2F10.2, 3I10)
1920  FORMAT(36X,    31H(INCIDENT WAVE RUN AT, I3, 1H/, I3, 1H/,I4,1H)//)
1940  FORMAT (30X,13HWATER DEPTH =,F6.2, 3HFT/)
      IF(NRAN.LT.NRUN) GO TO 9
1970  CONTINUE
      END
      SUBROUTINE AUTCOV ( X, N, Y, L , IPRINT )
C     SE AUTCOV  AUTOCOVARIANCE SUBROUTINE
      DIMENSION X(1), Y(1)
       IF ( IPRINT .EQ. 1 ) GO TO 900
      PRINT 3
3     FORMAT ( 1H1 )
      PRINT 200, L
200   FORMAT( 21H AUTO COVARIANCE WITHI4,5H LAGS//)
900   L1 = L + 1
      AN = N
      SUM = 0.
      DO 11 I = 1, N
11    SUM = SUM + X(I)
      E = (SUM / AN) **2
      DO 12 I = 1, L1
      Y(I) = 0.
      I1 = N- I + 1
      DO 13 J = 1, I1
      J1 = J + I - 1
13    Y(I) = Y(I) + X(J) * X(J1)
      Y(I) = Y(I) / FLOAT ( I1) - E
       IF ( IPRINT .EQ. 1 ) GO TO 12
      PRINT 210, Y(I)
210   FORMAT (5E20.12)
12    CONTINUE
      RETURN
      END
       SUBROUTINE DETRND ( X, N, Y, NDEG)
```

```
C      HE DETRND   MEAN AND LINEAR TREND REMOVAL                            DETRND01
       DIMENSIONX(1),Y(1)                                                   DETRND02
300    AN = N
       S1 = 0.
       S2 = 0.
       IF(NDEG)11,11,20                                                     DETRND06
11     DO13I=1,N                                                            DETRND07
13     S1=S1+X(I)                                                           DETRND08
       AVEX=S1/AN                                                           DETRND09
       DO15I=1,N                                                            DETRND10
       Y(I)=X(I)-AVEX
15     CONTINUE
       PRINT200,AVEX                                                        DETRND12
200    FORMAT(14H0REMOVE MEAN OF 1PE18.7)                                   DETRND13
       RETURN                                                               DETRND14
20     DO22I=1,N                                                            DETRND15
       S1=S1+X(I)                                                           DETRND16
22     S2=S2+S1                                                             DETRND17
       AVEI=0.5*(AN+1.0)                                                    DETRND18
       AVEX=S1/AN                                                           DETRND19
       SLOPE=-12.0*(S2-AVEI*S1)/(AN*(AN**2-1.0))                            DETRND20
       SUMRMS=0.0
       DO28I=1,N                                                            DETRND21
       AI=I                                                                 DETRND22
       Y(I)=X(I)-AVEX-SLOPE*(AI-AVEI)                                       DETRND23
       YSQ=Y(I)*Y(I)
       SUMRMS=SUMRMS+YSQ
   28  CONTINUE
       SUMRMS=SUMRMS/AN
       PRINT300,AVEX,SLOPE,SUMRMS                                           DETRND24
300    FORMAT(34H0REMOVE MEAN OF 1PE18.7,33H AND LINEAR TREND WITH SLOPE    DETRND25
      1OF 1PE18.7,17H AND MS VALUE OF 1PE18.7)                              DETRND26
       RETURN                                                               DETRND27
       END                                                                  DETRND28
        SUBROUTINE FOURTR ( X, N, Y, IND, IPRINT )
C      HE FOURTR   FOURIER TRANSFORM SUBROUTINE                             FOURTR01
       COMMON TAB (400)
       DIMENSIONX(2),Y(2)
        IF ( IPRINT .EQ. 1 ) GO TO 900
       PRINT 3
3      FORMAT (1H1)
       PRINT 200
200    FORMAT( 5X, 31HTABLE OF INPUT OF FOURIER TRANSFORM//)
       DO 400 I = 1, N
       PRINT 300, X(I)
300    FORMAT ( 5X, 5E20.12 )
400    CONTINUE
900    AN=N                                                                 FOURTR05
       N1=N+1                                                               FOURTR06
       N2=N+N                                                               FOURTR07
       ANGLE = 3.14159265358979 /FLOAT(N)
       GOTO(10,11,10,11),IND                                                FOURTR11
C      COSINE TABLE                                                         FOURTR12
10     DO 5  J= 1,N2
       JM1 = J - 1
       ANGLEJ = FLOAT(JM1) * ANGLE
       TAB(J) = COS( ANGLEJ )
```

```
5     CONTINUE
      ONE=1.0                                                          FOURTR18
      U=X(1)                                                           FOURTR19
      GOTO12                                                           FOURTR20
C     SINE TABLE                                                       FOURTR21
11    DO 6 J= 1, N2
      JM1 = J - 1
      ANGLEJ = FLOAT(JM1) * ANGLE
      TAB(J) = SIN( ANGLEJ )
6     CONTINUE
      ONE=0.0                                                          FOURTR27
      U=0.0                                                            FOURTR28
12    IF ( IPRINT .EQ. 1 ) GO TO 14
      PRINT 3
      PRINT 100
100   FORMAT ( 5X, 26HTABLE OF UNSMOOTHED OUTPUT//)
14    DO 15 I = 1, N1
      I1=I-1                                                           FOURTR30
      W=0.0                                                            FOURTR31
      DO16J=2,N                                                        FOURTR32
      JM1 = I1 * ( J - 1 )
      K = MOD( JM1, N2 )
16    W=W+X(J)*TAB(K+1)                                                FOURTR34
      Y(I)=(U+2.0*W+ONE*X(N+1))/AN                                     FOURTR35
      IF ( IPRINT .EQ. 1 ) GO TO 15
      PRINT 300, Y(I)
15    ONE=-ONE                                                         FOURTR36
      GOTO(17,18,19,21),IND                                            FOURTR37
17    PRINT200                                                         FOURTR38
      GOTO20                                                           FOURTR39
18    PRINT201                                                         FOURTR40
      GOTO20                                                           FOURTR41
19    W2=(Y(1)+Y(2))/2.0                                               FOURTR42
      W3=(Y(N)+Y(N+1))/2.0                                             FOURTR43
      PRINT202                                                         FOURTR44
      GOTO22                                                           FOURTR45
21    W2=0.0                                                           FOURTR46
      W3=0.0                                                           FOURTR47
      PRINT203                                                         FOURTR48
22    DO23I=2,N                                                        FOURTR49
      W=(Y(I-1)+Y(I+1))/4.0+Y(I)/2.0                                   FOURTR50
      Y(I-1)=W2                                                        FOURTR51
23    W2=W                                                             FOURTR52
      Y(N)=W2                                                          FOURTR53
      Y(N+1)=W3                                                        FOURTR54
20    RETURN                                                           FOURTR55
200   FORMAT(17H0COSINE TRANSFORM)                                     FOURTR56
201   FORMAT(15H0SINE TRANSFORM)                                       FOURTR57
202   FORMAT(26H0SMOOTHED COSINE TRANSFORM)                            FOURTR58
203   FORMAT(24H0SMOOTHED SINE TRANSFORM)                              FOURTR59
      END                                                              FOURTR60
```

APPENDIX B

```
RUN.

*
      PROGRAM CPEFT(INPUT,OUTPUT)
      COMPLEX X(2048)
      DIMENSION Y(2048),P(1024),PSD(1024),F(1024)
1000  FORMAT(I10,F10.7,I10,F10.7)
1001  FORMAT(8F8.5)
2000  FORMAT(1H1,* MEAN = *,E14.5,*   VARIANCE = *,E14.5,*  3RD MOM = *,
     1 E14.5,*  4TH MOM = *,E14.5/2X,*  I         TIME,SEC             Y(I)
     2     *)
2001  FORMAT (1X ,I5,3X,E14.5,3X,E14.5)
2002  FORMAT(1X,F10.5,F14.7)
2003  FORMAT (1H1,*  FREQUENCY,CPS       POW SPECT DENSITY  *)
2004  FORMAT (1X,2F14.7)
2005  FORMAT (////2X,*AREA UNDER SPECTRUM = *,E14.7)
2010  FORMAT(1H1,*      THE PERIODOGRAM                              *///
     11X,* FREQUENCY,CPS  POW SPECT DENS  *//)
2020  FORMAT(1H1,/////////////////////*                        THE FOLLOWING
     1RESULTS ARE FOR COSINE BELL TAPERED DATA*)
      READ 1000,N,DELT,NBLOCK,SIGN
      XBLOCK=NBLOCK
      NN=2**N
      XNX=NN
      DELF=1.0/(NN*DELT)
      READ 1001,(Y(I),I=1,NN)
      SUM1=0.
      SUM2=0.
      SUM3=0.
      SUM4=0.
      DO 1 I = 1,NN
      SUM1=SUM1+Y(I)
1     CONTINUE
      YMEAN=SUM1/XNX
      DO 2 I = 1,NN
      Y(I)=Y(I)-YMEAN
      Z2=Y(I)*Y(I)
      Z3=Y(I)*Z2
      Z4=Z2*Z2
      SUM2=SUM2+Z2
      SUM3=SUM3+Z3
      SUM4=SUM4+Z4
2     CONTINUE
      Y2=SUM2/XNX
      Y3=SUM3/XNX
      Y4=SUM4/XNX
      PRINT 2000,YMEAN,Y2,Y3,Y4
      TIM=-DELT
      DO 3 I = 1,NN
      TIM = TIM+DELT
      PRINT 2001,I,TIM,Y(I)
```

```
3       CONTINUE
        DO 4 I = 1,NN
        X(I)=CMPLX(Y(I),0.)
4       CONTINUE
        DO 5 M = 1,2
        IF(M.LT.2) GO TO 100
        PRINT 2020
        XX1=.1*XNX
        NXX=XX1
        NXF=NN-NXX
        XXF=NXF
        DO 6 I = 1,NXX
        RI=I
        R1=.5*(1.-COS(3.14162*(RI-1.)/(NXX-1)))*Y(I)
        X(I)=CMPLX(R1,0.)
6       CONTINUE
        DO 7 I = NXF,NN
        RI = I
        R=.5*(1.-COS(3.14162*((NN-1)-(RI-1.))/(NXX-1)))*Y(I)
        X(I)= CMPLX(R,0.)
7       CONTINUE
        JAP=NXF-1
        JAZ=NXX+1
        DO 8 I = JAZ,JAP
        X(I)=CMPLX(Y(I),0.)
8       CONTINUE
100     CALL NLOGN(N,X,SIGN)
        PRINT 2010
        XF=-DELF
        SUMP=0.0
        NN2=NN/2
        DO 9 I = 1,NN2
        X(I)=X(I)/XNX
        P(I)=2.*CABS(X(I))**2
        XF=XF+DELF
        SUMP=SUMP+P(I)
        PRINT 2002,XF,P(I)
9       CONTINUE
        PRINT 2005,SUMP
        KK=NN2/NBLOCK-1
        DO 10 K = 1,KK
        PSD(K)=0.0
        DO 11 IZ = 1,NBLOCK
        J=(K-1)*NBLOCK+IZ+1
        PSD(K)=PSD(K)+P(J)
        RK=K
        F(K)=(XBLOCK/2.+XBLOCK*(RK-1.))*DELF +DELF
11      CONTINUE
        PSD(K)=PSD(K)/(XBLOCK*DELF)
10      CONTINUE
        PRINT 2003
        PRINT 2004,(F(K),PSD(K),K=1,KK)
5       CONTINUE
        STOP
        END
        SUBROUTINE NLOGN(N,X,SIGN)
        DIMENSION M(10)
```

```
      COMPLEX X(2048)
      COMPLEX WK,HOLD,Q
      LX=2**N
      DO 1 I=1,N
    1 M(I)=2**(N-I)
      DO 4 L=1,N
      NBLOCK=2**(L-1)
      LBLOCK=LX/NBLOCK
      LBHALF=LBLOCK/2
      K=0
      DO 4 IBLOCK=1,NBLOCK
      FK=K
      FLX=LX
      V=SIGN*6.2831853*FK/FLX
      WK=CMPLX(COS(V),SIN(V))
      ISTART=LBLOCK*(IBLOCK-1)
      DO 2 I=1,LBHALF
      J=ISTART+I
      JH=J+LBHALF
      Q=X(JH)*WK
      X(JH)=X(J)-Q
      X(J)=X(J)+Q
    2 CONTINUE
      DO 3 I=2,N
      II=I
      IF (K.LT.M(I)) GO TO 4
    3 K=K-M(I)
    4 K=K+M(II)
      K=0
      DO 7 J=1,LX
      IF (K.LT.J) GO TO 5
      HOLD=X(J)
      X(J)=X(K+1)
      X(K+1)=HOLD
    5 DO 6 I=1,N
      II=I
      IF(K.LT.M(I)) GO TO 7
    6 K=K-M(I)
    7 K=K+M(II)
      IF(SIGN.LT.0.0) RETURN
      DO 8 I=1,LX
    8 X(I)=X(I)/FLX
      RETURN
      END
```

APPENDIX C

WAVE HEIGHTS IN FEET AND FREQUENCY (F) IN HERTZ
A AND B ARE CONSTANTS FOR EXPONENTIAL REGRESSION EQUATION H(F)=A*EXP(B*F)

TURBULENT CONDITION	H(9)	H(14)	H(20)	H(26)	A	B	F
	.115E-02	.533E-03	.673E-04	.104E-02	.404E-02	-.156E+00	6.07
	.211E-02	.143E-02	.273E-02	.265E-02	.523E-02	-.130E+00	5.04
	.261E-02	.219E-02	.141E-02	.103E-02	.404E-02	-.506E-01	4.12
	.251E-02	.246E-02	.215E-02	.200E-02	.278E-02	-.112E-01	3.43
	.236E-02	.233E-02	.211E-02	.226E-02	.225E-02	-.162E-02	3.75
	.111E-02	.662E-03	.286E-03	.147E-03	.250E-02	-.104E+00	6.13
	.197E-02	.162E-02	.116E-02	.800E-03	.295E-02	-.430E-01	5.02
	.249E-02	.225E-02	.187E-02	.186E-02	.287E-02	-.182E-01	4.12
	.237E-02	.238E-02	.207E-02	.223E-02	.240E-02	-.556E-03	3.43
	.222E-02	.224E-02	.198E-02	.233E-02	.224E-02	-.126E-02	3.73
	.339E-02	.288E-02	.250E-02	.246E-02	.286E-02	-.133E-01	3.43
	.247E-02	.193E-02	.152E-02	.801E-03	.273E-02	-.402E-01	5.15
	.560E-02	.461E-02	.410E-02	.375E-03	.650E-02	-.223E-01	3.43
A	.462E-03	.193E-03	.104E-03	.660E-04	.130E-03	-.132E+00	6.30
A	.337E-03	.306E-03	.221E-03	.210E-03	.432E-03	-.202E-01	5.01
A	.186E-02	.150E-02	.596E-03	.768E-03	.316E-02	-.620E-01	4.12
A	.221E-02	.174E-02	.120E-02	.142E-02	.277E-02	-.231E-01	3.43
A	.225E-02	.234E-02	.193E-02	.202E-02	.248E-02	-.073E-02	3.75
A	.180E-02	.717E-03	.242E-02	.300E-04	.723E-02	-.140E+00	5.13
A	.311E-02	.247E-02	.174E-02	.171E-03	.412E-02	-.208E-01	3.43
A	.532E-02	.372E-02	.273E-02	.230E-02	.772E-02	-.401E-01	3.54
B	.274E-03	.503E-04	.380E-04	.190E-04	.150E-02	-.231E+00	6.06
B	.888E-03	.145E-03	.355E-04	.300E-04	.075E-02	-.204E+00	5.00
B	.108E-02	.118E-03	.155E-03	.380E-04	.126E-01	-.213E+00	7.15
B	.145E-02	.871E-03	.650E-03	.768E-03	.305E-02	-.516E-01	3.43
B	.190E-02	.146E-02	.121E-03	.108E-03	.244E-02	-.226E-01	3.75
B	.220E-03	.152E-03	.380E-04	.308E-04	.550E-03	-.106E+00	6.06
B	.295E-03	.134E-03	.288E-04	.298E-04	.070E-03	-.140E+00	5.30
B	.673E-03	.548E-03	.310E-03	.180E-03	.117E-02	-.630E-01	4.33
B	.152E-02	.144E-02	.730E-03	.632E-03	.242E-02	-.506E-01	3.43
B	.160E-02	.200E-02	.128E-03	.028E-03	.236E-02	-.285E-01	3.75
B	.602E-03	.207E-03	.257E-03	.268E-03	.774E-03	-.400E-01	4.34
B	.268E-02	.111E-02	.072E-03	.026E-03	.478E-02	-.800E-01	3.43
B	.547E-02	.378E-02	.191E-03	.105E-03	.940E-02	-.680E-01	3.44
C	.378E-04	.136E-03	.856E-04	.503E-04	.002E-04	-.206E-02	6.06
C	.762E-04	.036E-03	.310E-04	.401E-04	.113E-01	-.237E+00	5.02
C	.608E-03	.406E-03	.163E-03	.300E-04	.145E-02	-.104E+00	4.31
C	.217E-02	.778E-03	.028E-03	.302E-03	.452E-02	-.081E-01	3.43
C	.215E-02	.151E-02	.145E-02	.705E-03	.220E-03	-.404E-01	3.80
C	.180E-03	.380E-04	.380E-04	.708E-04	.420E-03	-.110E+00	5.15
C	.265E-02	.117E-02	.665E-03	.886E-03	.550E-02	-.063E-01	3.44
C	.540E-02	.280E-02	.140E-02	.276E-03	.845E-02	-.653E-01	3.47